Synthesis of Metal-Containing Biomolecule Conjugates for Potential Use in ^{99m}Tc Molecular Imaging

DISSERTATION

zur

Erlangung der naturwissenschaftlichen Doktorwürde

(Dr. sc. nat.)

vorgelegt der

Mathematisch-naturwissenschaftlichen Fakultät

der

Universität Zürich

von

YUNJUN SHEN

aus der

V. R. China

Promotionskomitee

Prof. Dr. Roger Alberto (Vorsitz und Leitung)

Prof. Dr. Eva Freisinger

Zürich, 2014

Table of Contents

Acknowledgments

First and foremost, I would like to sincerely thank my supervisor, Prof. Roger Alberto for all his friendly guidance and patience during the whole time I was working on this thesis. I am so fortunate to join his research group and have the opportunity to carry out this great project.

I am very grateful to Dr Margret Schottelius from the University of Munich, Prof. Dr. Isabel Santos, Dr Paula Raposinho, Célia Maria from the Lisbon Instituto Tecnológico e Nuclear for collaboration on biological studies.

I am truly indebted to my dissertation committee members, Prof. Dr. Roger Alberto, Prof. Dr. Eva Freisinger for their valuable time and comments, to Prof. Dr. Roland Sigel for organizing our annual retreat program of the Graduate School of Chemical and Molecular Science Zurich (CMSZH), to Prof. Dr. Gilles Gasser for his helpful disscutions and suggestions.

Many thanks go to all the present and past members in our group for their help and encouragement while undertaking the work described in this PhD thesis. Special thanks to Michael Felber, Sebastian Imstepf, Dr. Paul Schmutz, Dr. Henrik Braband, Dr. Daniel Can, Dr. Jessica Steinmann, Dr Karel Zelenka for the nice time we spent together and for the interesting scientific discussions.

I am also grateful to Dr. Ferdinand Wild for his generous help with MS measurements, Dr. Felix H. Zelder for HPLC technical support, Dr. Laurent Bigler for HRMS measurements, Heinz Spring for elemental analyses.

I would like to express my deepest gratitude to my wife, Hui Qiu, for her continued support and sacrifice during my pursuit of a PhD in Switzerland. I dedicate my dissertation to her and our unborn child.

Finally, I acknowledge the financial support from the China Scholarship Council (CSC) and European Corporation in Science and Technology (COST).

Abbreviations

ADP	adenosine diphosphate
ATP	adenosine triphosphate
BBN	bombesin
BFC	bifunctional chelate
Bn	benzyl
Boc	tert-butoxycarbonyl
Cbz	carboxybenzyl
Dap	1,2-diamino-propionic acid
DCM	dichloromethane
DEAD	diethyl azodicarboxylate
DIPEA	diisopropylethylamine
DMAP	dimethylaminopyridine
DMF	dimethylformamide
DMSO	dimethyl sulfoxide
Fmoc	9-fluorenylmethoxycarbonyl
HBTU	o-(benzotriazol-1-yl)-N,N,N’,N’-tetramethyluronium
HMPA	hexamethylphosphoramide
HOBt	1-hydroxybenzotriazol
HPLC	high-performance liquid chromatography
Hz	hertz
Me	methyl
mg	milligram
MHz	megahertz
min	minute(s)
mL	milliliter(s)
mmol	millimole(s)

mol	mole(s)
NMM	N-methylmorpholine
NMR	nuclear magnetic resonance
OAc	acetate
$Pd(Ph_3P)_4$	tetrakis(triphenylphosphine) palladium(0)
Pd/C	palladium on activated carbon catalyst
PG	protecting group
Rf	retention factor
rt	room temperature
s	singlet
SAAC	solid phase peptide synthesis
t	triplet
TBSCl	tert-butyldimethylsilyl chloride
tBu	tert-butyl
TEA	triethylamine
TFA	trifluoroacetic acid
TFA	trifluoroacetic acid
TFA_2O	trifluoroacetic anhydride
THF	tetrahydrofuran
TIS	triisopropyl silane
TLC	thin layer chromatography
TMAH	tetramethylammonium hydroxide

1 General Introduction

1.1 Nuclear Medicine

In 1934, Irene and Frederic Joliot-Curie discovered the artificial radioactivity**,** representing the most significant milestone in nuclear medicine.(*1*) Nuclear medicine gained public recognition only after December 7, 1946, when an article was published in the Journal of the American Medical Association (JAMA) by S.M Seidlin.(*2*) The article described a successful treatment of a patient with thyroid cancer using radioactive iodine (I-131). Widespread clinical use of nuclear medicine, however, did not start until the early 1950s, as knowledge expanded about radionuclides, detection of radioactivity, and using certain radionuclides to trace biochemical processes. Despite considerable advance**s** in knowledge about the application of radiotracer technique for interrogating physiologic and pathophysiologic cardiopulmonary conditions in the early twentieth century, the spatial resolution of the scintigraphic instruments used to measure tracer concentration in different organs was limited. The development of single photon emission computed tomography (SPECT) in the late 1970s and PET in the 1980s dramatically changed the clinical utility of radiotracer techniques for the assessment of myocardial perfusion, and since that time, nuclear medicine has changed rapidly as a result of these technological developments.(*3-7*)

1.1.1 Radionuclide

A radioactive nuclide is an atom with an unstable nucleus that decays, emitting alpha, beta, or gamma rays. In alpha decay, the nucleus ejects a helium nucleus composed of two neutrons and two protons, dropping the mass of the original nucleus by four mass units. Atoms emit beta particles through a process known as beta decay. Beta decay occurs when an atom has either too many protons or too many neutrons in its nucleus. Two types of beta decay can occur. One type (β^+ decay) releases a positively charged beta particle called a positron, and a neutrino; the other type (β^- decay) releases a

negatively charged beta particle called an electron, and an antineutrino. The neutrino and the antineutrino are high energy elementary particles with little or no mass and are released in order to conserve energy during the decay process. Gamma decay occurs because the nucleus is at too high an energy. The nucleus falls down to a lower energy state and, in the process, emits a high energy photon known as a gamma particle (Table 1.1).

Table 1.1 Common isotopes used in nuclear medicine[a]

isotope	symbol	$T_{1/2}$	decay	gamma (keV)	positron (keV)
Imaging:					
fluorine-18	^{18}F	109.77 m	β^+	511 (193%)	249.8 (97%)
gallium-67	^{67}Ga	3.26 d	ec	93 (39%), 185 (21%), 300 (17%)	-
krypton-81m	^{81m}Kr	13.1 s	IT	190 (68%)	-
rubidium-82	^{82}Rb	1.27 m	β^+	511 (191%)	3.379 (95%)
nitrogen-13	^{13}N	9.97 m	β^+	511 (200%)	1190 (100%)
technetium-99m	^{99m}Tc	6.01 h	IT	140 (89%)	-
indium-111	^{111}In	2.80 d	ec	171 (90%), 245 (94%)	-
iodine-123	^{123}I	13.3 h	ec	159 (83%)	-
xenon-133	^{133}Xe	5.24 d	β^-	81 (31%)	0.364 (99%)
thallium-201	^{201}Tl	3.04 d	ec	69–83 (94%), 167 (10%)	-
Therapy:					
yttrium-90	^{90}Y	2.67 d	β^-	-	2.280 (100%)
iodine-131	^{131}I	8.02 d	β^-	364 (81%)	0.807 (100%)

$T_{1/2}$ = half-life; β+ = β+ decay; β- = β- decay; IT = isomeric transition; ec = electron capture

a) Retrieved from Wikipedia

Radiation can be absorbed by matter in its path. For example, alpha radiation travels only a few centimeters in air, beta radiation travels tens of centimeters in air, while gamma radiation travels many meters. Alpha and beta particles are effective only for a short distance because they use up their energy when they hit other atoms. Hence, these particles can cause internal radiation exposure hazard and affect health when they cause changes in the cells of the human body. These types of radiation can be used to kill cancer cells for therapeutic purpose. Gamma rays have a relatively long

range of penetration in air and matter and are not as ionizing as alpha or beta particles, hence, they can be detected outside the body and cause minimum damage to the patient. This type of radiation can be used to image the cancer cells for diagnosis purpose.(*8*)

1.1.2 Therapeutic nuclear medicine

Nuclear medicine treatments are technically a form of radiation therapy. Targeted tumor radiotherapy is a kind of radiation therapy that the radionuclides, which have high linear energy transfer particle emissions, are carried to a malignant site by appropriate carrier molecules in order to deliver lethal radiation dose to the tumors with minimal injury to normal tissue. There are three main types of radiation that can be emitted by radioactive particles (Table 1.2). They are called alpha, beta, and gamma and all three types of radiation come from the nucleus of the atom.(*9*) Physical characteristics include type and range of emissions, half-life, and chemical characteristics considered important for the selection of an appropriate therapy radioisotope. Most therapy agents utilize β-particle emissions for their ability to penetrate tissues. The ultimate target to achieve cell damage is the nucleus. The β emitter selected must therefore have an appropriate path length to reach the nucleus. There are several choices with respect to energy of the β emission. Lower energy β particles are desirable because they deposit all of their kinetic energy within a few cell diameters. These may be useful for microscopic targets and reducing damage to healthy tissue. Carrier molecules that target the cell surface require a longer particle path length to achieve nuclear damage and are ideally labeled with high energy β emitters such as P-32, Y-90, and Ho-166, which have excellent tissue penetration with a range beyond the source of several millimeters. Medium energy β particles such as those from iodine-131 have a shorter path length and may result in less dose homogeneity to the tissue, but still retain excellent therapeutic results.(*10*)

Although pre-clinical research and clinical trials suffer from limited availability of alpha emitters, there has been growing interest in alpha-particle emitters for targeted

radionuclide therapy over the past several years because of their high linear energy transfer and relative biological efficiency. The path length of alpha-particles in tissues only has a few cell diameters so that they can destroy tumor cells with minimal damage to surrounding healthy tissue. Cell damage essentially results from ionization and rupture of chemical bonds due to the kinetic energy transfer of alpha particles.

Table 1.2 Three Types of Radioactive Decay

Type	Symbol	Type of energy	Characteristics	Representative radionuclide
Alpha decay	α	Particle	Release of 2 protons, 2 neutrons	^{211}At, ^{212}Bi
Beta decay	β	Particle	Release of 1 electron	^{131}I, ^{90}Y
Gamma decay	γ	Electromagnetic	Release of photons	^{111}In

Ultra short-lived radioisotope of bismuth, Bi-213 has been studied for antibody mediated tumor targeting. Because of its short half-life (46 min), Bi-213 must be produced at the place of utilization. Radioisotopes with longer half-life, 225Ac and 212Pb, may be suitable for use in systemic treatment. 225Ac has a sufficiently long half-life (10 days) that results in optimal pharmacokinetics and is conveniently produced from Thorium 229 generators. 212Pb with half-life of 10.6 hours can be attached to monoclonal antibodies for cancer treatment.(*10*)

1.1.3 Diagnostic nuclear medicine

Diagnostic nuclear medicine generally uses small amounts of radioisotopes given intravenously or orally, and then external detectors capture and form images from the radiation emitted by the radiopharmaceuticals.(*11-13*). This diagnostic test helps evaluate different organ systems, including kidneys, liver, heart, lungs, thyroid, and bones. For many diseases, nuclear medicine is the most reliable method for making diagnoses.

Positron emission tomography (PET) and single-photon emission computed

tomography (SPECT) are noninvasive nuclear imaging modalities that provide clinical information regarding the living tissue in patients. In PET the radionuclides emit positrons (positively charged electrons) when they decay. The emitted positron travels in tissue until it interacts with an electron, resulting in the annihilation of both particles and the creation of two gamma rays which are used to create a tomographic image. The most important radiopharmaceutical used in the medical imaging modality PET is 2-^{18}F-fluoro-2-deoxyglucose (FDG), in which the hydroxyl group in the 2-position of D-glucose is replaced by ^{18}F. It can be used for the assessment of glucose metabolism in the heart, lungs, and the brain in PET imaging.(*14-17*) Unlike PET, radionuclides used in SPECT emit gamma rays, which are then recorded on cameras and reconstructed to determine the location of the decay events.(*18*) ^{99m}Tc is the most commonly used radionuclide for SPECT and the advantages of using this radionuclide are discussed in section 1.2. The ideal nuclear characteristics and its wide range availability are the main reason for widespread application of ^{99m}Tc based radiopharmercuticals.(*19, 20*) One widely used example in nuclear medicine imaging is technetium sestamibi (trade name Cardiolite), which is a lipophilic cation consisting of the radioisotope technetium-99m bound to six methoxyisobutylisonitrile ligands. The drug is mainly used to image the myocardium (heart muscle) and its lipophilicity leads to a favorable accumulation in the tissues.(*21-23*)

Table 1.3 Comparison of PET versus SPECT for imaging in nuclear medicine

Imaging modality	Radiation type	Type of energy	Characteristics	Representative radiotracer
SPECT	γ	Electromagnetic	Release of photons	^{99m}Tc ^{111}In ^{123}I
PET	β^+	Particle	Release of positively charged electrons	^{18}F ^{11}C ^{13}N ^{15}O

The comparison of the two imaging modalities, PET and SPECT, are shown in Table 1.3. One advantage of PET imaging is that there are more biologically relevant

isotopes available such as F-18, C-11, which can be covalently incorporated into a molecule.(*24, 25*) The main disadvantage is its high cost and not widely available. Up to now, there are only 3 FDA (U.S. Federal Drug Administration)-approved PET radiopharmaceuticals, ^{18}F-FDG (see Figure 1.1), ^{18}F-FDOPA (3,4-dihydroxy-6-fluoro- phenylalanine), and ^{18}F-Fluoride. This thesis focuses on the design of new SPECT based imaging agents. SPECT isotopes are generally cheaper than PET isotopes, and the gamma ray tracers used for SPECT usually have a longer half-life, like 6 hours for ^{99m}Tc, than the β^+ tracers used for PET, like 1.9 hours for ^{18}F. In addition, SPECT is based on much cheaper technology when compared to PET, Short-lived PET radiopharmaceuticals need to be produced by an expensive onsite cyclotron. SPECT, in contrast, produce images using gamma cameras which are available to most clinicians. These combined properties make SPECT much more widely applicable than PET.(*26-28*)

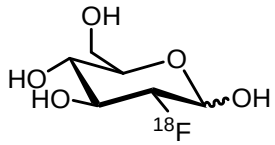

Figure 1.1 Structure of ^{18}F-FDG (2-deoxy-2-fluoro-glucose)

1.2 Tc-99m in diagnostic nuclear medicine

The most commonly used radioisotope in nuclear medicine is technetium-99m, a metastable nuclear isomer of technetium-99, used in over 85 percent of all nuclear medicine scans worldwide.(*20*) Technetium-99m was first discovered in 1938 as a product of cyclotron bombardment of molybdenum. This procedure produced a radionuclide molybdenum-99(^{99}Mo, $t_{1/2}$=66h), which decays to Tc-99m. As an ideal radionuclide for diagnostic imaging, ^{99m}Tc only emits gamma rays with energy of 141 keV and these are of an energy that is easily detected by a gamma camera. It has an ideal half life (6 h) which is long enough that the labeling synthesis of the radiopharmaceutical can be performed without significant loss of radioactivity but

short enough that the radioactivity administered to the body decreases rapidly with time, producing a radiation exposure equivalent to that obtained from a single normal X-ray.(*29*)

Technetium does not have any nonradioactive isotopes that permit the convenient characterization of compounds prepared by the new chemical methods. Rhenium (Re) is also a group VIIB transition metal that shares similar coordination geometries with technetium, thus it can be used as a nonradioactive surrogate for characterization of ^{99m}Tc radiopharmaceuticals. HPLC retention time comparison of the rhenium and technetium complexes derived from the same ligand is used as the primary method for identification of ^{99m}Tc complexes. If coinjection of both complexes shows the identical retention time, this is considered evidence of the technetium complex formation.

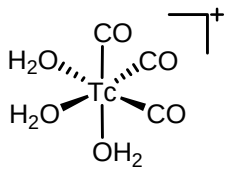

Figure 1.2 The structure of technetium (I) tricarbonyl core

Aside from traditional approach based on coordination chemistry for radiolabeling small molecules with ^{99m}Tc via stabilization of the $[Tc^{V}O]^{3+}$ metal core with ligands containing N or S chelating donors, organometallic labeling strategy has been investigated.(*30, 31*) The most well-known approach is using Alberto's reagent $[^{99m}Tc(CO)_3(OH_2)_3]^+$ (Figure 1.2).(*32*) The three aqua ligands can be readily replaced by many other donor atoms. Previous work from our laboratory has established the organometallic chemistry of Tc(I) and Re(I) tricarbonyl complexes containing the *fac*-$M(CO)_3$ moiety.(*33-37*) This core is of particular interest, not only because it is very small and stable over a wide range of pH values, but also because it provides excellent labeling efficiencies with a number of donor atoms. The new organometallic precursor $[^{99m}Tc(CO)_3(OH_2)_3]^+$ has been successfully used for radiolabeling of

biomolecules with low-valent ^{99m}Tc.(*38-46*) Our group previously reported the radiolabel Neurotensin by functionalizing the NH_2 terminus of Neurotensin with histidine or (N-histidinyl)acetic acid and obtained relatively high specific activity radiocomplexes, more importantly, the biological activity of the peptide was maintained.(*47*) In this thesis, we designed and synthesized several small tripod chelates with different number of nitrogen and oxygen donor atoms for $[^{99m}Tc(CO)_3(OH_2)_3]^+$ core. The reasons for this interest is that the tripod ligands have strong coordination ability with Alberto's reagent and the resulting complexes are quite small and hydrophilic, which are essential for the biological behavior of radiopharmaceuticals

1.3 Carbohydrate-based radiopharmaceuticals

1.3.1 Designing of diagnostic radiopharmaceuticals

Diagnostic radiopharmaceuticals are radiolabelled tracers that target specific organs or functions whose activity kinetics in tissue can be detected externally by specialised imaging systems such as gamma cameras and positron emission tomography scanners. An important part of the design of diagnostic radiopharmaceuticals is the chelating portion capable of strongly binding radioactive metals. The target-specific biomolecule itself usually does not bind strongly to metals, so a chelating portion needs to be introduced to the target molecule. This is bifunctional chelating agent (BFCA) approach for designing a targeted metal radiopharmaceutical, as illustrated in Figure 1.3. There are three essential parts designed into bioconjugates of this type: (i) Chelate (ii) Biomolecule (carrier) (iii) Linker or spacer. The primary function of the chelate is to produce radiometal complexes that are stable in vitro and in vivo. Biomolecules such as peptides, monoclonal antibodies and other receptor avid molecules carries a radionuclide as a payload and results in specific delivery of radioactivity to the desired site while sparing nearby organs from unnecessary radiation dose. The function of a linker is to prevents chelate's interference with biomolecule and adjust the lipophilic property of the bifunctional chelating agent.

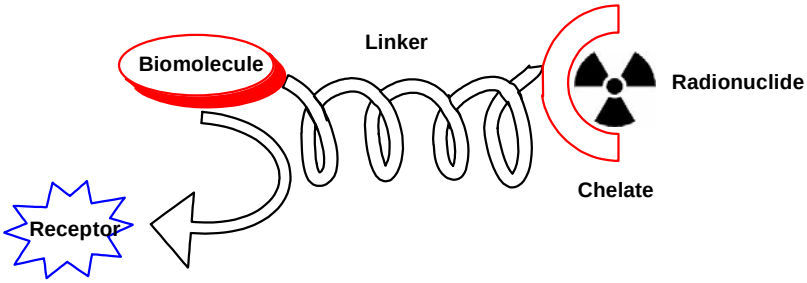

Figure 1.3 BFCA approach for the design of diagnostic radiopharmaceuticals

Biomolecules are molecules that occur naturally in living organisms and there are four major classes of biomolecules: Carbohydrates; Lipids; Proteins; Nucleic acids. The carbohydrates based bifunctional chelates that are the focus of this thesis are a class of attractive bioconjugates for the development of diagnostic radiopharmaceuticals due to the biological importance of carbohydrates that will be discussed in section 1.3.2.

^{99m}Tc is one of the most important medical radioisotopes in nuclear medicine applications due to its easy availability and ideal nuclear decay characteristics and therefore, the design of a ^{99m}Tc labeled glucose derivative as a SPECT analogue of the well established PET tracer [^{18}F]FDG is considered to be of great interest.(*48, 49*) Although some were recognized with relatively good affinity by hexokinase, the intracellular enzyme, the major problem to overcome is to effectuate transport through the cell membrane actively mediated by GLUT1.

In our endeavour for designing new carbohydrate derivatives able to be transported by GLUT1, we designed for this PhD project a number of new glucose derivatives, which are functionalized at different positions via a PEG spacer with the 1,2-diamino-propionic acid (Dap) chelator. Dap, replacing the ε-NH_2 group in Lysine was shown to yield a molecular imaging agent actively transported by the L-type amino acid transporter LAT1. Furthermore, we identified in previous work that Dap is a very strong chelator for the $[^{99m}Tc(CO)_3]^+$ core, yielding small and hydrophilic complexes.(*50-53*)

1.3.2 Carbohydrate metabolism *in Vivo*

Carbohydrates are a class of interesting building-block molecules for organic chemistry and drug development due to their involvement in various biological systems.(*54, 55*) Some carbohydrates are relatively small molecules. The most important to us is glucose, a simple sugar that is metabolized by nearly all known organisms. The breakdown of glucose to provide energy begins with the metabolic process called glycolysis. The free energy released in this process is used to form ATP (adenosine triphosphate) - the biological energy currency. Another important metabolic pathway is called oxidative phosphorylation that involves the conversion of ADP to ATP by the electron transport system in aerobic respiration. This pathway is a highly efficient way of releasing energy, generating 33.6 ATP per glucose molecule, compared to 2 ATP per glucose molecule for anaerobic glycolysis. Cancer cells have an altered cellular metabolism that promotes tumor survival and growth, which led to a high rate of glucose consumption compared with normal cells. This phenomenon, known as aerobic glycolysis or the Warburg effect, has important medical applications for the diagnosis and monitoring treatment responses of cancers by imaging uptake of 2-18F-2-deoxyglucose (FDG) with positron emission tomography (PET).(*56*) Thus glucose was widely used as a targeting vector for designing of diagnostic or therapeutic radiopharmaceuticals.

Hexokinase was first described by Meyerhof, who prepared the enzyme from baker's yeast.(*57*) It has a molecular weight of 100 kDa and is composed of an N-terminal regulatory domain a C-terminal catalytic domain. Each domain weighs about 50kD and contains a glucose binding site. It is an important enzyme that catalyzes the ATP-dependent phosphorylation of hexose to hexose-6-phosphate.The enzyme can catalyse this reaction on glucose, fructose, sorbitol and glucosamine as the first reaction in glycolysis pathway. The addition of a charged phosphate group at the 6-position of hexoses acts to trap it in a cell, since charged hexose phosphates cannot easily cross the cell membrane (Figure 1.4).

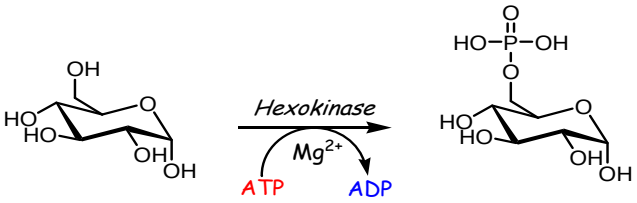

Figure.1.4 Phosphorylation of Glucose by hexokinase

Four different isozymes of hexokinase have been identified in mammals and each isozyme display distinct catalytic and regulatory properties. In contrast to normal cells, most malignant cells display increased expression and activity of hexokinase 2, which play a important role in tumor development by enhancing aerobic glycolysis.(*58*) There are many inhibitors of hexokinase that are being investigated as potential therapeutic agent in cancer treatment. Geschwind et al.(*59*) reported a novel therapeutic strategy for liver cancer by direct intraarterial injection of 3-bromopyruvate (3-BrPA), a potent inhibitor of cell ATP production, to liver-implanted rabbit tumors. The result showed that this strategy is highly effective, reducing the total number of viable cells to as low as 10% in a single injection without doing any apparent harm to the animals. Bertoni et al tested N-Appended glucosamine derivatives and found that several compounds exhibited competitive inhibition of hexokinase.(*60*)

Glucose is a uncharged polar molecule that is unable to cross the plasma membrane by passive diffusion and therefore requires specific carrier proteins to mediate its specific transport into the cell. Glucose transporters (GLUT) are a wide group of membrane proteins that facilitates glucose transport across these tissue barriers.(*61*) The human GLUTs family consists of 14 members and these facilitative glucose transporters are functionally distinct from the Na^+-dependent transporters which contribute to renal glucose reabsorption. The molecular weight of all Glut proteins range from 40 to 60 kDa and they are all glycosylated at or near the C terminus and are present on either cell surface or in intracellular sites. Tumor cells usually exhibit an altered metabolism characterized by exhanced aerobic glycolysis. Increases in glucose consumption help supply the energy for tumour cell proliferation and survival

that necessitate the overexpression of GLUTs. For example, GLUT1 appears to be the predominant glucose transporter in many types of cancer cells that include the breast, liver, pancreas, lung, thyroid, bone, cervix. Thus, metabolic changes of tumours can be used in the designing a carbohydrate based imaging agent.(*62*)

Glucose transporter type 1(GLUT1), a member of GLUTs family, is a major glucose transporter in the mammalian blood-brain barrier and is present at high levels in primate erythrocytes and brain endothelial cells. Although it has been proved that GLUT1 exhibits substrate specificity for glucose and galactose, the transport of non-natural substrates across biological membranes have been observed.(*63, 64*) When designing the glucose based imaging agents, it is important to keep the substrate specificity of glucose transporters and enhance the cell permeability. Zheng et al. described the synthesis of a porphyrin-glucosamine derivative (Figure 1.5a) and found that the compound was transported into cells.(*65*)

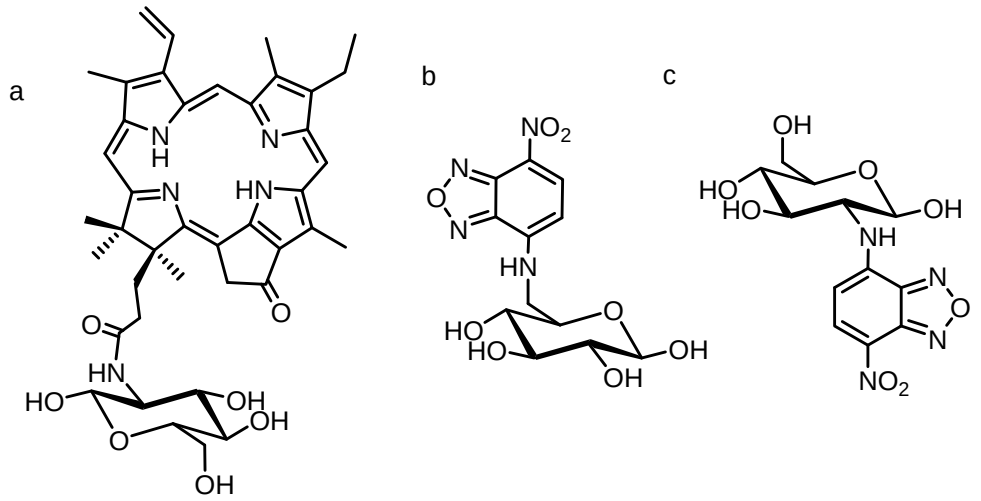

Figure 1.5 Functionalized glucose derivatives that exhibit GLUT glucose transporter activity: (a) porphyrin-appended glucosamine (b) 6-NBDG (c) 2-NBDG

Speizer and coworkers reported a fluorescent derivative of glucose 6-NBDG (Figure 1.5b) which was transported into human erythrocytes. It was found that the cellular uptake was competitively inhibited by D-glucose and that suggested the involvement of a glucose transporter in erythrocyte membrane.(*66*) 2-NBDG (Figure 1.5c) was also synthesized by Yoshioka et al,(*67*) it was shown that this compound is not only

transported into cells by GLUTs, but also phosphorylated by hexokinase.

^{18}F-FDG, as a glucose analogue, is actively transported into cells by GLUT transporters and subsequently phosphorylated by hexokinase to FDG 6-phosphate. The negative charged FDG 6-phosphate is unable to permeate the cell membrane and therefore accumulates once it has been absorbed. In addition, due to the absence of C2 hydroxyl group, ^{18}F-FDG-6-phosphate can not be further metabolized in cells. These properties make FDG a perfect imaging agent for glucose metabolism and give us inspiration in designing new carbohydrate based imaging agents.

1.4 Peptide-based radiopharmaceuticals

Peptide-based targeting vectors as carriers for radionuclides are in the focus of finding and developing new radiolabeled compounds for molecular imaging purposes. Since distinct peptide receptors are strongly overexpressed in many tumor cells, they represent attractive targets for radionuclide based diagnosis and therapy in oncology.(*68-74*) Most peptide radiopharmaceuticals, which are either used in clinical studies or currently under preclinical evaluation, are structurally derived from naturally occurring peptide ligands. These have intrinsically evolved to be highly active ligands, but also, being mostly peptide hormones, to be rapidly degraded in vivo.(*69*) For the applicability of a radiolabeled peptide probe for in vivo imaging, however, high metabolic stability, suitable pharmacokinetics (e.g. fast clearance from the blood pool, low binding to plasma proteins or non-target tissues, fast renal excretion) and high receptor affinity are crucial. Even if all these issues have been carefully addressed and an "optimized" small and metabolically stable peptide sequence with high affinity towards the target receptor is available, introduction of the radiolabel may represent a serious challenge on both receptor affinity and in vivo pharmacokinetics, depending on the radionuclide and labeling method chosen. For example, the use of radiometals requires the functionalization of the biomolecule with an usually bulky chelator for radiometal complexation. Even if this modification is well tolerated in a given position of the peptide sequence and does not seriously

challenge receptor affinity, it may still have substantial impact on the overall pharmacokinetics of the peptide radiopharmaceutical. This problem has been repeatedly observed for ^{99m}Tc-labeled peptides, and recent research has therefore been focused on the development of suitable bifunctional chelators (BFC) allowing ^{99m}Tc-labeling with high efficiency, leading to complexes with high stability. The influence of the type of chelator on labeling efficiencies and complex stabilities has recently been reviewed comprehensively several times.(*75-79*) However, in some cases, coordination chemistry and physicochemical characteristics such as lipophilicity of the complexes were not optimally compatible with the requirements for *in vivo* imaging applications.

1.4.1 Peptide synthesis

Chemical synthesis is one way for the production of peptides, by which unnatural amino acids can be incorporated and obtain larger peptides of the desired sequence.(*80*) There are two strategies for the chemical peptide synthesis: solution-phase and solid-phase peptide synthesis (SPPS) (Figure 1.6). Classical solution synthesis of peptides has been only used for the synthesis of small peptides due to the requirement of purification or work-up after each step. Bruce Merrifield developed in 1963 a method for peptide synthesis, based on reaction on a solid phase, for which he was awarded the Nobel Prize in Chemistry 1984.(*81*) The development of solid phase peptide synthesis was a major breakthrough allowing for the chemical synthesis of large complex peptides.

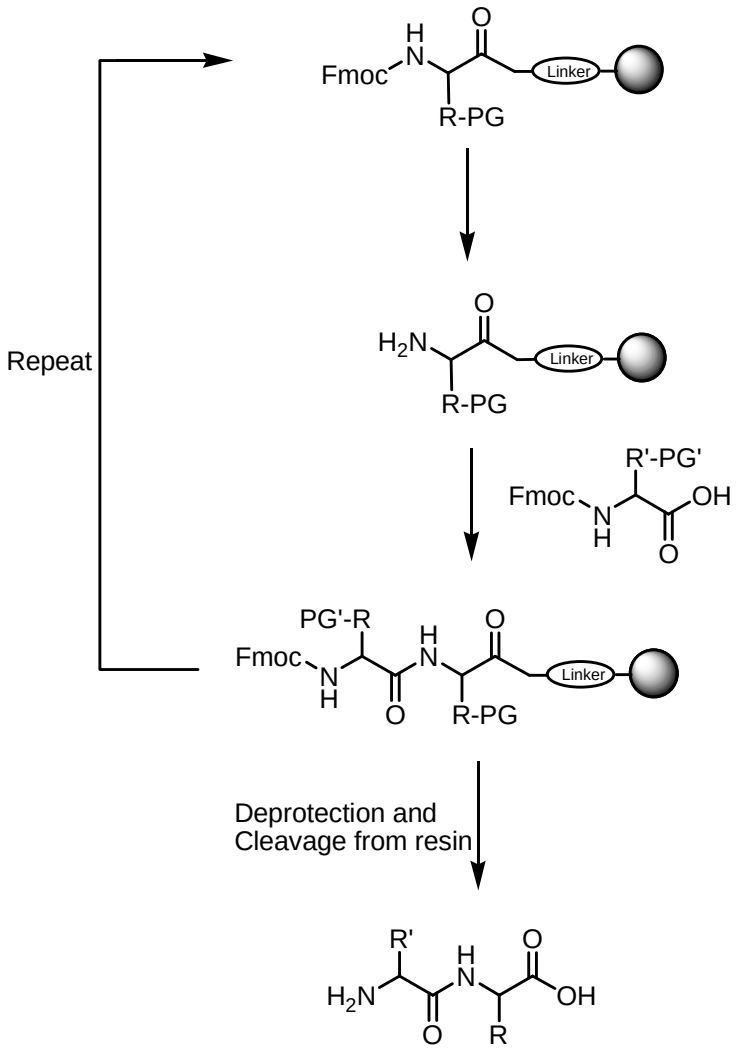

Figure 1.6 Solid Phase Peptide Synthesis using Fmoc methodology

Two major chemistries used for SPPS are Fmoc (base labile protecting group) and Boc (acid labile protecting group).(*82*) Unlike ribosome protein synthesis, SPPS is traditionally carried out in a C-terminal to N-terminal direction. The N-termini of amino acid monomers are protected by either of these two groups and introduced into a deprotected amino acid chain. Fmoc chemistry is known for peptide synthesis of avoidance of hydrofluoric acid and good yield compared with Boc chemistry and it is therefore used for most routine synthesis. In general, Solid phase peptide synthesis consists of three steps: 1) assembly of a protected peptide chain on a polymeric support 2) cleavage and deprotection of the resin-bound, fully protected peptide chain 3) chromatographic purification of the crude peptide. The selectivity of amino

protecting group for each amino acid monomer is the key point for the effectiveness of the peptide assembly process. Most widely used amino protecting groups for peptide synthesis have centered around three groups: Carboxybenzyl (abbreviated as Cbz or Z), removed by catalytic hydrogenation; tert-butoxycarbonyl (abbreviated as Boc or t-Boc), removed by mild acidolysis; and 9-fluorenylmethoxycarbonyl (abbreviated as Fmoc), removed by secondary amines. These groups are orthogonal to each other that the Boc group is stable to secondary amines and catalytic hydrogenation, the Fmoc group is stable to acidolysis, and the Cbz group is stable to secondary amines and mild acidolysis. Each of these protecting groups has found its place in SPPS.

1.4.2 Bombesin peptide analogues

Bombesin is a 14-amino acid peptide (pGlu1-Gln2-Arg3-Leu4-Gly5-Asn6-Gln7-Trp8-Ala9-Val10-Gly11-His12-Leu13-Met14-NH_2) (Figure 1.7), originally isolated from the skin of the oriental fire-bellied toad (Bombina orientalis). It shows high affinity and specificity for GRP (gastrin-releasing peptide) receptors, which is overexpressed on a variety of human cancer cells, like prostate, breast, lung, and pancreatic cancers.(*83*) To date, Four BN/GRP receptor subtypes have been characterized: the GRP preferring subtype (BRS-1), the neuromedin B preferring subtype (BRS-2) and the bombesin receptor subtype 3 (BRS-3) and the receptor subtype 4 (BRS-4). High expression of BBN/GRP receptors on a variety of human tumours provides an attractive target for molecular imaging and internal radiotherapy.
It has been show that 7-14 amino acid sequence of BBN with amidated C-terminus (Gln7-Trp8-Ala9-Val10-Gly11-His12-Leu13-Met14-NH_2) is critical for receptor binding affinity and biological activity.(*84*) Most reported BBN analogues therefore are based on 7-14 amino acid sequence, coupled with a chelator through a spacer group at the N-terminus of the peptide.(*84, 85*) As ^{99m}Tc is most commonly used radionuclide for diagnostic Nuclear Medicine, much attention has been focused on developing ^{99m}Tc-labeled BBN analogues with different types of chelators, such as

SN_3(triamidethiol), N_4 (tetraamine), P_2S_2(dithiadiphospine). In this work, we mainly focused on the small tripod chelators based on N_2O and NO_2 ligands due to their favourable properties as discussed in section 1.3.

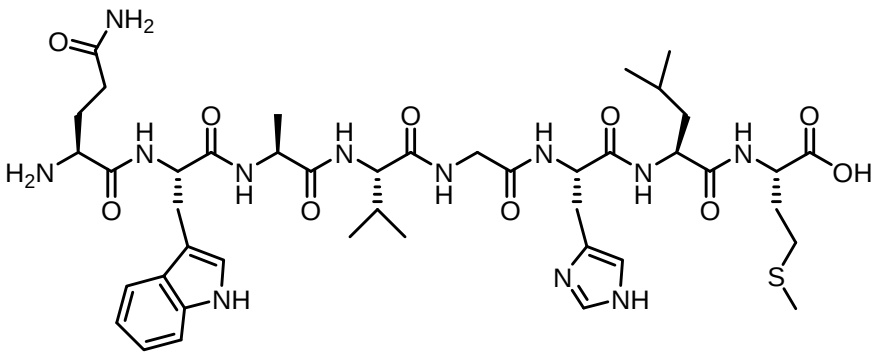

Figure 1.7 Structure of BBN (7-14)

Volkert et al. described the synthesis and the radiolabeling of P_2S_2 (dithiadiphosphine) -based BBN analogue. The ^{99m}Tc-P_2S_2-BBN (7-14) conjugate in vivo exhibited a favourable biodistribution profile after injection in normal mice. The radiopeptide was rapidly cleared from the blood and non-target tissues and more importantly, significant uptake of radioactivity was observed in the pancreas where acini cells express GRP receptors.(*86*)

Wiele et al. reported a ^{99m}Tc-labeled BBN (7-14) analogue based on SN_3 chelator (^{99m}Tc-RP-527). *In vitro* evaluation showed that this compound was rapidly and specifically bound and internalised by both PC-3 and CF-PAC-1 cells. In SCID mice with tumour xenografts study, the radiopeptide accumulated in tumour resulting in high tumour-to-muscle ratios. The preliminary clinical studies indicate that ^{99m}Tc-RP527 is a pharmacologically safe radioligand and the low brain, lung, and myocardial uptake and rapid hepatobiliary excretion of ^{99m}Tc-RP527 resulted in excellent imaging conditions for the supradiaphragmatic region.(*87*, *88*)

Maina and co-workers reported the synthesis of tetraamine (N_4) bombesin analogue, which is derived from the potent bombesin antagonist, wherein a tetraamine chelating unit was covalently attached to D-Phe residue through a benzylaminodiglycolic acid spacer. Preclinical study showed that the ^{99m}Tc-labeled BBN analogue exhibited high

affinity for the GRP-R and high specific uptake in PC-3 xenografts and pancreas in mice.(*89*)

1.4.3 RGD cyclic peptide

Integrins are heterodimeric transmembrane receptors containing the α (alpha) and β (beta) subunits that mediate the attachment between a cell and its surroundings. In mammals, eighteen α and eight β subunits have been characterized and the different combinations of them generate 24 unique integrins, although the number varies according to different studies.(*90, 91*)

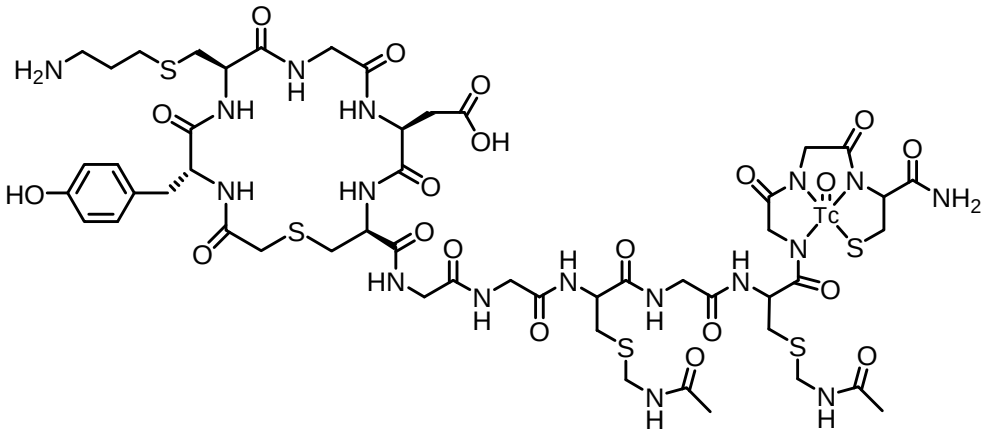

Figure 1.8 ^{99m}Tc-apcitide approved by FDA

The most studied $\alpha_{IIb}\beta_3$ or $\alpha_v\beta_3$ integrin-binding motif is the sequence arginine-glycine-aspartic acid (RGD), which is present in many extracellular matrix proteins and intracellular proteins. $\alpha_{IIb}\beta_3$ integrin-receptor is expressed only on activated platelets and many synthetic peptides targeting this integrin have been successfully radiolabeled with ^{99m}Tc. A successful example of such radio-imaging agent is ^{99m}Tc-apticide (AcuTect ® P280, Diatide, Nycomed Amersham) (Figure 1.8), which was the first RGD-mimicking peptide studied in humans.(*92, 93*) It is approved by the Food and Drug Administration and can be used for the detection of acute venous thrombosis.

The integrin receptor $\alpha_v\beta_3$ is highly expressed on tumor cells, endothelial cells and

stromal cells. It is involved in angiogenesis, osteoclast-mediated bone resorption and tumor metastasis and is being investigated intensively. Linear as well as cyclic RGD peptides targeting the αvβ3 integrin have been studied for many years. Cyclic pentapeptides such as cyclo(RGDfV), cyclo(RGDfE), c(RGDfK) and c(RGDyK), showed high binding affinity for integrin αvβ3. Among these peptides, the most commonly used for the delivery of diagnostic and therapeutic agents are c(RGDfK) and c(RGDyK), on which the ε-amino group of the L-Lysine is an ideal site for further modification. Thus, these RGD containing peptides are very useful tool for the targeting of imaging agents to $\alpha_v\beta_3$-integring expressing tumor vasculature.

Decristoforoa et al. reported the biological evaluation of [^{99m}Tc] labeled [c(RGDyK(HYNIC))].(*94*) The derivatization of c(RGDyK) with HYNIC at the ε-amino group of the Lysine gave the HYNIC RGD, which was radiolabeled using tricine, tricine–nicotinic acid (NA) or EDDA as coligands. Among these ^{99m}Tc-peptide conjugates, [^{99m}Tc]EDDA/HYNIC-RGD shows most favorable properties to target $\alpha_v\beta_3$ receptors with high stability *in vivo*. Thus, this RGD analogue was considered as a good candidate for imaging $\alpha_v\beta_3$ integrin receptor expression in tumors.

Smith and co-workers described the design and synthesis of a new cyclic RGD analogue [c(RGDyK(PZ))] (PZ =3,5-Me_2-pz$(CH_2)_2$N$((CH_2)_3$COOH)-$(CH_2)_2NH_2$) that can be radiolabeled with the metal precursor $[^{99m}Tc(CO)_3(H_2O)_3]^+$.(*95*) *In vivo* study showed a specific accumulation of radiolabeled peptide on $\alpha_v\beta_3$ receptor-positive melanoma cancer cells suggesting the potential utility of this new cyclic RGD derivative to image angiogenesis and tumor formation.

1.5 Conclusion

The design and synthesis of radiolabeled-biomolecule conjugates for receptor targeting is playing an increasingly important role in development of radiopharmaceuticals. Bifunctional chelator (BFC) approach is mainly used to design target specific radiopharmaceutical. In this approach, a suitable bifunctional chelate

was used to form a stable conjugate with the biomolecule and at the same time hold the radionuclide tightly. In the design of radiopharmaceuticals for the molecular imaging and targeted radiotherapy of disease, many important issues have to be considered including radioisotopes, bifunctional chelating agents, and targeting molecules. In this thesis, we chose to use ^{99m}Tc as the radionuclide, small tripod ligands as the chelating agents, and glucose and peptides as the targeting biomolecules. These units were assembled to build up the final radiopharmaceutical by using BFC approach.

2 Aims and Objectives

Although we have made huge progress in medicine, cancer remains the most feared disease, with more than 10 million new cases every year. Current radiopharmaceuticals for cancer imaging and treatment also detect and kill healthy cells and cause toxicity to the patient. It would therefore be desirable to develop more target-specific agents for molecular imaging and radiation therapy of tumours.

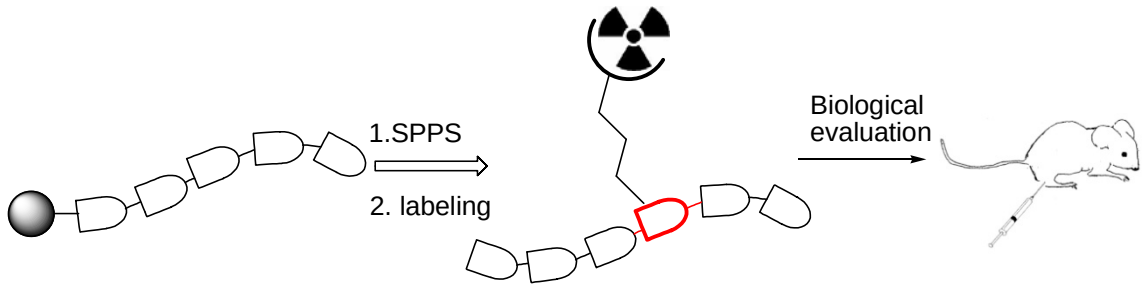

Figure 2.1 Design of peptide based radiopharmaceuticals for targeted tumor diagnosis

As discussed in section 1.3 and 1.4, Receptor-binding peptides and Glut1-mediated glucose are a class of useful biomolecules for the development of such tumor-specific radiopharmaceuticals. Hence, the design and evaluation of radiolabeled biomolecules for early diagnosis or systemic radiotherapy of tumors is very meaningful in nuclear medical research. In previous work in our group, it has already been shown that 1, 2-diamino-propionic acid (Dap) is a very strong tripod chelator for $[^{99m}Tc(H_2O)_3(CO)_3]^+$ core, providing very small and hydrophilic complexes. The main goal of this PhD thesis is the design, synthesis and biological evaluation of metal tripod chelate-containing biomolecule conjugates. Towards this goal, cyclic as well as linear peptide and glucose were selected to be modified with different small tripod ligands and their analogues.

For the synthesis of peptide conjugates, the objective was to incorporate the bifunctional chelates into the peptide sequence such as BBN analogues, RGD cyclic

peptides (Figure 2.2). The resulting peptides were then labeled with organometallic tricarbonyl precursor[^{99m}Tc$(H_2O)_3(CO)_3]^+$, yielding very hydrophilic metal-peptide conjugates, which were then finally evaluated *in vitro* and *in vivo* as potential peptide radiopharmaceuticals (Figure 2.1).

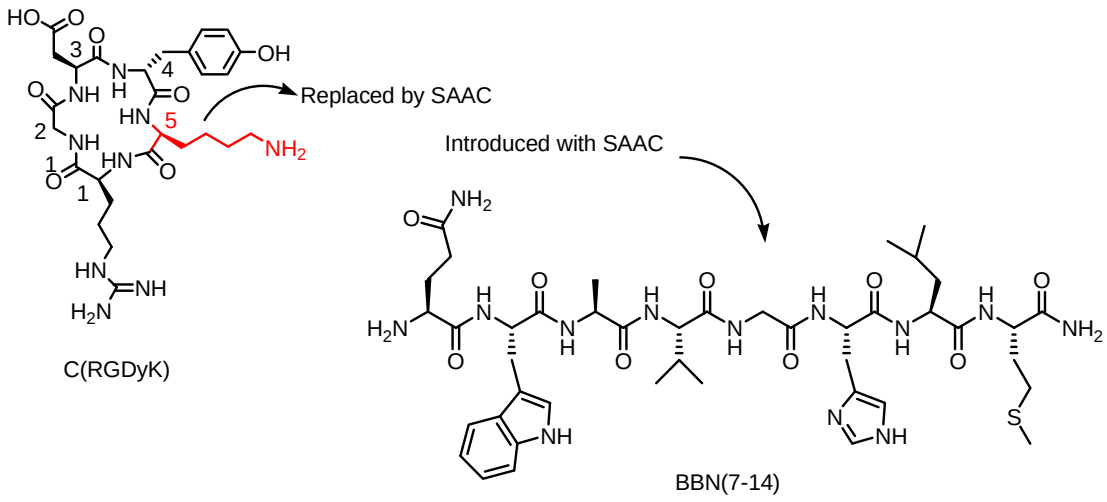

Figure 2.2 Synthetic strategies for bifunctional chelate-peptide conjugates

Carbohydrates are a class of interesting building blocks due to their involvement in various biological systems. PET Imaging of glucose metabolism has gained considerable interest in recent years.(*96-100*) 2-[^{18}F]-fluoro-2-deoxy-D-glucose ([^{18}F]-FDG) is the most successful and widely used imaging agent in PET in clinical routine so far. Since 18F has some disadvantages, especially cost and half life time, there has been growing interest in the design of ^{99m}Tc labeled glucose derivatives as surrogates of [^{18}F]-2-fluoro-desoxy glucose ([^{18}F]-FDG). We therefore designed for this PhD project a number of new glucose derivatives. Such derivatives are functionalized at position C1, C2, C3, C6 via a PEG spacer with the Dap chelator (Figure 2.3). Our approach involved i) radioactive labeling of these promising candidates at low concentration (10^{-5}M) and ii) testing of ^{99m}Tc complexes for cell internalization and transport via Glut1.

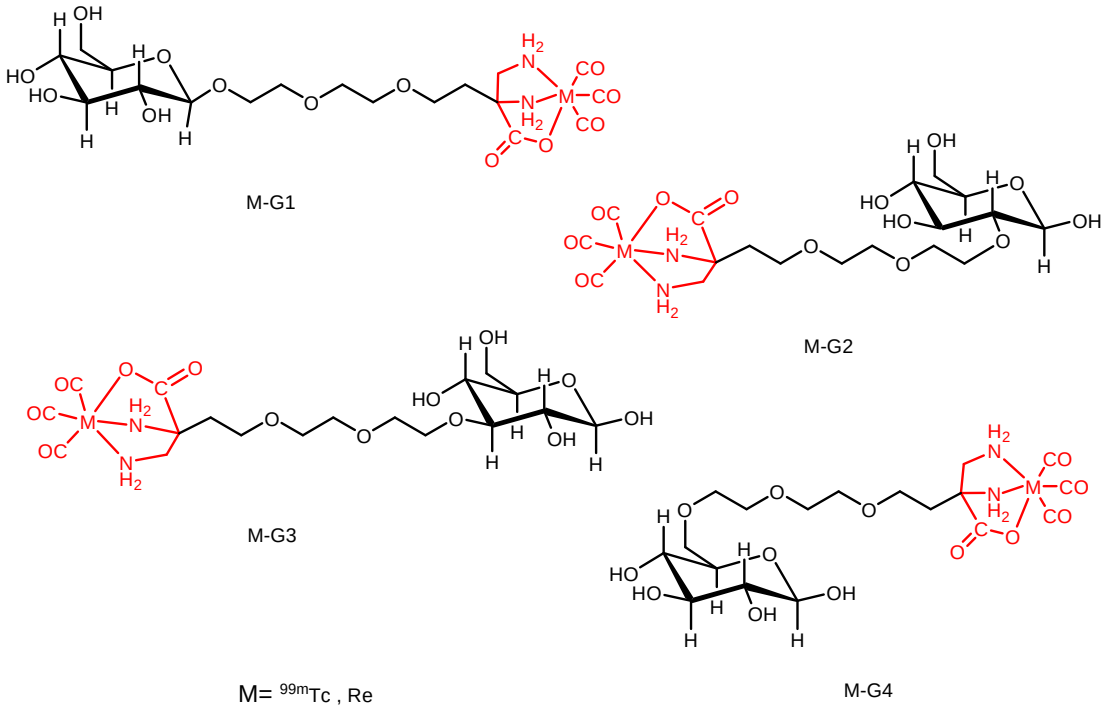

Figure 2.3 Structures of glucose derivatives functionalized at different positions

3 Synthesis of N_2O, NO_2, and N_3 bifunctional chelate ligands containing PEG spacers

3.2 Results and discussion

PEG is the abbreviation for polyethylene glycol. Conjugation of a biomolecule with poly (ethylene glycol) polymers is designed to improve the pharmacological properties of a drug molecule. It enhances aqueous solubilities and give minimal loss of biological activity. To couple PEG to a biomolecule, the modification of PEG molecule with different functional group at one or both termini is necessary. In this work, we choose triethylene glycol as the spacer, which one end was attached to the small tripod chelate and the other end was a biomolecule.

3.1.1 α-amination of ethyl or methyl cyanoacetate

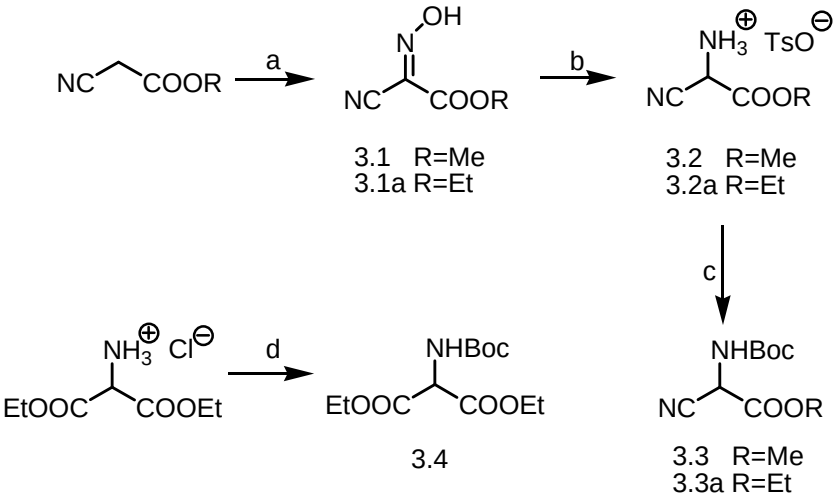

Scheme 3.1 Synthesis of cyanoacetate derivatives; (a) AcOH, $NaNO_2/H_2O$ (b) i) $Na_2S_2O_4$, $NaHCO_3/H_2O$ ii) TsOH, EtOH/Ether (c) Boc_2O, Toluene (d) Boc_2O, CH_2Cl_2/H_2O

The total synthesis of small tripod ligands ethyl or methyl 2-(tert-butoxy

carbonylamino)-2-cyanoacetate is shown in Scheme 3.1. The nitrosylation of ethyl or methyl acetate using sodium nitrite in aqueous acetic acid afford oxime 3.1. Sodium dithionite reduction of 3.1 followed by treatment with *p*-toluenesulfonic acid gives the tosylate of ethyl or methyl aminocyanoacetate 3.2. The final Boc protection of 3.2 afforded the desired compound 3.3 in 20% overall yield for the three steps. The commercial available aminomalonate hydrochloride was protected as its *N*-Boc derivative 3.4 in 88% yield (Scheme 3.1). The ^{1}H spectra of 3.4 agreed well with literature data.(*101*)

3.1.2 Synthesis of triethylene glycol derivatives

For conjugation to other molecules, we synthesized mesylate 3.6 and iodide 3.7 (Scheme 2). Benzyl protected alcohol 3.5 was synthesized from triethylene glycol; the free hydroxyl group was then mesylated to afford compound 3.6 in 90% yield. The formation of 3.6 was confirmed by ^{1}H NMR spectroscopy, with the presence of a singlet at about 3.00 ppm (integrating as three proton in total) corresponding to the proton of the methyl group.The displacement of mesylate group with sodium iodide gave pure compound 3.7 (90% yield). Iodide and mesylate are both good leaving groups in nucleophilic substitution reactions that facilitate the attachment of binding site to one end of PEG linker.

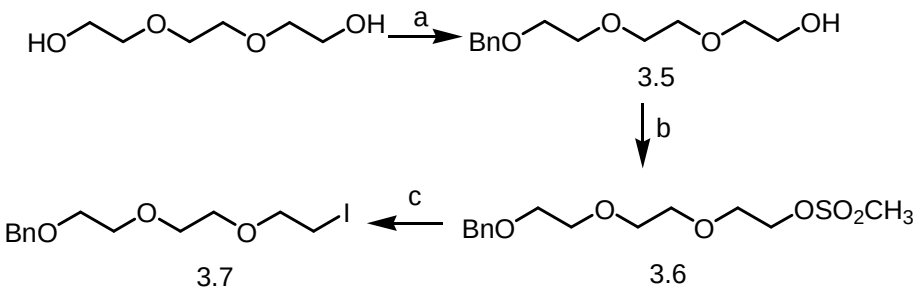

Scheme 3.2 Synthesis of mesylate 3.6 and iodide 3.7; (a) BnBr, K_2CO_3, acetone (b) $MeSO_2Cl$, Et_3N, CH_2Cl_2 (c) NaI, 2-butanone

3.1.3 Synthesis of protected N_2O bifunctional chelate ligands

Bifunctional chelate ligand 3.11 and 3.13: The synthesis of protected N_2O bifunctional chelate ligands 3.11 and 3.13 starting from mesylate 3.6 was shown in scheme 3.3. In a first step, the deprotonation of methyl 2-(tert-butoxycarbonylamino)-2-cyanoacetate with sodium methylate (freshly prepared by dissolving sodium in MeOH) gave the corresponding sodium salt, which was then treated with mesylate 3.6 in DMSO at 70° to afford 3.8 in excellent yield. We found that nucleophilic displacement of mesylate by the sodium salt in THF was difficult but proceed in good yield when carried out in DMSO.(*102*) Reduction of nitrile 3.8 employing catalytic quantities of nickel (II) chloride with excess sodium borohydride gave Boc protected amine 3.9. The removal of benzyl group using catalytic hydrogenation gave the desired alcohol 3.10, which was then converted to bromide 3.11 by triphenylphosphine and CBr_4 in THF.

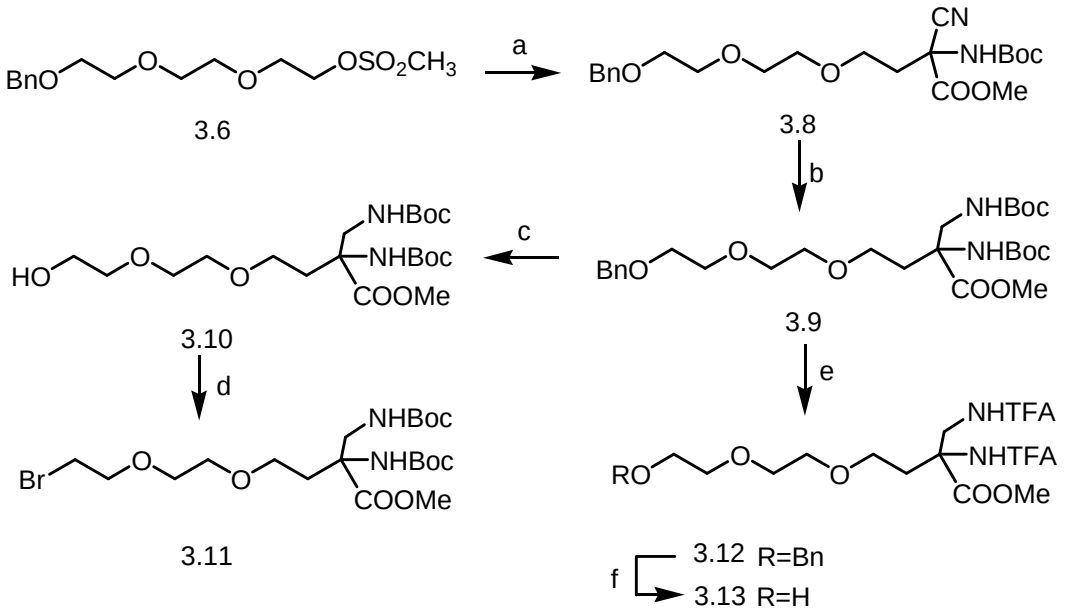

Scheme 3.3 Synthesis of fully protected N_2O bifunctional chelate ligand 3.11 and 3.13; (a) **3.3,** NaOMe, DMF (b) $NaBH_4$, Boc_2O, MeOH (c) Pd/C, EtOH (d) Ph_3P, CBr_4,THF (e) i) TFA/DCM ii) Tfa_2O, Et_3N (f) Pd/C, MeOH

Both Boc protecting groups of 3.9 were replaced with base labile group trifluoroacetyl

(TFA) followed by removing of benzyl group to produce alcohol 3.13 in 63% overall yield after two steps. The successful formation of 3.12 was confirmed by ^{1}H NMR spectroscopy in $CDCl_3$, with two broad singlets at 8.63 and 7.56 ppm corresponding to the NH hydrogen.

Bifunctional chelate ligand 3.18: The ligand 3.18 was synthesized from methyl ester 3.9, as summarized in scheme 3.4. Direct reduction of 3.9 gave alcohol 3.14 by using $LiBH_4$ in THF in 70% yield. The protection of hydroxyl group in the compound 3.14 was accomplished with TBSCl in the presence of imidazole, followed by removal of the benzyl protecting group by hydrogenolysis, furnishing the desired alcohol 3.16. Formation of the product 3.15 was confirmed by ^{1}H NMR spectroscopy, with two singlets at 0.86 and 0.03 ppm corresponding to the methyl protons of the TBS group. Mesylation of the OH of 3.16 with methanesulfonyl chloride in the presence of TEA and followed by an SN_2 substitution using NaN_3 in DMF, led to the desired azide 3.17 in 79% yield. Finally, reduction of the azide group in 3.17, accomplished by catalytic hydrogenation, resulted in the formation of the desired bifunctional chelate ligand 3.18 in 80% yield.

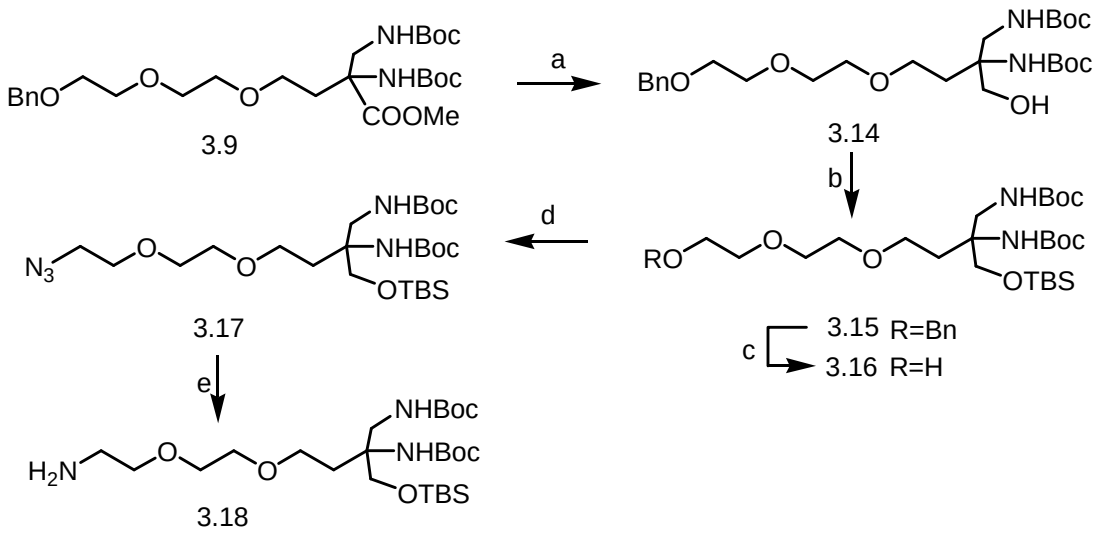

Scheme 3.4 Synthesis of fully protected N_2O bifunctional chelate ligand 3.18; (a) $LiBH_4$, THF (b)TBSCl, imidazole, DMF (c) Pd/C, MeOH (d) i) MsCl, CH_2Cl_2, Et_3N ii)NaN_3, DMF (e) Pd/C, EtOH

We initially tried to use triphenylphosphine (Staudinger reduction) to reduce the azido group, but it proved difficult to separate the reaction mixture. Thus, we tried to reduce the azide 3.17 via catalytic hydrogenation over 10% palladium on carbon under 2 bar. hydrogen at room temperature, a general method for the reduction of azides, but the yield of the target amine 3.18 was only 30% due to the formation of secondary amine (Scheme 3.5).(*103*) When the reaction was conducted at 0° C over 10% palladium on carbon at an initial hydrogen pressure of 2 bar, the yield of 3.18 increased to 80% and the production of secondary amine was negligible.

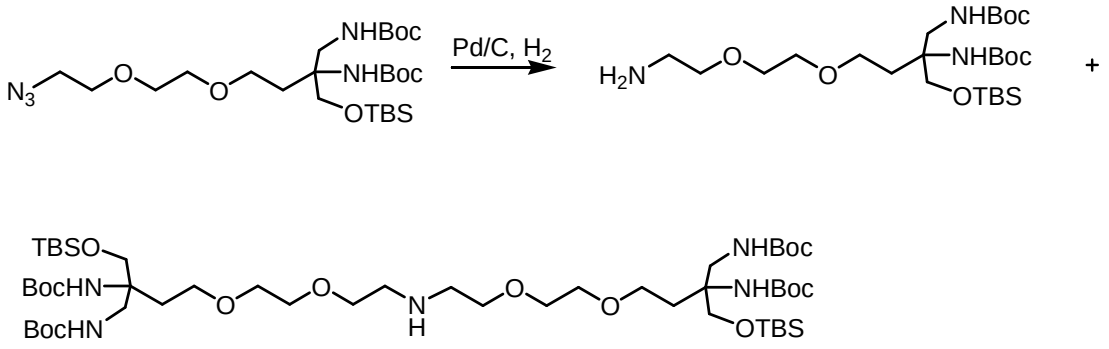

Scheme 3.5 The dimerization of azide 3.17 by catalytic hydrogenation

3.1.4 Synthesis of protected NO_2 and N_3 bifunctional chelate ligands

Bifunctional chelate ligand 3.22 and 3.27: The preparation of ligand 3.22 and 3.27 are summarized in Scheme 3.6. Nucleophilic displacement of the mesylate 3.6 by using the sodium salt of diethyl 2-(tert-butoxycarbonyl)malonate in DMSO had only marginal success. Instead, iodide 3.7 was used for the nucleophilic displacement by the sodium salt of diethyl 2-(tert-butoxycarbonyl)malonate in dry THF, furnishing diester 3.19 in excellent yield (90%). The removal of benzyl protection group in the diester 3.19 provided alcohol 3.20, which was then converted to amine 23 using procedures analogous to those described for 3.18. Removal of Boc protecting groups in diester 3.19, followed by reaction with aq NH_3 in MeOH, furnished amide 3.23 in 76% yield.

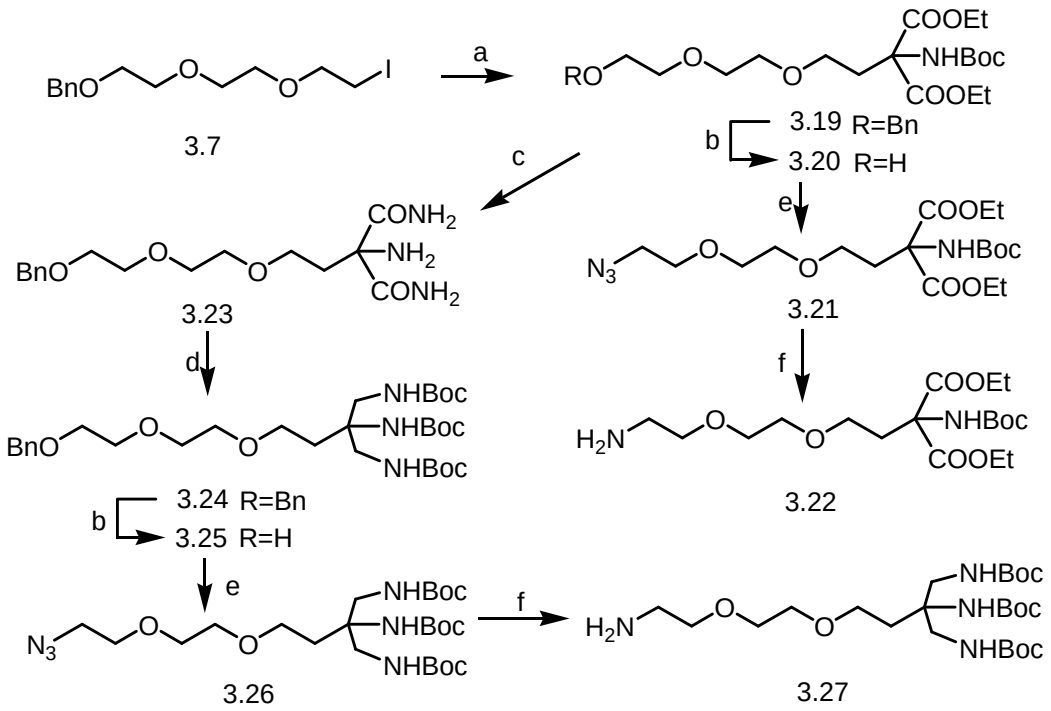

Scheme 3.6 Synthesis of fully protected N_2O bifunctional chelate ligand 3.22 and 3.27; (a) **3.4**, NaH, THF (b) Pd/C, MeOH (c) i) TFA/CH_2Cl_2 ii) aq NH_3, MeOH (d)i) $LiAlH_4$, THF ii) Boc_2O, dioxane, $NaHCO_3$ (e) i) MsCl, CH_2Cl_2, Et_3N ii) NaN_3, DMF (f) Pd/C, EtOH

The ^1H NMR spectrum of 3.23 exhibited additional broad singlets corresponding to the amino group. Two singlets at 7.83 and 6.43 ppm with an integration of 2H for each were assigned to the amide groups and one singlet at 2.57 ppm to the terminal NH_2 group. Reduction of 3.23 using $LiAlH_4$ in THF followed by Boc protection afforded target compound 3.24. The desired alcohol 3.25 was then obtained by catalytic hydrogenation. Conversion of the alcohol 3.25 to the amine 3.27 was accomplished by employing conditions similar to those used for the preparation of 3.18 in Scheme 3.4.

Bifunctional chelate ligand 3.31: The ligand 3.31 was prepared using the protocol as outlined in Scheme 3.7. Selective hydrolysis of the diester 3.19 by LiOH in THF/Water gave the carboxylic acid, which was converted to the HOBt ester with BOP reagent and DIPEA (Caution: highly carcinogenic HMPA formed).The active ester was then reacted with $NaBH_4$ to give the alcohol 3.28 (54% yield), followed by

the protection of the hydroxyl group with TBS to produce 3.29 in 87% yield.

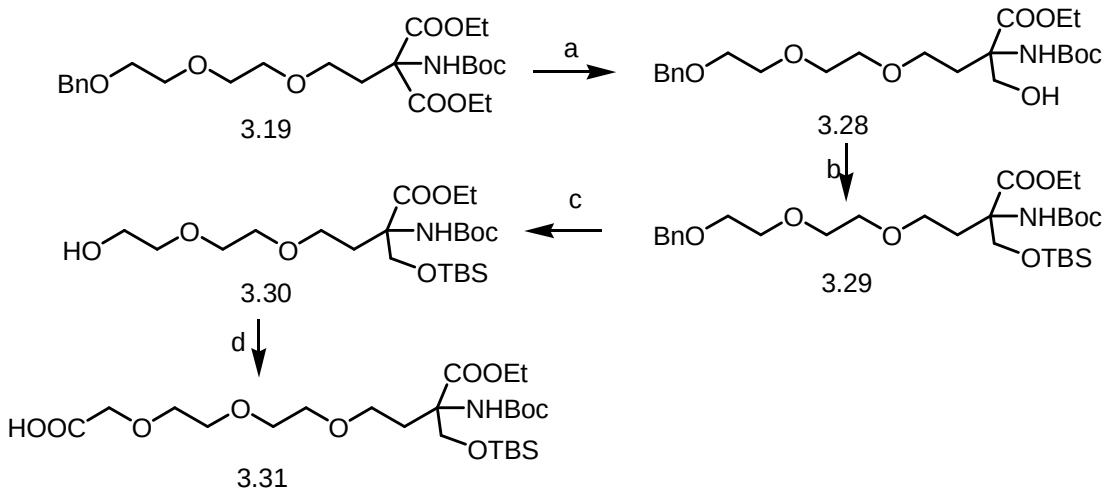

Scheme 3.7 Synthesis of protected N_2O bifunctional chelate ligand 3.31; (a) i) LiOH, H_2O THF ii)BOP, $NaBH_4$, THF(b) TBSCl, imidazole, DMF (c) Pd/C, MeOH (d) sodium iodoacetate, NaH/DMF

^{1}H NMR spectroscopy of 3.29 showed the signals of to the protection groups, two singlets at 0.81 and 0.03 ppm due to the methyl protons of the TBS group, a triplet at 1.23 ppm with an integration of 3H for the methyl protons of the ester group, a singlet at 1.39 ppm with an integration of 9H for the methyl protons of the Boc group. The alkylation of alcohol 3.30 with sodium iodoacetate provide the carboxylic acid 3.31 (77% yield).

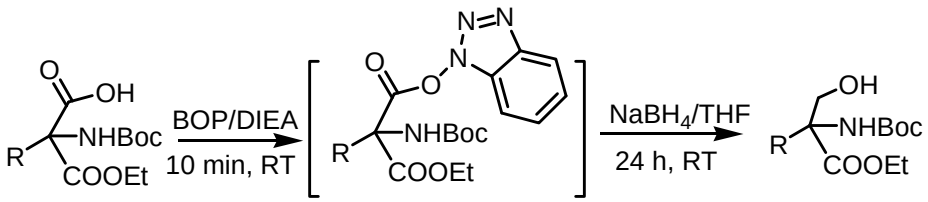

Scheme 3.8. Reduction of Carboxylic acid by BOP reagent and $NaBH_4$

Scheme 3.8 illustrates the reduction process of carboxylic acid using BOP reagent. In comparison with other reductants (eq, $LiAlH_4$, Borane) for carboxylic acids, this method can tolerate many functional groups, such as esters, nitriles, amides, halides,

azides. Therefore, this protocol offers a wide range of applications for reduction of carboxylic acids.(*104*)

3.2 Conclusion

In this chapter, synthetic strategies for bifunctional chelate ligands containing triethylene glycol spacer are described. Small tripod chelating agents with different nitrogen, oxygen donor atoms were successfully introduced to one end of triethylene glycol spacer. The other terminus contains chemical reactive functional groups, through which these newly synthesized bifunctional chelate ligands could be introduced to the biomolecules.

4 Synthesis of orthogonally protected artificial amino acid as bifunctional chelators

4.1 Results and discussion

The design of single amino acid chelates, designed from derivatized amino acids or amino acid analogues, was considered suitable for development of novel radiopharmaceuticals, since the introduction of the single amino acid chelates does not result in significant alterations of the structure and function of the biomolecules. To introduce the single amino acid chelates into the peptide by solid phase synthesis, Fmoc protected amino acid with chelating agents were designed. In our study, L-Lysine was selected for the modification, and a series of Fmoc-protected amino acids with small tripod chelators carrying acid-labile side chain protecting groups were synthesized.

4.1.1 Synthesis of L-Lysine derivatives

Starting from L-Lysine, iodide 4.6, 4.10 and mesylate 4.5, 4.9 were synthesized as shown in Scheme 4.1. In the first step, ε-amino group of Lysine was masked by formation of the benzylidene imine 4.1. Benzyloxycarbonyl was then introduced to protect the α-amino group. Hydrolytic *in situ* cleavage of the ε-imine gave N-α-benzyloxycarbonyl-L-Lysine 4.2. For the conversion of ε-amino group to a hydroxyl group, two different approaches were adopted. The first approach was to use $NaNO_2$ in acetic acid at 40° C. The amino group was converted to an acetyl protected alcohol which was then treated with Boc_2O in the presence of 4-DMAP to afford *tert*-butyl ester 4.3. After hydrolytic removal of the acetyl group, the alcohol 4.4 was treated with methanesulfonyl chloride. The resulting mesylate 4.5 was finally converted to iodide 4.6. The other approach was with sodium nitroprusside at pH 9.5. The resulting alcohol was extracted as yellow oil after removal of complex

decomposition products and used without purification in the next step.(*105, 106*) The carboxylic acid was then protected to give the benzyl ester 4.8, followed by the synthesis of iodide 4.10 which was achieved by mesylation and displacement with sodium iodide. In contrast to compound 4.9, the ^{1}H-NMR spectrum of 4.10 exhibited a triplet at 3.13 ppm, assigned to the methylene protons adjacent to iodide.

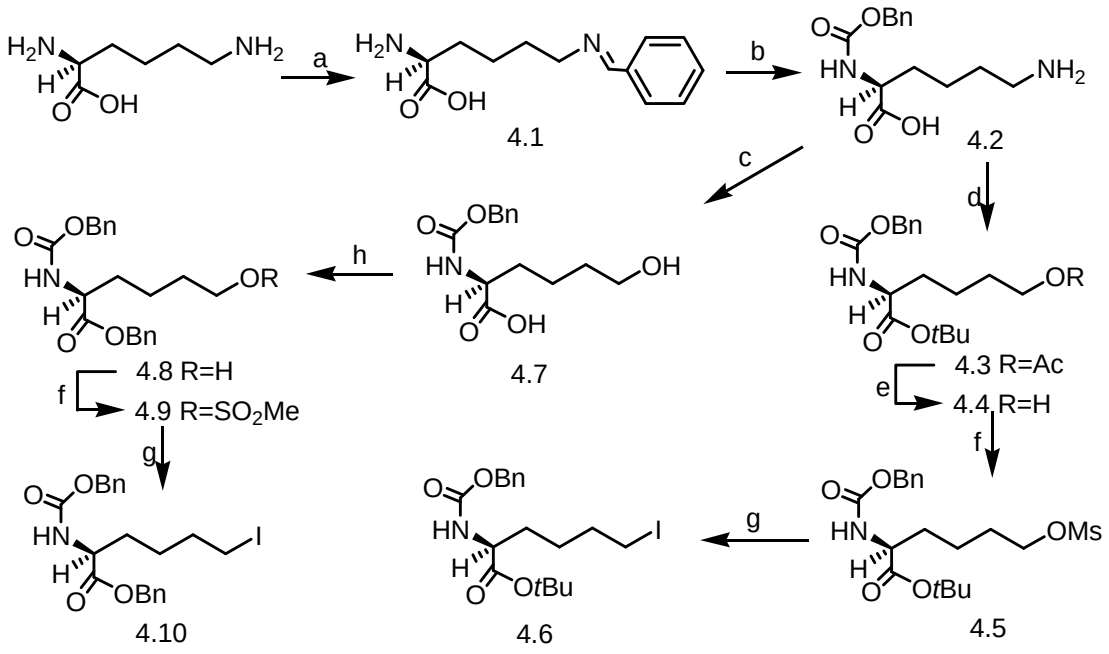

Scheme 4.1 Synthesis of L-Lysine derivatives; (a) LiOH, benzaldehyde (b) EtOH/1M NaOH, Benzyl chloroformate (c) 4M NaOH, sodium nitroprusside (d) i) HOAc, NaOAc, $NaNO_2$ ii) Boc_2O, DMAP, t-BuOH (e) K_2CO_3, MeOH/water (f) MsCl, Et_3N (g) NaI, 2-butanone (h) BnBr, TEA, Acetone.

4.1.2 Synthesis of L-Lysine based bifunctional chelators

Scheme 4.2 illustrates the synthesis of tridentate single amino acid chelates (SAAC) derived from L-Lysine. Compound 4.11, 4.16 and 4.12, 4.17 were prepared by using the same conditions as described for 3.8 and 3.9 in chapter 3. Formation of the products was confirmed by ESI-MS and NMR spectroscopy was in agreement with the presence of the tripod ligand moiety. Deprotection of the carboxybenzyl (Cbz) and benzyl (Bn) protecting group in 4.17 was accomplished by hydrogenolysis with 10%

Pd/C to furnish amino acid 4.18, which was protected as its N-Fmoc derivative 4.19 (87% yield). Hydrolysis of the methyl ester functionality of 4.12, followed by the reduction of the carboxylic acid using BOP reagent and Na[BH_4], gave the desired compound 4.13 (50% yield). Selective deprotection of the *tert*-butyl ester in the presence of N-Boc protecting group under the described conditions ($ZnBr_2/CH_2Cl_2$, $CeCl_3/CH_3CN$) failed to get the desired compound 4.14. (*107, 108*) LC-MS analysis showed that simultaneous removal of Boc and *tert*-butyl protecting group occurred in the presence of these Lewis acids. On the other hand, a two-step reaction sequence involving acid deprotection of both *tert*-butyl and Boc group followed by re-introduction of N-Boc function provided 4.14 in excellent yield (87%).

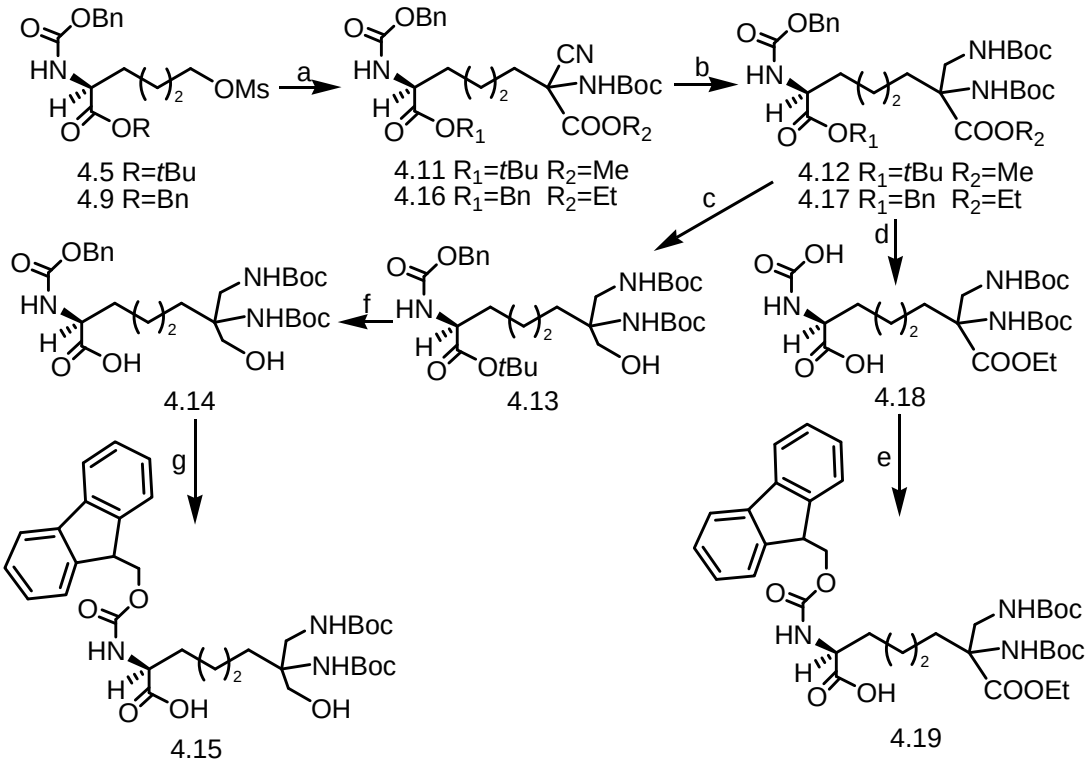

Scheme 4.2 Synthesis of orthogonally protected BFC based on L-Lysine; (a) **3.3**, NaOMe, DMF or **3.3a**, NaOEt, DMF (b) $NaBH_4$, $NiCl_2$ $6H_2O$ (c) i) LiOH,THF/H_2O ii) BOP, $NaBH_4$,THF (d) Pd/C, EtOH (e) FmocCl, $NaHCO_3$, dioxane/H_2O ii)NaN_3, DMF (f) i)TFA, CH_2Cl_2, ii) TMAH, Boc_2O, CH_3CN (g) i)Pd/C, MeOH ii) FmocOSu, acetone, DIEA

We found that the re-introduction of N-Boc group did not succeed with standard

conditions ($NaHCO_3$, Boc_2O, and H_2O/dioxane) after stirring for 24h due to the steric hindrance of one amino group. Employing another, more efficient method for N-*tert*-butoxycarbonyl protection with TMAH in acetonitrile, provided 4.14 in good yields.(*109*) After hydrogenolytic cleavage of the Cbz-protecting group and Fmoc protection using the more reactive Fmoc-OSu instead of Fmoc-Cl, 4.15 was obtained in 90% yield.

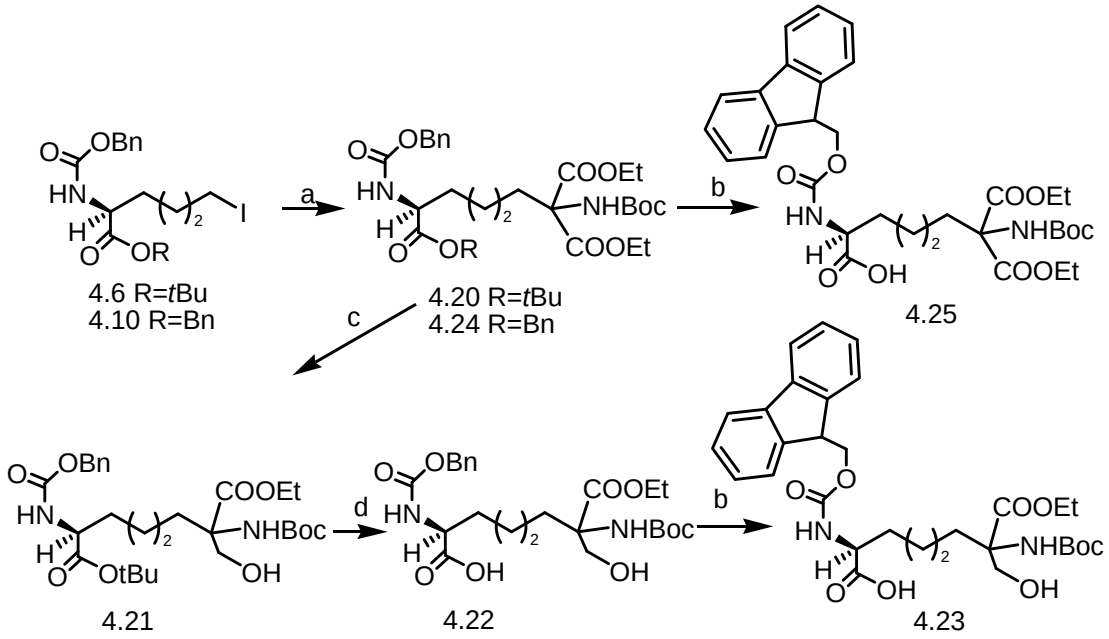

Scheme 4.3 Synthesis of orthogonally protected BFC based on L-Lysine; (a) **3.4**, NaH, THF (b) i) Pd/C, MeOH ii) FmocOSu, acetone, DIEA (c) i) LiOH, THF/H_2O ii) BOP, $NaBH_4$, THF (d) i) TFA, CH_2Cl_2 ii) TMAH, Boc_2O, CH_3CN

Bifunctional chelators 4.25 and 4.23 were synthesized as summarized in Scheme 4.3. After extensive experimentation with various bases and conditions, the nucleophilic displacement of iodide in 4.6 and 4.10 with sodium salt of diethyl 2-(*tert*-butoxycarbonyl)malonate (deprotonated by sodium hydride) in THF (refluxing overnight), afforded pure diesters 4.20 and 4.24, respectively, in yields from 85 to 95%. The ^{1}H NMR spectrum of both compounds showed signals corresponding to the N-protected amino acid; a doublet at 5.21 ppm with an integration of 1H was assigned to NH proton adjacent to Cbz protecting group and a broad singlet at 5.87 ppm to the

NH proton adjacent to Boc protecting group. The simultaneous removal of the benzyl and benzyloxycarbonyl groups in 4.24, followed by the 9-fluorenylmethoxycarbonyl (Fmoc) protection of the amino group led to the desired bifunctional chelator 4.25 in 92% yield. Conversion of 4.20 to the primary alcohol 4.21 by using similar conditions as described for 4.13, followed by the acid deprotection and re-introduction of Boc protecting group, provided carboxylic acid 4.22 (74% yield). The formation of 4.21 was confirmed by HR-MS (ESI), with a peak at m/z = 575.2939 corresponding to $[M + Na]^+$. ^1H NMR spectroscopy showed a doublet at 3.71 ppm with an integration of 1H that was assigned to one of the methylene protons adjacent to hydroxyl group. For the re-introduction of the Boc group, no reaction was observed with standard conditions ($NaHCO_3$, Boc_2O, H_2O/dioxane), probably due to steric hindrance of the amino group. Thus, we employed the same methodology (TMAH, acetonitrile, Boc_2O) as used for preparation of 4.14. Under this condition and as previously observed, the solubility of the $[N(CH_3)_4]^+$ salt proved to be crucial for the success of the reaction.(*110*) In our reaction, the precipitation of the amino acid $[N(CH_3)_4]^+$ salt dissolved rapidly in acetonitrile so that the reaction proceeded very quickly and gave good yields. Final removal of Cbz group followed by Fmoc protection provided the desired bifunctional chelator 4.23 in 78% yields.

4.1.3 Synthesis of D-Tyrosine based bifunctional chelators

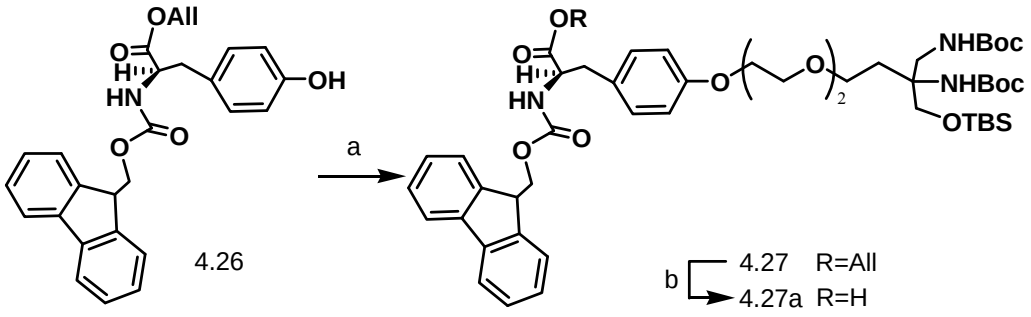

Scheme 4.4 Synthesis of orthogonally protected BFC based on D-Tyrosine; (a) DEAD, Ph_3P, toluene (b) $Pd(PPh_3)_4$, N-methylaniline, THF

The carboxylic acid 4.27a was synthesized from D-Tyrosine derived compound 4.26 (Scheme 4.4), which was prepared according to a known literature procedure.(*111*) The coupling of 4.26 with alcohol 3.16 under Mitsunobu protocol provided compound 4.27 in 50% yield. Interestingly, the reaction did not go to completion and compound 4.26 was recovered.(*112*)

4.1.4 Synthesis of L-Glutamic acid based bifunctional chelators

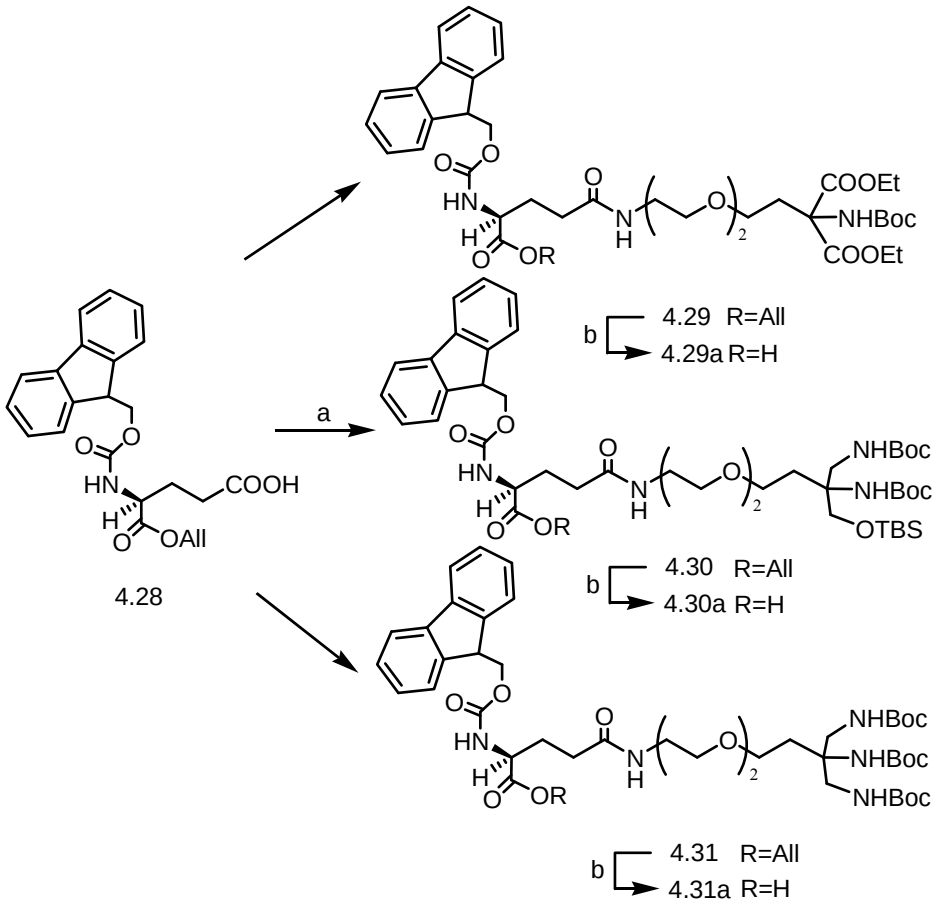

Scheme 4.5 Synthesis of orthogonally protected BFC based on L-Glutamic acid; (a) EDC, HOBt, NMM, THF (b) $(Ph_3P)_4Pd$, N-methylaniline, THF

Three L-Glutamic acid based bifunctional chelators 4.29a, 4.30a, 4.31a were prepared from the known L-Glutamic acid-derived compound 4.28, as shown in scheme 4.5. Thus, the commercially available Fmoc-L-Glutamic acid 5-*tert*-butyl ester was converted to the corresponding allyl ester and then to the carboxylic acid 4.28,

according to a published procedures.(*113*) The coupling of the carboxylic acid 4.28 with amine by EDC·HCl and HOBt in THF, followed by removal of allyl protecting group in the presence of tetrakis(triphenylphosphine)palladium(0), led to the desired building block 4.29a, 4.30a, 4.31a, respectively.

4.2 Conclusion

Multistep syntheses of single amino acid chelates (SAAC) based on L-Lysine, L-Glutamic acid and D-Tyrosine was described in this chapter. These artificial amino acids offer the possibility for conjugation to biomolecules via the carboxylic acid group without significant effect on the structure and function. Deprotection of these ligands produce very strong chelators with different donor atoms for the $[^{99m}Tc(CO_3)]^+$ moiety.

5 Synthesis and in vitro evaluation of ^{99m}Tc-Carbohydrate conjugates

5.1 Results and discussion

Glucose plays an important role in human metabolism as one of the primary molecules which serve as energy sources for plants and animals. Tracers for imaging of glucose metabolism have gained considerable interest in recent years. In this work，a small tridentate chelate was introduced to the different position of glucose via a PEG spacer. Radiolabeling of these glucose derivatives was performed and the resulting tehcnetium complexes were tested for their transport through cancer cell membranes via Glut1.

5.1.1 Synthesis of glucose derivatives

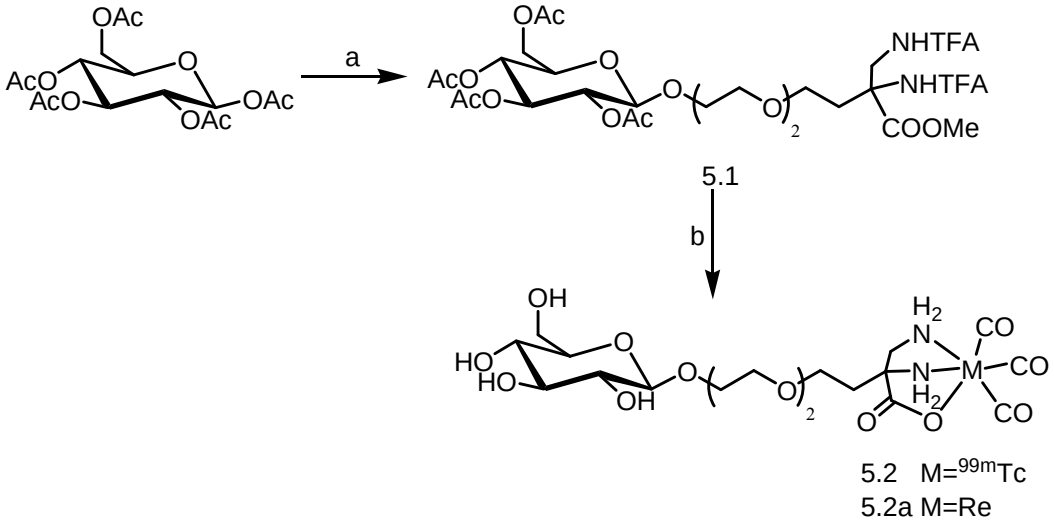

Scheme 5.1 Synthesis of a glucose analogue substituted at the C1 position; (a) **3.13**, $BF_3 \cdot Et_2O$, CH_2Cl_2 (b) i) LiOH, THF/H_2O ii) $[NEt_4]_2[Re(CO)_3Br_3]$, H_2O

Substitution at C1 position The synthesis of metal glucoconjugate 5.2 is shown in Scheme 5.1. In a first step, glycosylation of 3.13 with beta glucose pentaacetate in the presence of $BF_3{\cdot}OEt_2$ in dichloromethane afford compound 5.1 in 82% yield. Only the

beta-anomere was observed under these conditions, in agreement with literature reports.(*114, 115*) Simultaneous removal of all the protection group by LiOH in water/THF, followed by the reaction with $[^{99m}Tc(CO)_3(H_2O)_3]^+$ or $[ReBr_3(CO)_3]^{2-}$, furnished the metal complex 5.2 (^{99m}Tc-G1) and 5.2a, respectively. The successful formation of 5.2a was confirmed by ^{1}H NMR spectroscopy in D_2O. Although an unambiguous assignment of the signals is difficult, a doublet signal for C-l β proton can be clearly seen at 4.53 ppm. The synthetic strategy described here has many advantages for the preparation of glucose analogues substituted at C1 position. For instance, the starting material β-glucose-pentaacetate is easily prepared and even commercially available. The coupling of β-glucose-pentaacetate with alcohol 3.13 afforded compound 5.1 in high yields. This method is simpler and more convenient than those previously reported in view of the easiness of the synthetic method for substitution at C1 position.(*116, 117*) Moreover, the use of base labile N-protecting trifluoroacetyl group remarkably simplified the synthetic procedures and greatly enhanced the overall yield.

Substitution at C2 position: Unlike the synthesis of 5.1, the synthesis of glucose analogue 5.5 started with the protected glucofuranose instead of glucopyranose as shown in Scheme 5.2. According to the previous study, an effort to alkylate the unprotected C2 hydroxyl group of benzyl protected glucopyranose in the presence of different bases with an alkylbromide failed to give the desired products.(*118*) The most probable explanation for the synthetic problem is the steric hindrance of C2 hydroxy groups on the sugar in pyranose form with the bulky benzyl groups. However, the protected furanose ring is considered as planar, with the C2 hydroxyl group below and the protecting group above the plane. The steric hindrance was thus reduced and the alkylation became much easier.(*118*) Our synthetic approach is therefore to alkylate the hydroxyl group at C2 position of the benzyl protected glucofuranose, followed by the conversion of furanose to pyranose and complexation with Re or ^{99m}Tc.

The benzyl protected glucofuranose 5.3, with an unprotected hydroxyl group at C2 position was synthesized from 1, 2-O-isopropylidene-α-D- glucofuranose.(*119*) The

latter was protected to yield O-benzylated glucofuranose, which was then converted to 5.3 by treatment with acidic ion exchange resin in MeOH. The alkylation of 5.3 using NaH in DMF with the bromide 3.11 (56% yield), followed by the replacement of acid labile amino-protecting group Boc with acid stable TFA group, furnished derivative 5.6 (73% yield). After the reductive removal of benzyl groups, the substitution of the methoxy by an acetoxy group occurred in the presence of TMSOtf and acetic anhydride.(*118, 120*) Simultaneous removal of all the protecting groups by basic hydrolysis give the unprotected glucose derivative, which was sufficiently pure to be directly used for the synthesis of Re and ^{99m}Tc complexes (^{99m}Tc-G2). In ^{1}H NMR spectroscopy of 5.8a, two doublets were observed at 5.25 and 4.62 ppm (with a coupling constant of 3.5 Hz, 8.0 Hz, respectively) and assigned to the anomeric protons at the C-1 position.

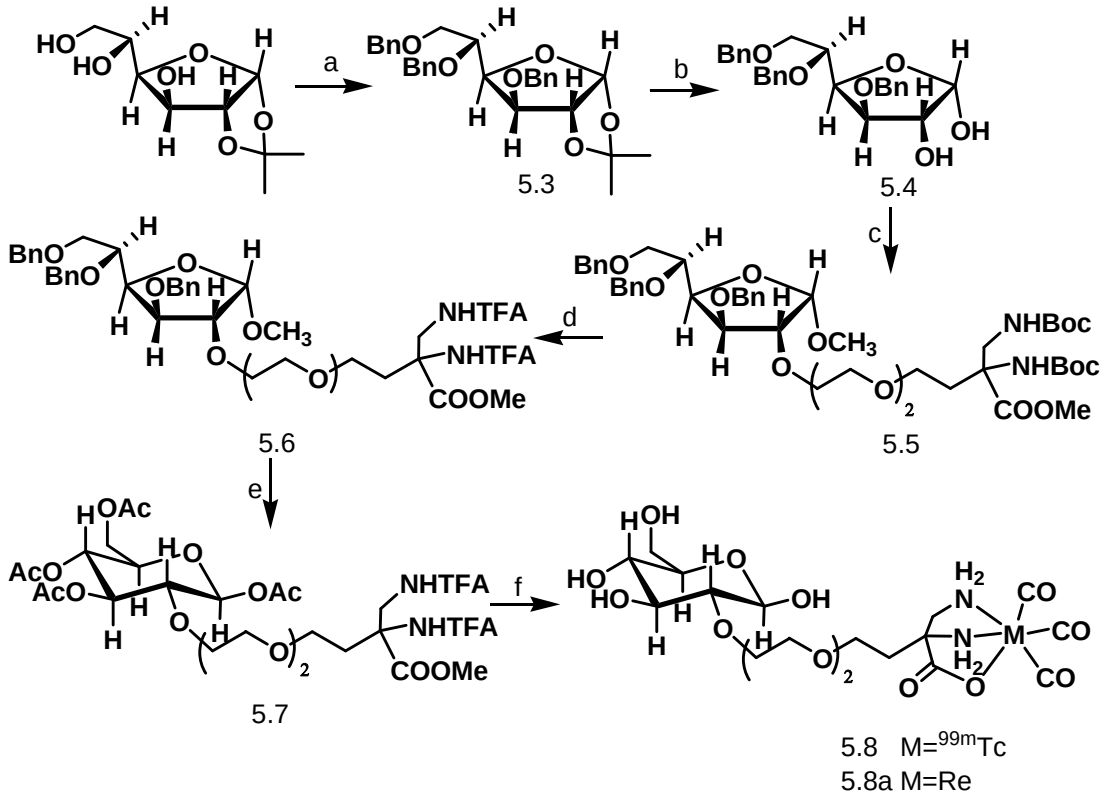

Scheme 5.2 Synthesis of glucose analogue substituted at C2 position; (a) BnBr, NaH, DMF (b) AmberliteH^+, MeOH (c) **3.11**, NaH, DMF (d) i) TFA/CH_2Cl_2 ii) Tfa_2O, Et_3N (e) i) Pd/C, MeOH ii) TMSOtf, Ac_2O (f) i) LiOH, THF/H_2O ii) $[NEt_4]_2[Re(CO)_3Br_3]$, H_2O

Substitution at C3 position: Scheme 5.3 illustrates the synthesis of glycoconjugate 5.11. Acetonation of D-glucose to 1,2:5,6-diisopropylidene-α-D-glucofuranose and the alkylation of the latter with bromide 3.11 to 5.10 have been accomplished in 70% yield. Final removal of Boc protecting group and the acetone substituent, followed by treatment with the transition metal precursor $[^{99m}Tc(OH_2)_3(CO)_3]^+$ and $[Re(OH_2)_3(CO)_3]^+$, provided the sugar-metal complex 5.11(^{99m}Tc-G3) and 5.11a, respectively. In ^{1}H NMR spectroscopy of the rhenium compex 5.11a, the signals of anomeric proton occur at 4.60 (J = 8Hz) and 5.18(J = 3Hz), respectively, due to the presence of a mixture of α- and β-anomers.

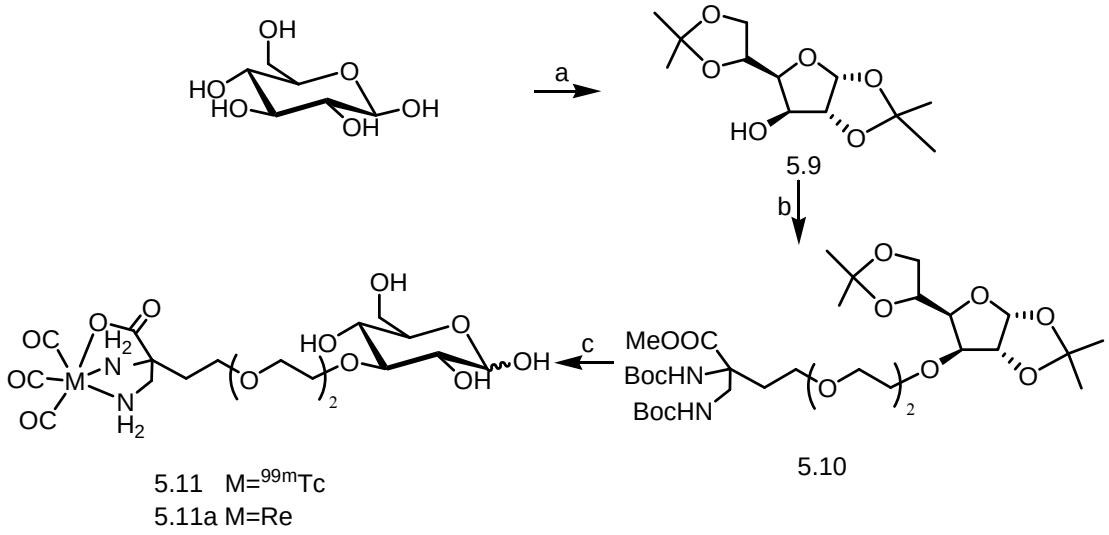

Scheme 5.3 Synthesis of glucose analogue substituted at C3 position; (a) Con H_2SO_4, acetone (b) **3.11**, NaH, DMF (c) i) CF_3COOH, H_2O ii) $(NEt_4)_2[Re(CO)_3Br_3]$, H_2O

Substitution at C6 position: The technetium and rhenium glucoconjugates 5.16, 5.16a were synthesized starting from D-glucose as shown in Scheme 5.4. Conversion of D-glucose to alcohol 5.14 began with the benzylation of all hydroxyl groups using benzyl bromide to provide 5.12 in 60% yield. Selective acetolysis of the benzyl protecting group at C-6 took place when 5.12 was treated with a mixture of HOAc-Ac_2O in the presence of $ZnCl_2$.(*121*) Deacetylation of 5.13 under "Zemplen" conditions (catalytic amount of sodium methoxide in methanol) afforded alcohol 5.14, which was subjected to an alkylation of the hydroxyl group with bromide 3.11 to give

compound 5.15 (52% yield). Acidic removal of the tert-butyloxycarbonyl group and reductive removal of the benzyl group in 5.15, followed by strong coordination to Tc(I) and Re(I) using the same condition as for preparation of 5.2, led to the desired metal glucoconjugate 5.16 (^{99m}Tc-G4) and 5.16a, respectively. Elementary analysis of 5.16a confirmed the composition. The ^{1}H NMR spectrum clearly exhibited a doublet at 4.58 ppm with a coupling constant of 8.0 Hz that was assigned to the C1β proton.

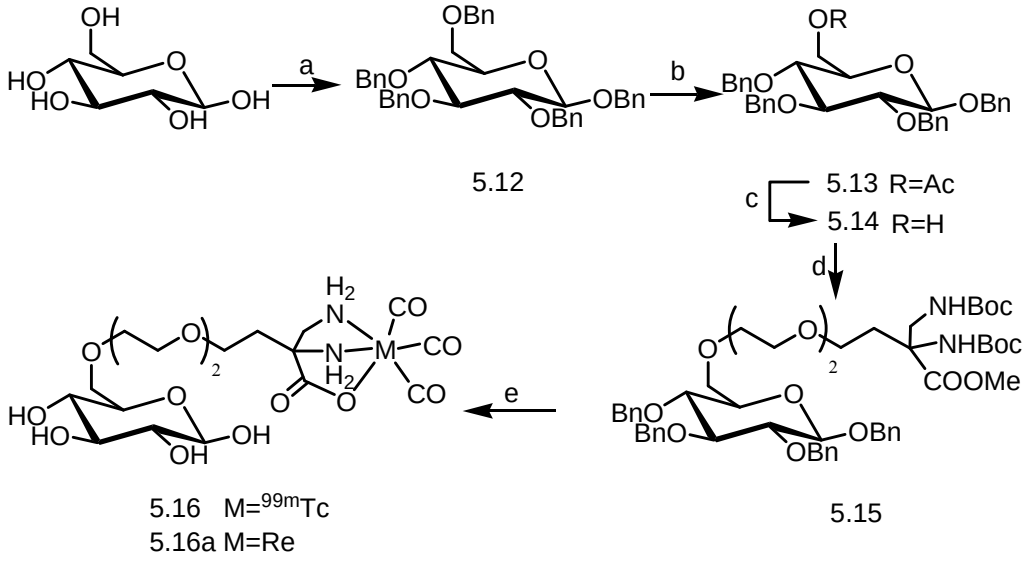

Scheme 5.4 Synthesis of glucose analogue substituted at C6 position; (a) BnBr, KOH, DMSO (b) $ZnCl_2$ HOAc-Ac_2O (c) NaOMe, MeOH (d) **3.11**, NaH, DMF (e) i) CF_3COOH, CH_2Cl_2 ii) Pd/C, MeOH iii) $(NEt_4)_2[Re(CO)_3Br_3]$, H_2O

5.2 Hexokinase inhibition studies

Hexokinase is an important enzyme that phosphorylates glucose by ATP, forming glucose-6-phosphate and ADP. Glucose-6-phosphate dehydrogenase (G6PDH) catalyzes the oxidation of G6P by $NADP^+$ to form 6-phosphogluconate and NADPH (Scheme 5.5), which is determined by measuring the increase in absorbance at 340 nm. Thus, the rate of glucose phosphorylation can be monitored spectrophotometrically in the presence and absence of inhibitory compounds.(*122-124*)

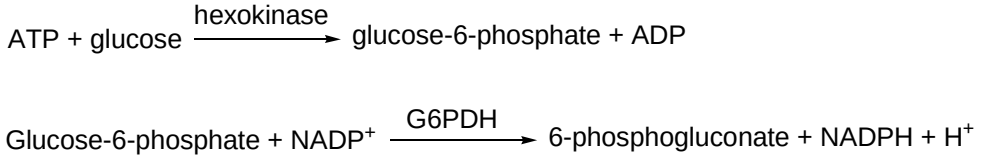

Scheme 5.5 Test principle of the rate of glucose phosphorylation

The Re complexes 5.2a, 5.8a and 5.16a have been tested for competitive inhibition of yeast hexokinase: 5.2a: K_i = 2.38 ± 0.05 mM, 5.8a: K_i = 0.81 ± 0.06 mM, the inhibition of 5.16a was not observed. The Lineweaver-Burk plot, also known as the double reciprocal plot, was used to calculate the inhibition constant K_i. For comparison, the known hexokinase inhibitor N-acetyl-glucosamine has an inhibition constant of 3.5 mM in this assay (literature value 2.72 ± 0.05 mM).(*123*) The K_i values of these two rhenium complexes suggest that they may have interaction with hexokinase. It is worth noting that the C-1 functionalized rhenium glucose analogues have the comparable K_i value to the one of glucosamine. To the best of our knowledge, none of the C-1 functionalized glucose Re derivatives showing inhibition of hexokinase, was previously reported in the literature.(*125, 126*) One possible reason for 5.2a exhibiting interaction with hexokinase is that a PEGylated linker increases the water solubility of the complexes. This can also explain the result that no inhibition was observed for the C-1 functionalized glucose rhenium complex with a alkyl linker.(*125*)

5.3 Cellular uptake of ^{99m}Tc-labeled glucose derivatives

5.3.1 ^{99m}Tc labelling

The small tridentate ligands have strong coordination ability with the $[^{99m}Tc(CO)_3]^+$ core. The labeling traces are shown in Figure 5.1. Over a concentration range of 10^{-3}-10^{-5} M, the labeling of glucose derivatives with $[^{99m}Tc(CO)_3]^+$ was achieved in very good yields (>99%) by heating a buffered solution (pH 7.4) of the corresponding peptide and ^{99m}Tc-tricarbonyl precursor at 70° C for 15-30 min. The rhenium

complexes were synthesized by heating each ligand with the $[Re(OH_2)_3(CO)_3]^+$ precursor in water at 70℃ for 6 h. The identity of complexes was confirmed by HPLC coinjection with the corresponding rhenium complexes, due to the well-known chemical similarities between rhenium and technetium complexes.

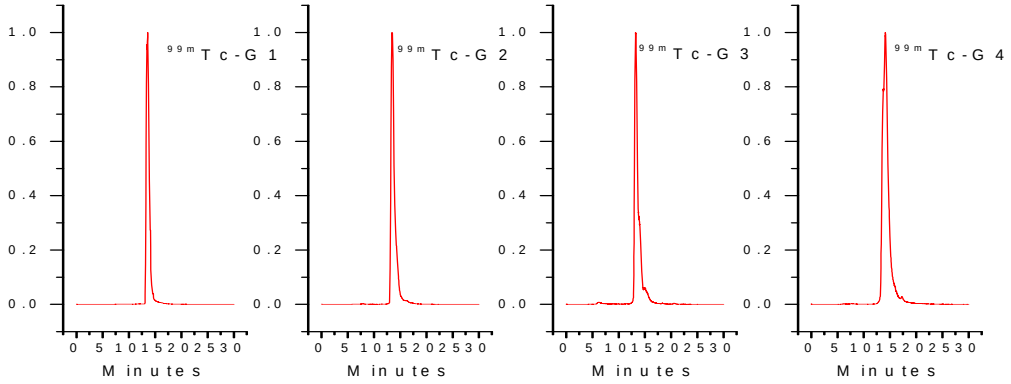

Figure 5.1 HPLC traces of ^{99m}Tc-labelled glucose derivatives; Retention time (Gradient B): ^{99m}Tc-G1: 13.60 min; ^{99m}Tc-G2: 13.48 min; ^{99m}Tc-G3: 13.27 min; ^{99m}Tc-G4: 14.17 min

5.3.2 Cellular uptake

Glucose transporter 1 is an integral membrane protein used to facilitate transport of glucose and other sugars. In this study, we tested all four technetium complexes for transport through the cell membrane via Glut1. Five different cell lines were used for these experiments (Figure 5.1). Low to moderate cellular uptake was observed for all radiolabeled glucose derivatives. The uptake was quite rapid as no significant increase was observed for higher incubation periods. The highest values of uptake were observed for MDA-MB-231 breast carcinoma cells, probably because the cells are bigger and have epithelial-like morphology that phenotypically appear as spindle shaped cells which may facilitate the uptake of glucose derivative.

In vitro, the MDA-MB-231 cell line has a high invasive phenotype, displaying a relatively high colony forming efficiency (cells grow quite fast), which can also contribute for the highest uptake glucose. We could also think about an eventual higher expression of glucose transporters, namely Glut1, in the cells MDA-MB-231

that could, and will be, evaluated by western blot analysis. However, such eventual higher expression is probably not the responsible for the higher uptake observed as the uptake appeared to be not Glut1 mediated.

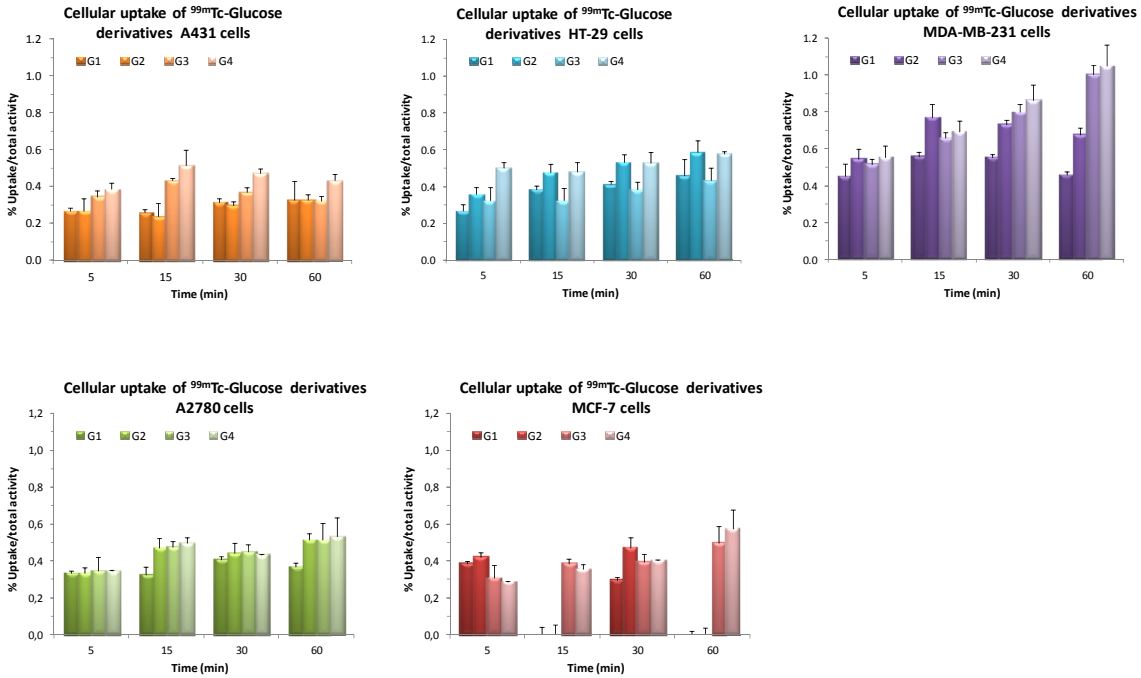

Figure5.3 Cellular uptake of ^{99m}Tc Glucose derivatives in different cells

Effect of assay medium in the uptake of radiolabeled glucose derivatives: The assay medium used in the uptake assays is very important and strongly influences the results of such assays. The modified Eagles Medium (MEM) with 25 mM of HEPES is frequently used and herein was used it as a first attempt. Compared to the high-glucose culture mediums like DMEM with gluta$_{max}$ (4500 mg/L D-glucose, Gibco 61965-026), MEM is a low-glucose medium (1000 mg/L D-glucose). However, such low amounts of glucose may compete with the radiolabeled glucose derivatives to the binding to glucose transporters, reducing thereby their uptake. Thus, other assays mediums were applied as well: MEM (Gibco: 21090-022) with 25mM HEPES (glucose conc.: 1000 mg/L, 5.5 mM), Opti-MEM (Gibco: 31985) (glucose conc.: 2500 mg/L) , Dulbecco's PBS (without glucose), Hanks Balanced Salt Solution (without glucose). The cellular uptakes of ^{99m}Tc-G2 in different assay mediums are

shown in Figure 5.4.

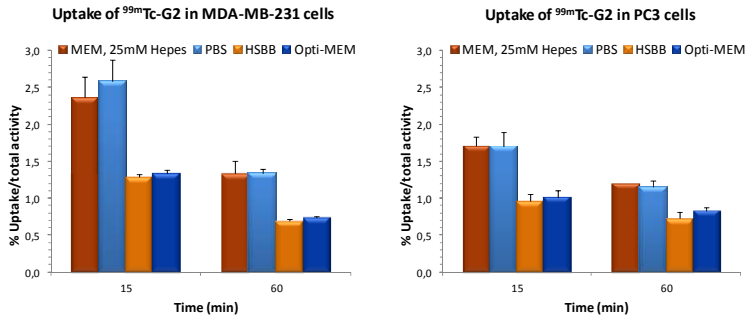

Figure 5.4 Cellular uptake of ^{99m}Tc-G2 in different assay mediums

The highest values of uptake were obtained for MEM with 25 mM Hepes and for Dulbecco's PBS. However, the morphology of cells incubated in DPBS changed during the incubation and it is believed that labeled compounds entered in the cells because cell membrane is damaged. Indeed, PBS or DPBS is not recommended as assay mediums for long incubation periods, but often used for washing steps.

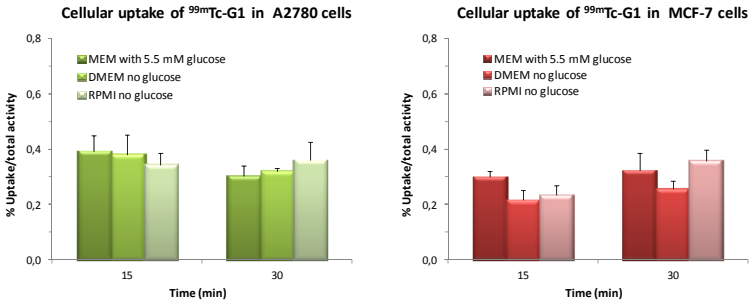

Figure 5.5 Cellular uptake of ^{99m}Tc-G1 in different assay mediums

Since the radiolabeled glucose derivatives are in a very low concentration, orders of magnitude lower than the 5.5 mM of glucose in MEM medium. Since our aim was to minimize the competition/saturation of glucose transporter Glut1 with cold glucose to maximize the uptake of radiolabeled compounds, the use of an assay medium without glucose, but richer than PBS or glucose-free HBSS could improved that uptake. Therfore, the effect of two different no-glucose mediums (DMEM, no glucose and RPMI 1640, no glucose) was evaluated in the uptake of ^{99m}Tc-G1 in A2780, MCF-7

and MDA-MB-231 cells, at 15 and 30 min (Figure 5.5), and compared with MEM with low glucose (5.5 mM), all mediums with 25 mM HEPES. The uptake of ^{99m}Tc-G1 was not improved with these assay mediums without glucose as compared to assay medium with low glucose concentration (5.5 mM). These results suggested that uptake was probably not mediated by transporters of glucose.

Effect of Cytochalasin B (Glut1 inhibitor) in the uptake of ^{99m}Tc-labeled glucose derivatives

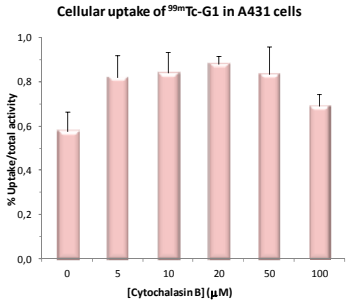

Figure 5.6 Cellular uptake of ^{99m}Tc-G1 in different concentration of Cytochalasin B

In a previous study the uptake of ^{99m}Tc-G2 in MDA-MB-231, cells were challenged in the presence of different concentrations (0, 5, 10 and 20 µM) of the potent Glut1 inhibitor cytochalasin B to verify specific transport via Glut1. The radiolabeled complexes and cytochalasin B were added to the cells simultaneously and the uptake was evaluated after 15 and 60 min at 37ºC. No inhibition of the uptake was observed. The effect of higher concentrations of cytochalasin B (0-100µM) was herein evaluated in the uptake of ^{99m}Tc-G1 in A431 cells at 37ºC during 15 min. Cytochalasin (400 µL) was added to the cells 15 min before the radiolabeled glucose derivative (100 µL). However, no significant uptake inhibition of ^{99m}Tc-G1 was observed in the presence of cytochalasin B (Figure 5.6).

Effect of high concentrations of glucose in the uptake of ^{99m}Tc-labeled glucose derivatives: Since cytochalasin B binds intracellularly to Glut1, it could still be speculated that the ^{99m}Tc-glucose derivatives are interacting at different binding sites, at the extracellular binding site of glucose. Therefore, the uptake (after 15 min) of

radiolabeled compounds was also evaluated in the presence of increasing concentrations of 2-deoxy-D-glucose (0-20 mM) (Figure 5.7).

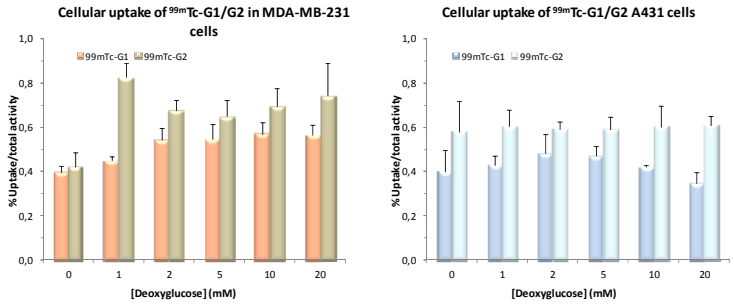

Figure 5.7 Cellular uptake of ^{99m}Tc-G1 in different concentration of 2-deoxy-D-glucose

MDA-MB-231 and A431 cells were incubated with 2-deoxy-D-glucose 15 min before the addition of the radiocomplexes. A large excess of 2-deoxy-D-glucose did not reduce internalization of ^{99m}Tc-G1 and ^{99m}Tc-G2, giving final evidence that they do not compete with 2-deoxy-D-glucose for a common binding site.

These complexes appeared to be transported into the cells by an unspecific uptake mechanism (e.g. passive diffusion) rather than by active transport via the sodium-independent Glut1 transporter. It is likely that the ^{99m}Tc-complexes are sterically too demanding for recognition at the extracellular binding site and/or transportation via Glut1.

5.4 Conclusion

In this Chapter, glucose derivatives functionalized at position C1, C2, C3, C6 with the Dap chelators were successully synthesized and radiolabeled. The rhenium complexes were accessed for competitive inhibition of hexokinase. The cellular uptakes of the corresponding ^{99m}Tc-complexes have been test in different tumor cells. No significant uptake inhibition of the radiocomplexes observed in the presence of cytochalasin B or 2-deoxy-D-glucose suggest that the cellular uptake is not mediated by GLUT-1.

6 Solid phase synthesis and biological evaluation of Peptide-^{99m}Tc conjugates

6.1 Results and discussion

The overexpression of many peptide-targeted receptor proteins provides the basis for new imaging methods. Radiolabeled peptides that bind with high affinity and specificity to receptors on tumor cells have emerged as an important class of radiopharmaceuticals. In this chapter, we described the design and synthesis of radiolabeled linear peptide and cyclic RGD peptides that target GRPrs, $\alpha_v\beta_3$ receptor, respectively. *In vitro* and *in vivo* studies of RGD peptide based conjugates were carried out for assessing binding affinity and internalization.

6.1.1 BBN analogues synthesis

To assess the utility of SAAC 4.19, three different peptide sequences, each containing nine residues but with a variable L-lys(Dap) position, were selected for the synthesis of BBN analogues. In those sequences, the single amino acid chelate L-lys(Dap) was introduced at the N-, the C-terminus or near the centre of the peptide. Dap containing peptide **L1** was prepared by solid phase peptide synthesis (Scheme 6.1). In this BBN derivative, the tripod chelate was introduced into N-terminus of BBN (7-14). For the solid phase synthesis, Rink amide MBHA resin was used as the solid support, which consists of the Rink amide linker attached to MBHA resin and is an ideal tool for the Fmoc SPPS of peptide amides with high yields and purities.(*127*) After removal of Fmoc protecting groups on the resin, the first amino acid Fmoc-Met-OH was immobilized on the resin by the reaction of HBTU activated carboxyl groups with the amino group. The protected amino acids were assembled sequentially on the Rink amide resin using a standard HOBt/HBTU/DIPEA coupling protocol. Each coupling was performed once for 50 min using a fourfold excess of the amino acid and

coupling reagents. Two equivalents of SAAC 4.19 were coupled manually to the growing peptide using a more expensive HATU coupling protocol which is preferred to HBTU due to the faster reaction with less epimerization during coupling. After final Fmoc deprotection, peptides were cleaved from the resin with simultaneous Boc protecting group removal using a cocktail consisting of 85% TFA, 5% thioanisole, 5% phenol and 5% water. At this point, the carboxylate group in the Dap unit was still esterified.

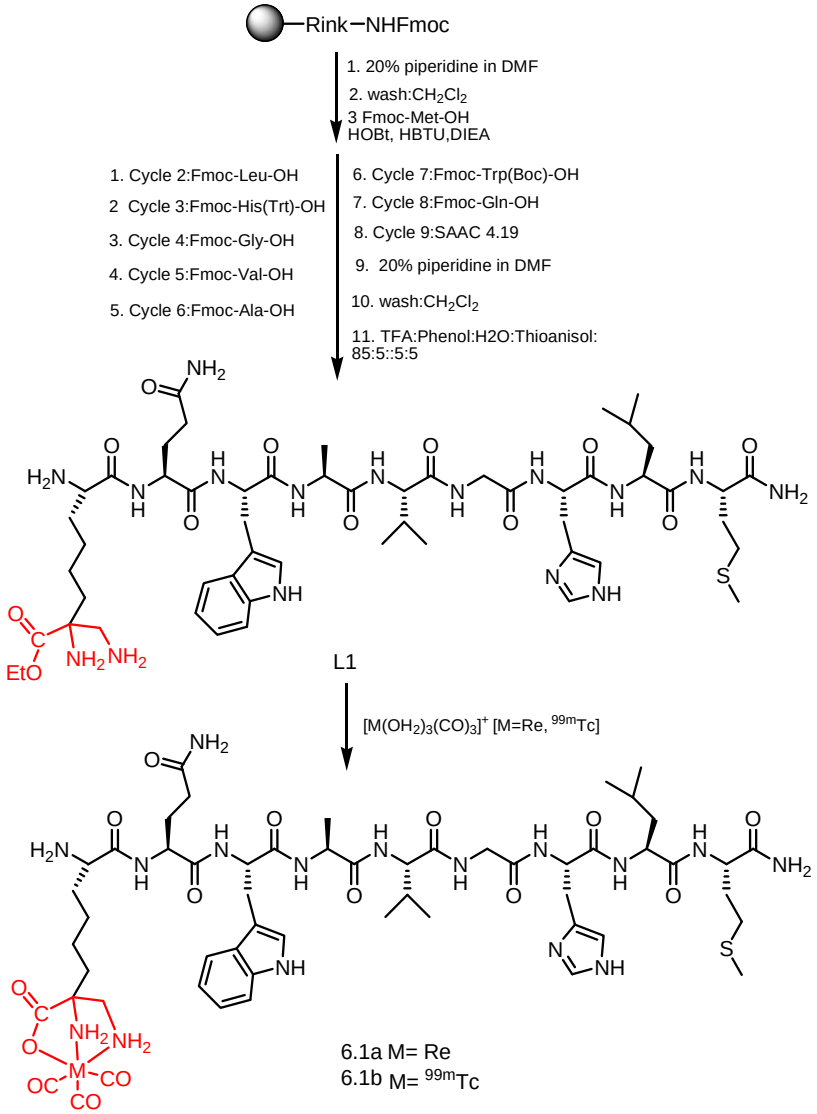

Scheme 6.1 Solid-Phase Synthesis of peptide conjugate 6.1 and peptide metal complex 6.1a,b

Coordination to the $\{Re(CO)_3\}^+$ or to the $\{^{99m}Tc(CO)_3\}^+$ moiety hydrolyzes this group concomitantly. It is important to exclude oxygen during the cleavage reaction in order

to avoid oxidation of the methionine containing peptides.(*128*) Following precipitation with cold methyl-t-butyl ether and centrifugation, the peptide-chelator conjugate 6.1 was purified by RP-HPLC and obtained in overall yields of 46% based on the initial resin loading of 0.69 mmol g^{-1}. Aqueous solution of the target peptide was treated with $[M(OH_2)_3(CO)_3]^+$ [M=Re, ^{99m}Tc] in H_2O under N_2 at 70°C for 20 h to give the corresponding metal bound peptide conjugates in quantitative yields.

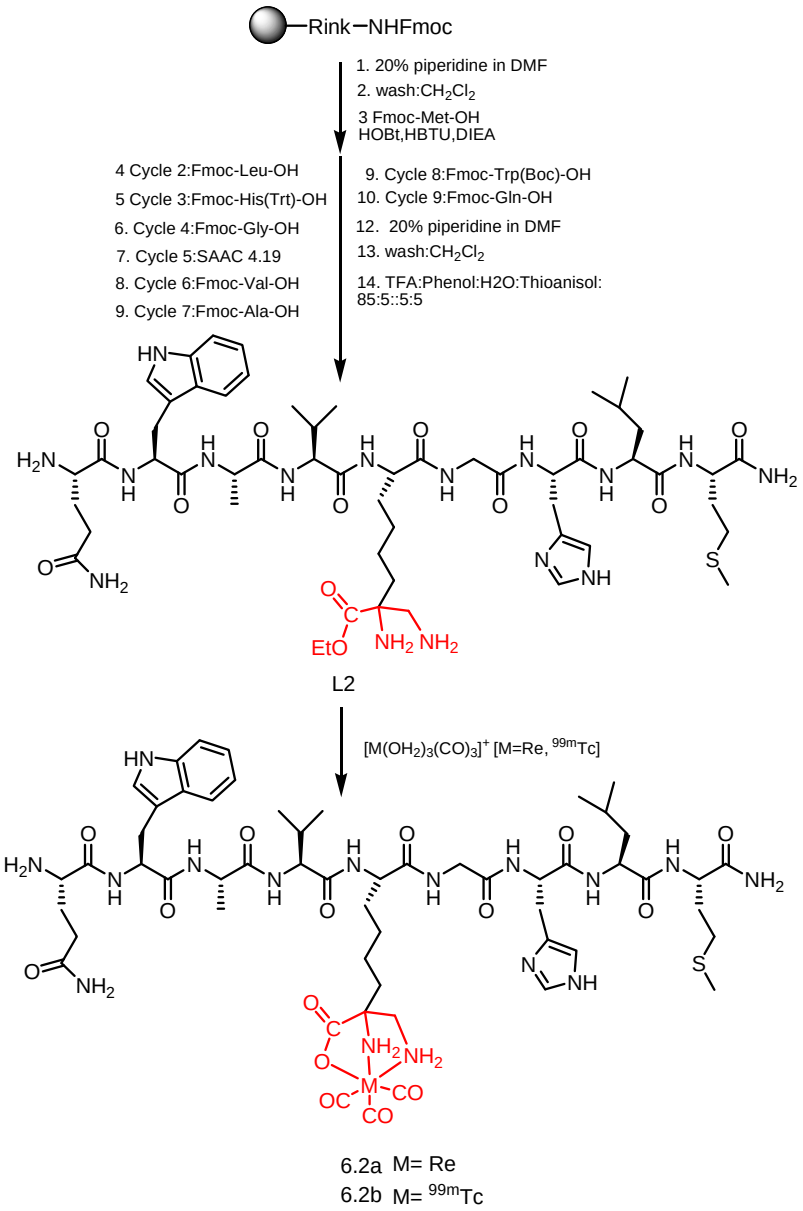

Scheme 6.2 Solid-Phase Synthesis of peptide conjugate 6.2 and peptide metal complex 6.2a,b

The same approach was used to prepare the Dap containing peptide **L2**, in which the

tripod chelate was introduced into middle position of BBN (7-14) (Scheme 6.2). Two equivalents of SAAC 4.19 were coupled after the completion of cycle 4 by using two equivalents of coupling reagents (HATU/DIEA). After deprotection and resin cleavage, the final peptide 6.2 was treated with metal precursor $[M(OH_2)_3(CO)_3]^+$ [M=Re, ^{99m}Tc] to give the corresponding metal-peptide conjugates 6.2a, b.

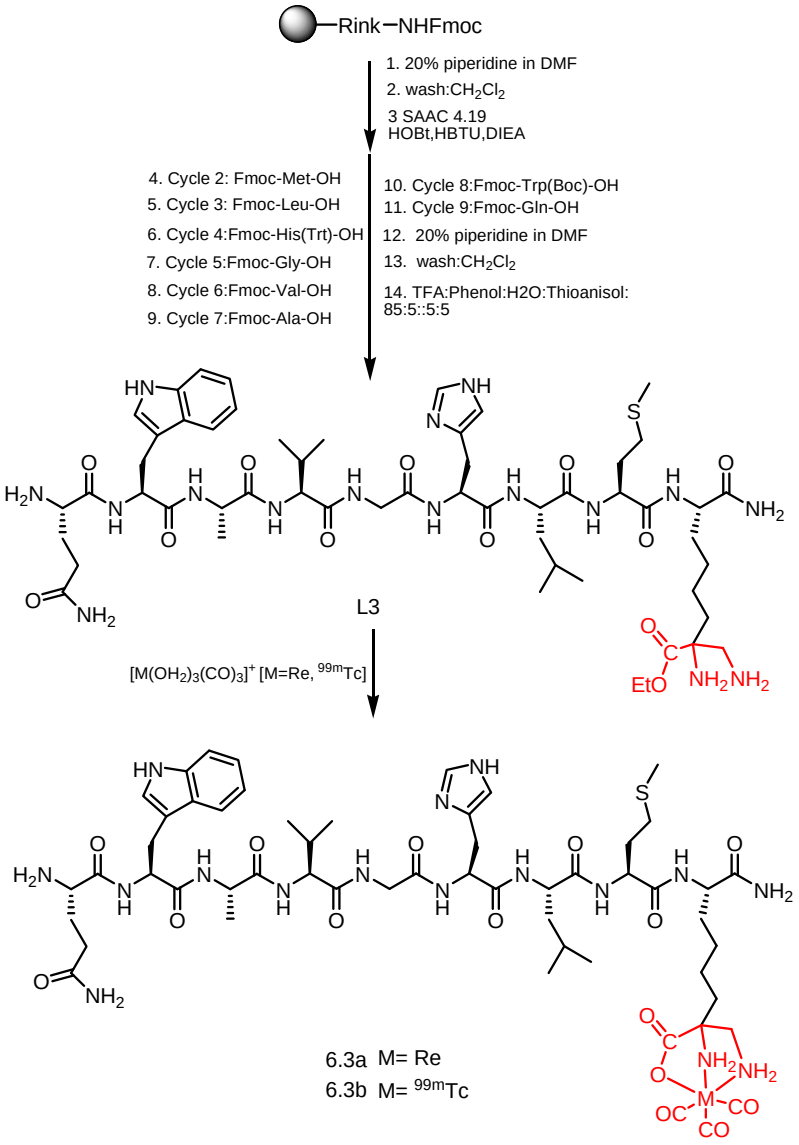

Scheme 6.3 Solid-Phase Synthesis of peptide conjugate 6.3 and peptide metal complex 6.3a,b.

In the synthesis of peptide **L3** (Scheme 6.3), the SAAC 4.19 was first immobilized on the rink amide resin, and the remaining Fmoc-amino acids (4 equiv) were sequentially coupled with standard HBTU protocol. The final product was cleaved from the resin

and precipitated into cold MTBE. The metal bound peptide conjugates 6.3a, b were obtained by the same method for preparation of 6.1 a, b.

6.1.2 Cyclic RGD peptide analogues synthesis

The synthetic strategy for preparation of the cyclic RGD peptide **L4** is shown in Scheme 6.4. Essentially, the synthesis involved three key steps: (1) attachment to the solid support via the α-carboxyl of Fmoc-Gly-OH, (2) linear chain formation, and (3) head-to-tail cyclization in solution through amide bond formation between the α-carboxyl group of Gly and the α-amino group of Asp.

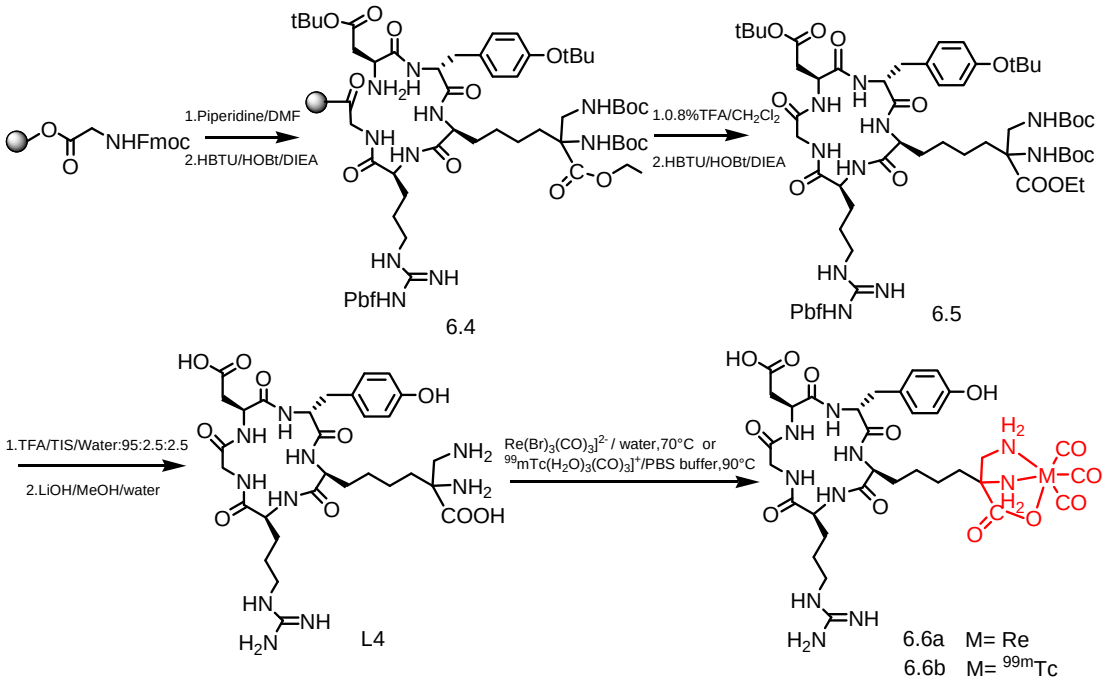

Scheme 6.4 Synthesis of cyclic RGD peptide 6.6 and its complexes

SPPS was performed using 2-chlorotrityl chloride resin and standard Fmoc chemistry. The resin is a super acid-labile resin for the solid phase immobilization of carboxylic acids that provides the possibility of selective cleavage of peptide from the resin in the presence of moderate acid-labile protecting groups.(*129*) To initiate the synthesis, Fmoc-gly-OH was immobilized onto 2-chlorotrityl chloride resin via its carboxylic acid and then the linear, side-chain-protected peptide was assembled with the glycine at the C-terminus using HBTU/HOBt activation in the presence of DIPEA in DMF.

The completion of each coupling cycle was monitored after 50 min of agitation by means of the Kaiser test.(*130*) Cleavage from the resin was accomplished under mildly acidic conditions (0.8% TFA in DCM) to give the fully protected linear peptide which was then subjected to intramolecular head-to-tail cyclization in solution to furnish the macrocycle 6.5. Side chain deprotection was achieved in almost quantitative yield by treating the product with TFA in the presence of free radical scavenger (triisopropylsilane). Purification of the crude products with preparative reverse-phase HPLC gave the target compound **L4** in 20% overall yield, with >95% purity (as determined by analytical HPLC with monitoring at 226 nm).

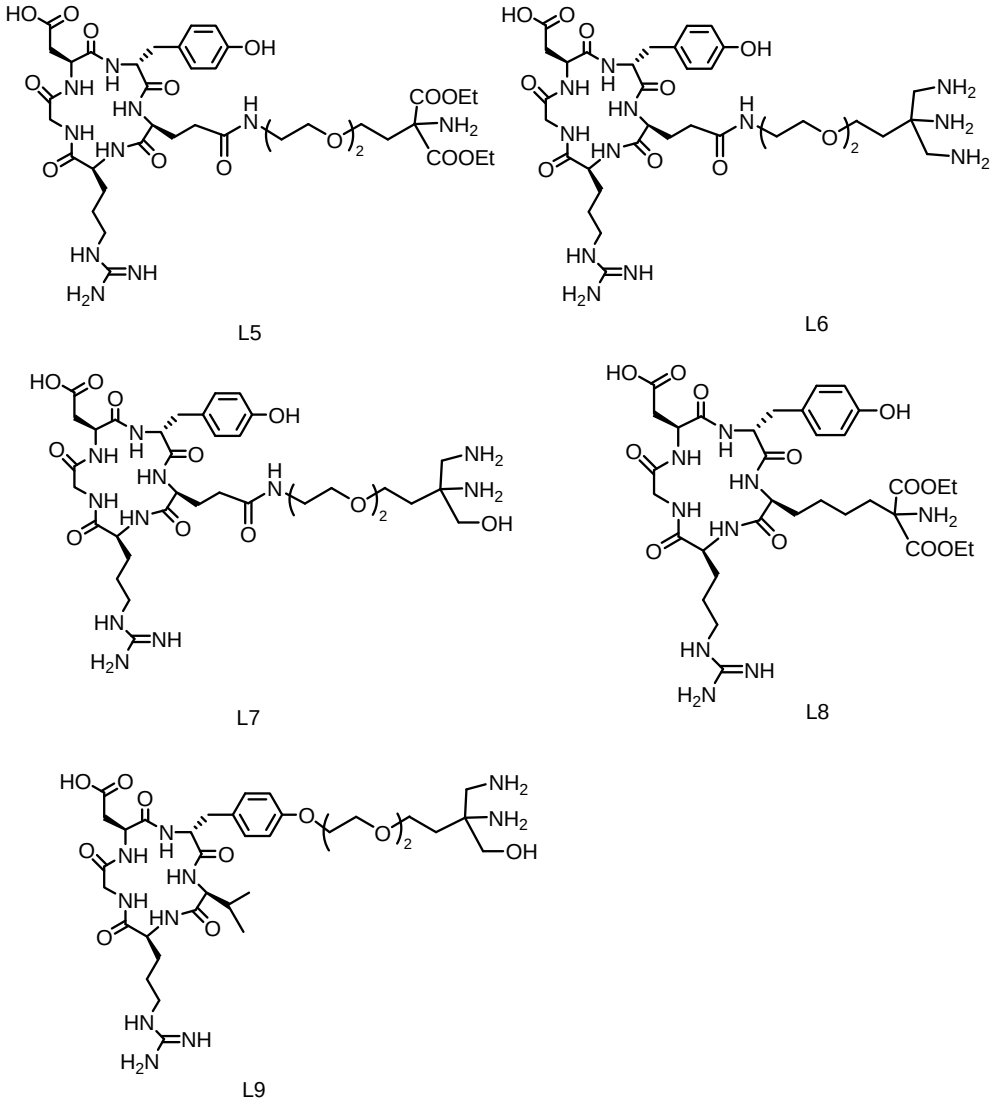

Scheme 6.5 Cyclic RGD peptide analogues

cyclo(Arg-Gly-Asp-D-Tyr-Glu(NO_2))(**L5**),cyclo(Arg-Gly-Asp-D-Tyr-Glu(N_3))(**L6**),cyclo(Arg-Gly-Asp-D-Tyr-Glu(N_2O))(**L7**),cyclo(Arg-Gly-Asp-D-Tyr-Lys(NO_2))(**L8**), cyclo(Arg-Gly-Asp-D-Tyr(N_2O)-Val)(**L9**) (Scheme 6.5) were prepared using the same strategy as for the preparation for peptide **L4**. All the couplings were performed manually using a DMF solution of HOBt/HBTU in the presence of DIPEA. Each coupling was performed once for 60 min using a fourfold excess of Fmoc-amino acids and activating reagents. In the case of SAAC, the coupling was performed for 90 min by using two equivalents of the amino acids. After purification by preparative HPLC, peptides were obtained in overall yields of 20-25%.

6.1.3 Rhenium complexes

The complexes were synthesized as references for the corresponding ^{99m}Tc labeled peptides. Aqueous solutions of peptides (**L1-L4**) were reacted with $[Re(OH_2)_3(CO)_3]^+$ in H_2O under N_2 at 70°C for 6-20 h to give the Re compounds in quantitative yields. The synthesis of complexes 6.7-6.10 (Scheme 6.5) were performed using a microwave reactor. The reactions were complete in 2 min at 120 °C. The metallated conjugates were purified by reverse-phase HPLC and lyophilized. Electrospray mass spectrometry allowed for the determination of the molecular ion of the nonradioactive Re(I) conjugates. No dissociation between the *fac*-$\{Re(CO)_3\}^+$ moiety and the ligand framework was observed, demonstrating the stability of the M(I)-N_2O coordinate bond.

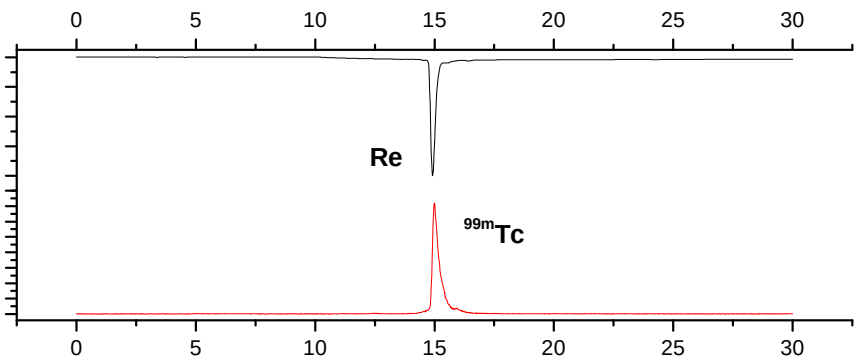

a)

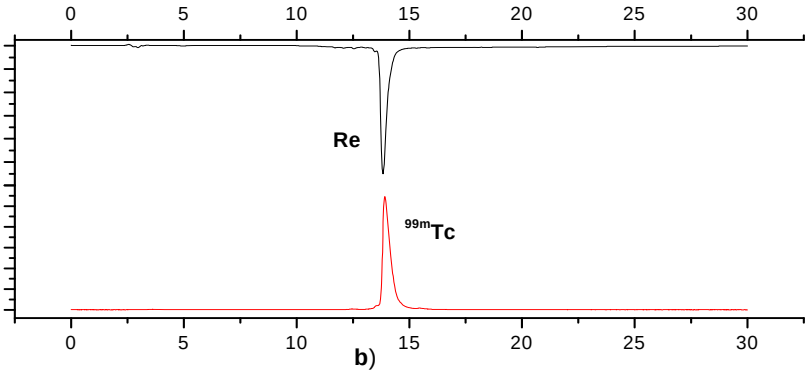

Firgure 6.1 a) HPLC traces of N terminus of BBN(7-14)-Metal(M=Re, ^{99m}Tc) conjugates b)HPLC trace of [M(CO)$_3$-cyclo-(Arg-Gly-Asp-D-Tyr-Lys(DAP))](M=Re,^{99m}Tc)

6.1.4 ^{99m}Tc-labeling studies

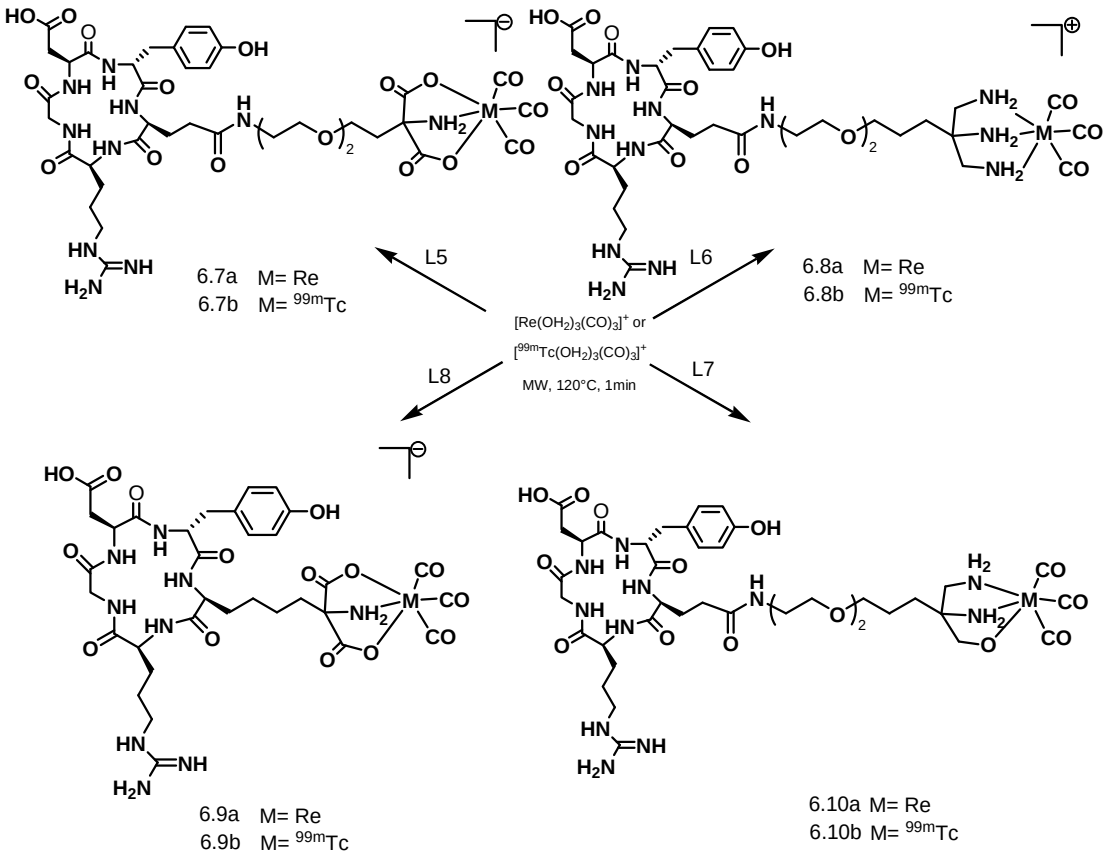

Scheme 6.5 Synthesis of Re and [^{99m}Tc] chelator-cyclic RGD peptide conjugates

$[^{99m}Tc(OH_2)_3(CO)_3]^+$ was prepared from $Na^{99m}TcO_4$ according to literature methods. Aqueous ^{99m}Tc solutions in the concentration range of 10^{-6} to 10^{-9} M were adjusted to pH=7 with 1 M HCl and labeling efficiencies determined by reacting these stock solutions with peptide concentration from 10^{-3}-10^{-5}M. Over this range, these peptides could be labeled with $[^{99m}Tc(OH_2)_3(CO)_3]^+$ at 90°C after 30 min in yields better than 98%. Even at a concentration of 10^{-6} M, the peptides could be labeled in 85% yield after 70 min, underlining the efficacy of the Dap chelator. In the presence of 0.1 M cysteine or histidine at 37°C, no trans-metallation was found after 24h further confirming the chemical robustness of the Dap complex.

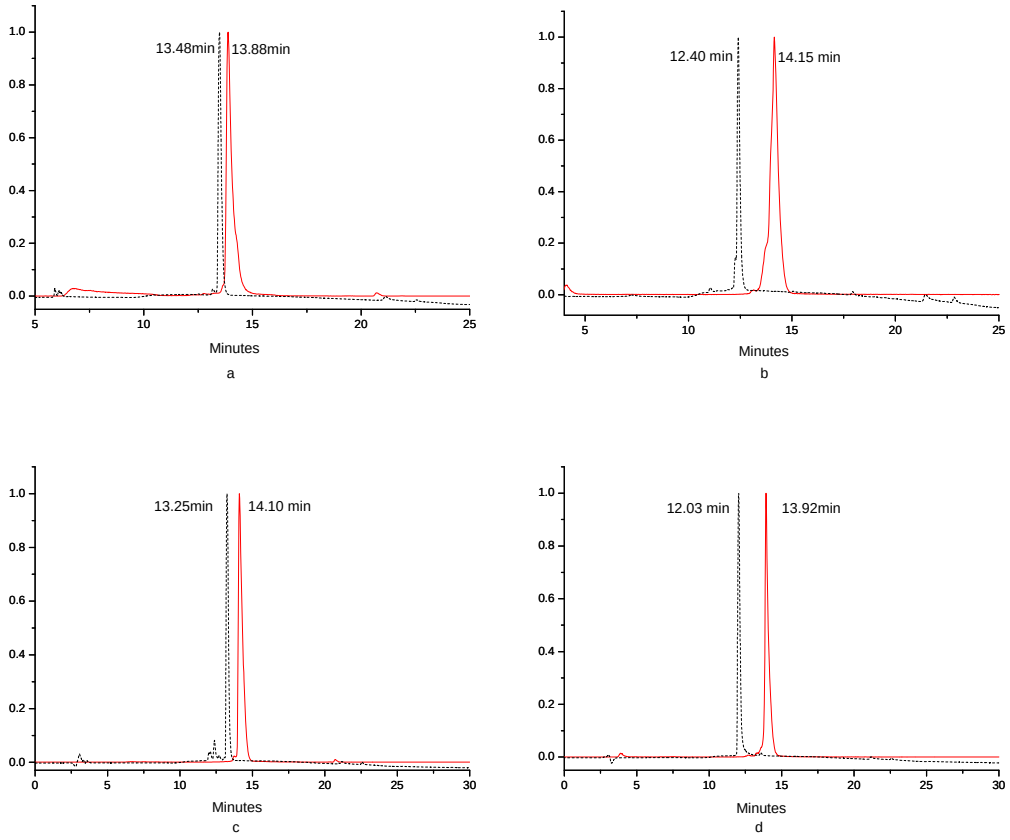

Figure 6.2 HPLC traces of cyclic RGD peptides without metal complex and the ^{99m}Tc conjugates (a) L5(dash line), $[^{99m}Tc(L5)(CO)_3]$ (red line), (b) L7(dash line), $[^{99m}Tc(L7)(CO)_3]$(red line), (c) L8(dash line), $[^{99m}Tc(L8)(CO)_3]$(red line), (d) L6(dash line), $[^{99m}Tc(L6)(CO)_3]^+$(red line).

It should be emphasized at this point that the labeling yield did not depend on the

absolute amount of ^{99m}Tc activity, an observation in agreement with the pseudo first order labeling kinetics in Dap. Typical specific activities as achieved in our labeling studies were in the order of 1.1TBq/μmol. Dap is, thus, suitable for labeling biomolecules to very high specific activities. The identities of the ^{99m}Tc labeled conjugates were confirmed by HPLC co-injection with the corresponding rhenium analogues (Figure 6.1). Due to the close structural similarity between Re and Tc homologues, retention times should be close to identical. It was found that if the labeling was conducted using a microwave reactor instead of normal heating, the labeling reactions were complete in 1 to 2 min at 120° C (Scheme 6.5). All the RGD peptides with the tridentate ligands have relatively high reaction rates with the $[^{99m}Tc(OH_2)_3(CO)_3]^+$ moiety as compared with those tridentate ligand frameworks containing bulky coordinating functional groups. The radioactive HPLC traces are shown in Figure 6.2, and the biological evaluation of these labelled peptide conjugates are still under investigation.

6.2 Biological evaluation

In vitro evaluation: For an exemplary evaluation of the effect of Lys by Lys(Dap) substitution on receptor binding affinity of cyclic RGD analogs, we investigated the binding affinity of $[Re(L4)(CO)_3]$ to different clinically relevant integrin receptor subtypes.(*131, 132*)

The integrins with the highest documented relevance for imaging applications contain the α_v subunit, especially the $\alpha_v\beta_3$ and $\alpha_v\beta_5$ subtype. The former is known to be overexpressed on many tumor types and tumor neovasculature, but is also expressed at lower levels in non-cancerous tissues.(*133*) Table 6.1 summarizes the binding affinities (IC_{50} in nM) of $[Re(L4)(CO)_3]$ as well as of the uncomplexed labeling precursor L4 to these and three other integrin receptor subtypes.

The rhenium reference peptide $[Re(L4)(CO)_3]$ and the uncomplexed labeling precursor L4 display similar IC_{50} values for all integrin subtypes investigated. However, in the case of the $\alpha_v\beta_6$, $\alpha_v\beta_5$ and $\alpha_v\beta_3$ integrins, complexation with the

$[Re(CO)_3]^+$ fragment leads to a loss in binding affinity by a factor of 2. Nevertheless, binding affinity of L4 integrates well into a series of different RGD-based precursors for ^{99m}Tc-labeling such as Pz1-RGD, HYNIC-RGD, Cys-RGD and L2-cRGD with IC50 values of 3, 6, 6.6, and 11.8 nM, respectively, in a comparable assay.(*134*) The $\alpha_v\beta_3$-integrin affinity of $[Re(L4)(CO)_3]$ is comparable to that of other clinically used radiolabeled RGD-analogs such as [^{18}F]Galacto-RGD. [^{18}F]Galacto-RGD shows an affinity of 5 nM to the immobilized $\alpha_v\beta_3$ receptor, but significantly higher $\alpha_v\beta_3$ selectivity (IC_{50} ($\alpha_v\beta_3$) = 1000 nM, IC_{50} ($\alpha_{IIb}\beta_3$) = 6000 nM) than the peptides investigated in this study.(*135*)

Table 6.1 Competitive binding affinities of L4 and $[Re(L4)(CO)_3]$ to different solubilized integrins determined via ELISA. Data represent IC50 values [nM] (mean of duplicate experiments (SD))

	$\alpha_v\beta_6$ [a]	$\alpha_v\beta_1$ [b]	$\alpha_v\beta_5$ [c]	$\alpha_{IIb}\beta_3$ [d]	$\alpha_v\beta_3$ [e]
reference peptide*	30 (3.5)	6.1(0.5)	41(1.2)	1.5 (0.3)	0.2 (0.02)
L4	254 (4.1)	41 (1.9)	30 (3.1)	440 (8.3)	3.4 (0.05)
$[Re(L4)(CO)_3]$	540 (3.9)	42 (1.4)	72 (1.2)	432 (5.1)	7.1(1.2)

* data for the respective reference peptides are cited from the literature; Reference peptides are a) RTDlinear IC50=30 nM (*136*), b) Cilengitide IC50=15 nM (*137*), c) Cilengitide IC50=50 nM (*138*), d) Tirofiban IC50=0.6 nM (*137*), e) Cilengitide IC50=0.5 nM (*139, 140*)

The results obtained in the binding study using M21 cells and [^{125}I]echistatin as the radioligand show the same tendency: $Re(CO)_3$-complexation of L4 leads to a loss in binding affinity (IC_{50} (L4) = 242 nM, IC_{50} ($[Re(L4)(CO)_3]$) = 866 nM), albeit somewhat more pronounced than observed when using immobilized integrin. The affinity determined for [^{18}F]Galacto-RGD in the same assay is 319 nM.(*141*)

In vivo biodistribution study: The biodistribution data obtained for $[^{99m}Tc(L4)(CO)_3]$ in M21 melanoma bearing nude mice are summarized in Table 6.2.

$[^{99m}Tc(L4)(CO)_3]$ shows rapid clearance from the circulation and no particular predominance of renal vs. hepatobiliary clearance or vice versa, but modest

accumulation in all excretion organs. This represents a major advantage of this new Lys(Dap)-coupled RGD analog over previous derivatives using other BFC's for $[^{99m}Tc(CO)_3]^+$ complexation.(*142*) For example, $[^{99m}Tc(CO)_3]$Pz1-cRGD, in which pyrazolyl functionalities serves for $[^{99m}Tc(CO)_3]^+$ complexation, shows fivefold higher hepatic and intestinal accumulation. This may be due to the significantly reduced lipophilicity of $[^{99m}Tc(L4)(CO)_3]$ as compared to $[^{99m}Tc(CO)_3]$Pz1-cRGD (log P = -1.82 vs -0.92). Surprisingly, the accumulation of $[^{99m}Tc(L4)(CO)_3]$ in the excretion organs is as low as or even lower than that of [^{99m}Tc]EDDA/HYNIC-cRGD, which shows an even lower log P of -3.57.(*134*) This underlines once more the observation, that especially in the case of ^{99m}Tc-labeled peptide radiopharmaceuticals, the labeling method itself rather than the physical parameter "hydrophilicity" governs excretion pathways from the circulation.

Table 6.2: Biodistribution of $[^{99m}Tc(L4)(CO)_3]$ in M21 melanoma bearing nude mice 60 min p.i.. Control animals (n = 5) were injected with tracer only, for the blocking study (n = 3), the tracer and 590 µg Cilengitide per mouse (23.5 mg/kg body weight) were coinjected. Data are given as %ID/g and are means ± SD.

Organ	Control	Blocking study	Tumor/organ ratio
blood	0.37 ± 0.02	0.31 ± 0.25	3.8 ± 0.5
heart	0.34 ± 0.02	0.20 ± 0.04	4.2 ± 0.5
lung	0.78 ± 0.13	0.41 ± 0.06	1.8 ± 0.4
spleen	0.63 ± 0.13	0.22 ± 0.04	2.3 ± 0.5
pancreas	0.24 ± 0.01	0.10 ± 0.01	5.9 ± 0.7
liver	2.10 ± 0.50	1.42 ± 0.27	0.7 ± 0.2
stomach	1.02 ± 0.15	0.35 ± 0.23	1.4 ± 0.3
intestines	1.89 ± 0.45	1.31 ± 0.77	0.8 ± 0.2
kidney	2.02 ± 0.29	1.22 ± 0.22	0.7 ± 0.1
muscle	0.18 ± 0.01	0.07 ± 0.02	7.7 ± 1.0
tumor	1.41 ± 0.16	0.25 ± 0.14	

Absolute tumor accumulation of [^{99m}Tc(L4)(CO)$_3$] is lower than that observed for [^{99m}Tc(CO)$_3$]Pz1-cRGD or [^{99m}Tc]EDDA/HYNIC-cRGD in the same tumor model at 1 h p.i. (2.5 and 2.7 %ID/g, respectively). However, as demonstrated by the blocking experiment (coinjection of an excess of unlabeled Cilengitide), tumor uptake is almost exclusively integrin-mediated, which highlights the integrin targeting efficiency of [^{99m}Tc(L4)(CO)$_3$].

Due to its comparably low accumulation in non-target tissues, [^{99m}Tc(L4)(CO)$_3$] shows reasonable tumor-to-background ratios (Table 6.2), which approximates or even exceeds those previously achieved with ^{99m}Tc-labeled monomeric RGD peptides with higher tumor accumulation such as [^{99m}Tc]EDDA/HYNIC-cRGD (t/blood: 2.8, t/liver: 1.0, t/intestines: 1.3, t/kidney: 0.7, t/muscle: 3.6). These features make [^{99m}Tc(L4)(CO)$_3$] a promising candidate for future evaluation in small animal SPECT-imaging of integrin expression.

6.3 Conclusion

Orthogonally protected L-Lys(N_xO_y) and L-Glu(N_xO_y) represent artificial, single amino acid chelates which can be implemented into solid phase peptide syntheses. Being orthogonally protected amino acids, incorporation into any desired position in the peptide sequence is possible and thus enables facile preparation of libraries of peptides including a single amino acid chelate at any position. We have demonstrated this concept by conjugating L-Lys(Dap) to three different positions in BBN(7-14). In addition, we have replaced the original L-Lysine in the c-RGDyK sequence or glutamine in the c-RGDyE sequence . As shown in a receptor binding study, both introduction of the Lys(Dap)-moiety as well as complex formation with $[Re(CO)_3]^+$ do not seriously affect binding affinity of the peptide to different integrin subtypes, in particular to the $\alpha_v\beta_3$ receptor. Labeling of L-Lys(Dap)-functionalized peptides with the [^{99m}Tc(CO)$_3$]$^+$ core usually proceeds quantitatively at around 10 μM concentrations, leading to ^{99m}Tc-labeled peptide radiopharmaceuticals with high specific activities. Overall, the investigated N_xO_y-based tripod ligand is one of the

smallest and most efficient tridentate ligands for $[^{99m}Tc(CO)_3]^+$ complexation described so far, and is not only suited for labeling of peptides but also of other biomolecules or pharmacophores. As HYNIC, it has the potential to become a standard in ^{99m}Tc-based molecular imaging, but unlike for HYNIC-based ^{99m}Tc complexes, the authenticity of the conjugates is well defined.

7 Summary and Outlook

In this work, we designed and synthesized a series of small tripod ligands which have very low molecular weight with different hydrophilic functional groups including amino groups, carboxyl groups, hydroxyl groups (Figure 7.1). These tripod ligands are strong chelators for the $[^{99m}Tc(CO)_3]^+$ core and the resulting complexes are therefore very small and hydrophilic.

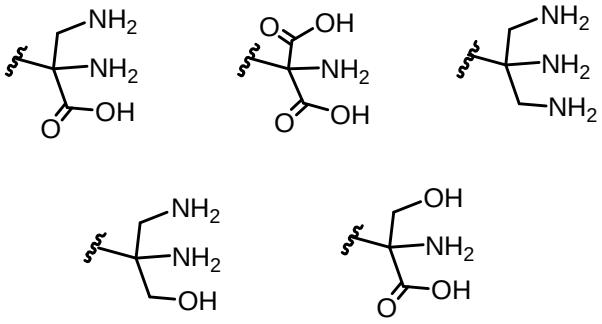

Figure 7.1 Small tripod chelates with different donor atoms

In order to introduce these tripod chelators into the peptide sequence, we prepared the L-Lysine derivatives in which the ε-NH_2 group was replaced by the tripod through conjugation to its α-carbon and glutamic acid derivatives in which the γ-COOH group was conjugated with the tripod via PEG linker. The synthetic strategy produced orthogonally protected single amino acid chelates (SAACs). The -NH_2 group of the α-amino acid portion is Fmoc- and the -NH_2 groups of the tripod are Boc-protected. Fmoc-L-Lys(N_2O(Boc)) was either conjugated to the N- and C-terminus of bombesin BBN(7-14) or integrated into the sequence using solid phase peptide synthesis (SPPS). We also replaced the amino acid at position 5 in a cyclic RGD peptide with L-Lysine or L-Glutamic acid based chelators. For all peptides, quantitative labeling was achieved with the $[^{99m}Tc(CO)_3]^+$ core at 10 μM concentrations in PBS buffer (pH=7.4). For comparison, the rhenium homologues were prepared from $[Re(OH_2)_3(CO)_3]^+$ and Lys(N_2O)-BBN(7-14) or cyclo-(RGDyK(N_2O)) or cyclo-(RGDyE(N_xO_y)) respectively.

Determination of integrin receptor binding showed low to medium nM affinities for various receptor subtypes. The IC_{50} of cyclo-(RGDyK(N_2O[$Re(CO)_3$])) for $\alpha_v\beta_3$ is 7.1 nM as compared to 3.1 nM for non-ligated RGD derivative. Biodistribution studies in M21 melanoma bearing nude mice showed reasonable $\alpha_v\beta_3$-integrin specific tumor uptake. Altogether, orthogonally protected L-Lys(N_2O) represents a highly versatile building block for integration in any peptide sequence. Lys(N_2O)-precursors allow high yield ^{99m}Tc-labeling with [$^{99m}Tc(H_2O)_3(CO)_3]^+$, forming small and hydrophilic complexes, which in turn leads to peptide radiopharmaceuticals with excellent in vivo characteristics.

The design of a ^{99m}Tc labeled glucose derivatives as SPECT imaging analogues of the well established PET tracer [^{18}F]FDG is considered to be of great interest. In our endeavor for designing new carbohydrate derivatives able to be transported by GLUT1, we designed a number of new glucose derivatives. In this work, we present the synthesis of glucose derivatives which are functionalized at position C1, C2, C3, C6 via a PEG spacer with the 1, 2-diamino-propionic acid (Dap) chelator. Labeling studies showed quantitative labeling at low glucose concentrations. Inhibition studies with hexokinase showed good affinity with inhibition values in the range of 0.8 to 2.3 mM which are comparable to one of the standard inhibitor glucosamine (3.5 mM). The cellular uptakes of the corresponding Tc complexes have been test in different tumour cells. Low to moderate cellular uptakes were observed for all radiolabeled glucose derivatives. Since no significant uptake inhibition of the radiocomplexes was observed in the presence of cytochalasin B or 2-deoxy-D-glucose, it is evident that these complexes are transported into the cells by an unspecific uptake mechanism rather than by active transport via the sodium-independent Glut1 transporter.

The small size of these tripod chelators as well as their strong coordination with the [$^{99m}Tc(CO)_3]^+$ core make them attractive building blocks in the design of ^{99m}Tc based radiopharmaceuticals. The new methodologies developed for the synthesis of these metal-biomolecule conjugates will facilitate forthcoming studies that would have to extend investigations to the correlation of structure and properties. The investigation should include the incorporation of longer spacer into the metal-biomolecule

conjugates to reduce the interaction between the biomolecules and ligand binding sites and provide favourable binding characteristics *in vivo*. An amphiphilic polyethylene glycol (PEG) linker was incorporated into the cyclic RGD peptide to improve the pharmacokinetics, it may also reduce the receptor binding affinity, we will report on the overall effect of the introduction of PEG linkers in due course. Furthermore, the synthesis of ^{99m}Tc labeled glucose derivatives transported by Glut1, would be of importance for the design of carbohydrate-based radiopharmaceuticals. Important future tasks are to find out the transport mechanism of the glucose derivatives we reported in this work and develop more promising glucose analogues that would be probably used as surrogates of [^{18}F]-2-fluoro-desoxy glucose ([^{18}F]-FDG).

Zusammenfassung

Im Rahmen dieser Arbeit wurde eine Reihe von kleinen, tripodalen Liganden mit verschiedenen funktionellen Gruppen konzipiert und synthetisiert. Die resultierenden Komplexe mit der $[^{99m}Tc(CO)_3]^+$ Einheit sind klein und hydrophil.

Des Weiteren wurden diverse Glucose Derivate synthetisiert, welche an den Positionen C1, C2, C3 und C6 über einen PEG Linker mit dem 1,2-Diaminopropionsäure Chelator funktionalisiert sind. Markierungs-Studien mit ^{99m}Tc waren selbst bei tiefen Glucose Konzentrationen möglich. Die Zellaufnahme von den entsprechenden ^{99m}Tc Komplexen wurde in verschiedenen Tumorzelllinien untersucht. Dabei wurde eine schlechte bis moderate Zellaufnahme für die verschiedenen Glucose Derivate beobachtet. Aufgrund der Tatsachte, dass keine signifikante Hemmung der Zellaufnahme in der Gegenwart von Cytochalasin B oder 2-Deoxy-D-Glucose gefunden wurde, ist eine unspezifische Zellaufnahme offensichtlich und nicht ein aktiver Transport in die Zelle über den GLUT-1 Transporter.

Um die Chelatoren in Peptidsequenzen einzufügen, wurde die Aminogruppe an der ε-Position von L-Lysine durch die tripodalen Liganden ersetzt oder die Carbonsäure γ-Position von Glutaminsäure über einen PEG Linker mit dem tripodalen Liganden verbunden. Die sogenannten orthogonal geschützten „Single Amino Acid Chelates (SAACs)“ wurden entweder an den N- und C-Terminus von Bombesin angehängt oder direkt in die Sequenz integriert mittels Festphasenpeptidsynthese. Ausserdem wurden die Aminosäurederivate in ein zyklisches RGD Peptid inkorporiert. Die verschiedenen Peptide konnten bei μM-Konzentrationen quantitative mit der $[^{99m}Tc(CO)_3]^+$ Einheit markiert werden. Die Bestimmung der Affinität zum Integrin Rezeptor zeigte geringe bis mittelmässige Werte im nM Bereich für diverse Rezeptor-Subtypen. Die Biodistributionsstudien in Nacktmäusen mit einem M21 Melanom ergab eine vernünftige $\alpha_v\beta_3$-Integrin spezifische Tumoraufnahme.

8 Experimental part

8.1 General information, materials and instrumentation

All reagents and organic solvents were purchased from Aldrich, Acros, or ABCR in reagent grade or better and used without further purification. Dry DMF, acetonitrile were purchased from Aldrich. Dry ethanol, methanol and THF were freshly distilled. Yeast hexokinase, glucose, Adenosine triphosphate (ATP), Nicotinamide adenine dinucleotide phosphate (NADP), glucose-6- phosphate-dehydrogenase (G6PDH) were purchased from Roche diagnostics. Thin-layer chromatography (TLC) was carried out using Merck silica gel 60, F254 with a thickness of 0.25 mm. Column chromatography was accomplished on silica gel 60 (20-40 mesh). Electrospray ionization mass spectrometry (ESI-MS) spectra were recorded a Bruker HCT spectrometer, NMR spectra on a Bruker 400 or 500 MHz spectrometer in $CDCl_3$ solutions. All NMR chemical shifts are in ppm, coupling constants (*J*) are given in Hz. High-resolution electrospray ionization mass spectrometry was performed on a FinniganMAT 900 (Finnigan MAT95, San Jose, CA; USA) double-focusing magnetic sector mass spectrometer (geometry BE). Compoud 3.1-3.5, 4.1-4.3, 4.7-4.8, 5.3-5.4, 5.9, 5.12-5.14 were synthesized by slightly modified literature procedures.(*105, 119, 121, 143-149*)

HPLC-MS (ESI) spectra were measured on a Bruker HCT spectrometer (Bruker) with Aquinity UPLC (Waters), using either a Macherey-Nagel EC 250/3 Nucleodur C18 Gravity 5 µm or a Macherey-Nagel EC 250/3 Nucleosil C18 Gravity 5 µm. HPLC solvents were 0.1% formic acid (solvent A) and methanol or acetonitrile(solvent B), The following gradient was used: Gradient A: 0% B for 2 min, and increased to 100% in 10 min, and held at 100% for 5 min and then back to 0% in 8 min, flow 0.3 mL.min-1. HPLC analyses were performed on a Merck-Hitachi L-7000 system equipped with a diode array UV/Vis spectrometer and Macherey Nagel Nucleosil C18 columns (5µm particle size, 100 Å pore size, 250 x 3 mm) for radioactive compounds.

HPLC solvents were acetonitrile(0.1% TFA, solvent B) in water (0.1%TFA, solvent A). Gradient B: 0-3 min 0% B, 3-20 min 0-100% B, 20-25 min 100% B, 25-30 min 100%-0% B, flow 0.3 mL.min-1; Gradient C: 0-3 min 0% B, 3-40 min 0-100% B, 40-42 min 100% B, 42-45 min 100%-0% B, Gradient D: 0-5 min 5% B, 5-20 min 5-18% B, 20-30 min 18% B, 30-35 min 18%-5% B, flow 0.5 $mL.min^{-1}$. Gradient E: 0-3 min 5% B, 3-20 min 5-20% B, 20-30 min 20%, flow 0.5 $mL.min^{-1}$. Gradient F: 0-3 min 5% B, 3-20 min 5-30% B, 20-30 min 30%, flow 0.5 $mL.min^{-1}$. Preparative HPLC was performed on a Varian ProStar system by using a Macherey-Nagel VP 250/40 Nucleosil 100-7 C18 column with a flow rate of 40 $mL.min^{-1}$. The mobile phase for preparative HPLC consisted of 0.1% aqueous trifluoroacetic acid (A) and acetonitrile (B). Samples were purified with a linear gradient (100% solvent A to 20% or 30% solvent B over 70min).

8.2 General procedures

8.2.1 In vitro evaluation of glucose derivatives

Hexokinase assay: The cold rhenium complexes were tested for their ability to inhibit glucose phosphorylation by hexokinase. Commercial yeast hexokinase has been used instead of human HK1. The phosphotransferase activity was followed spectrophotometrically by reduction of $NADP^+$ in the presence of an excess of G6PDH. Our assay was validated and confirmed using a known HK inhibitor 2-N-acetyl glucosamine. Stock solution of 10^{-2} M of the complexes 5.2a, 5.8a, 5.16a in triethanolamine hydrochloride buffer (TEOA; Ph=7.6) have been prepared. Inhibition with respect to glucose was studied at three different concentrations. The reagent for the determination of inhibitory effect of the compounds on HK was a reaction mixture composed of 0.1 M TEOA, 100 µL of 10 mM NADP, 50 µL of 0.66 mM ATP, 200 µL of 10 mM $MgCl_2$, 100-200 µL of 1 mM glucose, 5 µL of a stock solution of glucose-6-phosphate dehydrogenase (G6PDH; 140 U/mL). After 5 min of pre-incubation of the enzyme with the compound in the assay buffer, the reaction mixture was added to trigger off the reaction (The final total volume was 1 ml). The

rate of NADPH formation was determined by measuring the increase in absorbance at 340 nm.

Protocol for the uptake studies:

The uptake of radiolabeled glucose derivatives was evaluated in five cancer cell lines, for different incubation periods (5, 15, 30 and 60 min) at 37ºC

- A431 vulva carcinoma cells
- HT-29 colon carcinoma cells
- MDA-MB-231 breast carcinoma cells
- MCF-7 breast carcinoma cells
- A2780 ovarian carcinoma cells

Radiolabeling of glucose derivatives with ^{99m}Tc(I) for cell upake: Na[$^{99m}TcO_4$] was eluted from a ^{99}Mo/^{99m}Tc generator, using 0.9% saline. Using a Covidean kit, the precursor fac-[$^{99m}Tc(CO)_3(H_2O)_3]^+$ was prepared and its radiochemical purity checked by RP-HPLC. Radioconjugates ^{99m}Tc-G1, ^{99m}Tc-G2, ^{99m}Tc-G3 and ^{99m}Tc-G4 were obtained by reaction of the conjugates G1-G4 with *fac*-[$^{99m}Tc(H_2O)_3(CO)_3]^+$. Briefly, a solution of *fac*-[$^{99m}Tc(H_2O)_3(CO)_3]^+$ (450 μL) was added to a capped vial, previously flushed with N_2, containing conjugates G1-G4 (50-60 μL, 10^{-4} M). The mixture reacted for 20-40 min, at 90ºC and the radiochemical purity of radiolabeled glucose derivatives was checked by RP-HPLC in a C18 Nucleosil column (250/4 mm, 10 μm) eluted with flow rate of 1.0 mL min^{-1} and using the following method: (mobile phase A, 0.1% TFA aq; mobile phase B, CH3CN) 0–3 min, 100% A; 3-20 min, 0–100% B; 20–28 min, 100% B; 28-29 min, 100–0% B; 29-30 min, 100% A.

Cell culture: Cells were grown in DMEM containing GlutaMax I or RPMI 1640 supplemented with 10% heat-inactivated fetal bovine serum and 1% penicillin/streptomycin antibiotic solution (all from Gibco-Invitrogen). Cells were cultured in a humidified atmosphere of 95% air and 5% CO_2 at 37°C with the medium changed every other day. The cells were adherent in monolayers and, when confluent, were harvested from the cell culture flasks with trypsin EDTA and seeded farther apart.

Uptake assays: cells were seeded at a density of 0.2 million per well in plates of 24 wells and allowed to attach overnight. The cells were incubated at 37 ºC for a period of 5, 15, 30 and 60 min with about 200,000 cpm of the ^{99m}Tc-labeled glucose derivatives in 0.5 mL of assay medium (MEM with 25 mM N-(2-hydroxyethyl)piperazine-N-ethanesulfonic acid). Incubation was terminated by removing the radiocomplexes and washing the cells with ice-cold assay medium. The cells were subsequently lysed by 10 min incubation with 1 M NaOH at 37 ºC and the radioactivity in the lysate fraction was measured in a gamma counter.

8.2.2 Determination of binding affinity and specificity using solubilized integrins

The inhibitory activity and selectivity of L4 and [Re(L4)(CO)$_3$] were determined using an ELISA assays based on previously reported methods with some optimizations.(*150, 151*)

Human integrins $\alpha_v\beta_3$ and $\alpha_v\beta_5$ were purchased from Millipore, αIIbβ3 from Enzyme Research Laboratories, $\alpha_5\beta_1$ and $\alpha_v\beta_3$ from R&D Systems. Vitronectin was purchased from Millipore, fibronectin from Sigma, fibrinogen from Calbiochem and LAP protein from R&D Systems.

Blocking and binding steps were always performed with TS buffer (20 mM Tris-HCl pH 7.5, 150 mM NaCl, 1 mM $CaCl_2$, 1 mM $MgCl_2$, and 1 mM $MnCl_2$) containing 1% BSA (TSB-buffer). Washing steps after the incubation time were done with PBST buffer (10mM Na_2HPO_4, pH 7.5, 150 mM NaCl, and 0.01% Tween 20).

For the integrins $\alpha_v\beta_3$ and $\alpha_v\beta_5$, the binding was visualized using a Mouse anti-human integrin α-V monoclonal antibody for α_v subunit (MAB 1978 purchased from Chemicon); for $\alpha_5\beta_1$ and $\alpha_{IIb}\beta_3$ were used antibodies from BD Biosciences (mouse anti-human CD49e for $\alpha_5\beta_1$ and mouse antihuman CD41b for $\alpha_{IIb}\beta_3$) and Sigma (anti-mouse IgG-peroxidase). Peroxidase development was performed using the substrate solution 3,3,5,5'-tetramethylethylenediamine (TMB from Seramun Diagnostic GmbH) and 3 M H_2SO_4 to stop the reaction.

The absorbance (450, 492 nm) was recorded with a POLARstar Galaxy plate reader

(BMG Labtechnologies). Every concentration was analyzed in duplicate and the resulting inhibition curves were analyzed using OriginPro 7.5G software. Each plate also contained either Tirofiban (*152*) or Cilengitide (*139*) as reference compounds.

$\alpha_v\beta_3$ assay. Flat-bottom 96-well ELISA plates (from Brand) were coated with 100 µL of vitronectin (2µg/mL) overnight at 4 °C in 15 mM of Na_2CO_3, 35 mM $NaHCO_3$, pH 9.6 (carbonate buffer).

After removal of the coating solution, the wells were blocked for 1h at R.T. with 150 µL/well of TSB. Plates were then washed three times with 200 µL/well of PBST.

Next, 4.0 µg/mL of soluble integrin $\alpha_v\beta_3$ and a serial dilution of integrin inhibitors and the control cilengitide were incubated in the coated wells for 2 h at r.t.

After washing three times, the plate was treated with 100 µL/well of primary antibody (MAB1978 diluted 1:500 in TSB) and the secondary antibody (antimouse IgG-peroxidase) at 2.0 µg/mL for 1 h at r.t. After three washing steps, integrin binding was visualized with TMB. The oxidation was allowed to proceed for 5 min, and the product absorbance was measured at 450 nm.

$\alpha_v\beta_6$ assay. For this assay, ELISA plates were coated with 100 µL of LAP protein (0.4 µg/mL) overnight at 4 °C in coating TS buffer. Blocking and washing steps were performed as described for $\alpha_v\beta_3$. Next, 0.5 µg/mL of soluble integrin αvβ6 and a serial dilution of integrin inhibitors and the control cilengitide were incubated in the coated wells for 1 h at r.t. All subsequent steps were performed as described for $\alpha_v\beta_3$.

αvβ5 assay. ELISA plates were coated with 100 µL of vitronectin (5µg/mL) overnight at 4 °C in coating TS buffer. Blocking and washing steps were performed as described for $\alpha_v\beta_3$. Next, 3.0 µg/mL of soluble integrin $\alpha_v\beta_5$ and a serial dilution of integrin inhibitors and the control cilengitide were incubated in the coated wells for 1 h at r.t. After washing three times, the plate was incubated with 100 µL/well of primary antibody (MAB1978) diluted 1:500 in TSB and secondary antibody (antimouse IgG-peroxidase) at 1.0 µg/mL for 1 h at r.t. All subsequent steps were performed as described for $\alpha_v\beta_3$.

$\alpha_5\beta_1$ assay. Flat-bottom 96-well ELISA plates were coated overnight at 4 °C with 100 µL/well of 0.50 µg/mL of fibronectin in carbonate buffer (see $\alpha_v\beta_3$). Blocking and

washing steps were performed as described. Next, 1.0 µg/mL of soluble integrin α5β1 and a serial dilution of integrin inhibitors and the control cilengitide were incubated in the coated wells for 1 h at r.t. After washing three times, the plate was treated with 100 µL/well of primary antibody (CD49e) at 1.0 µg/mL (1:500 dilution) and secondary antibody (antimouse IgG-peroxidase) at 2.0 µg/mL (1:385 dilution) for 1 h at r.t. All subsequent steps were performed as described for $\alpha_v\beta_3$

$\alpha_{IIb}\beta_3$ assay. ELISA plates were coated overnight at 4 °C with 100 µL/well of 10.0 µg/mL of fibrinogen in carbonate buffer. After washing and blocking, 2.5 µg/mL of soluble integrin $\alpha_{IIb}\beta_3$ and a serial dilution of integrin inhibitors and the control molecules cilengitide and tirofiban were incubated in the coated wells for 1 h at r.t. After three washing steps, wells were treated with 100 µL/well of primary antibody (CD41b) at 2.0 µg/mL (1:250 dilution) and secondary antibody (anti-mouse IgG-peroxidase) at 1.0 µg/mL (1:770 dilution) for 1 h at r.t. All subsequent steps were performed as described for $\alpha_v\beta_3$.

8.2.3 Determination of binding affinity using M21 cells

The in vitro integrin binding affinities were assessed via a cellular displacement assay using 125I-echistatin as an integrin specific radioligand on M21 human melanoma cells. One day prior to the experiment M21 cells were harvested using trypsin/EDTA (0.05 % and 0.02 %) in PBS (Biochrom), centrifuged and re-suspended in culture medium. The cells were transferred into 24-well plates (approx. 200'000 cells per well in 1 mL) and placed in the incubator overnight. The plates were used when confluence reached approx. 80 %. Before the experiment the culture medium was removed and binding buffer (20 mM tris(hydroxymethyl)aminomethane (Tris) pH 7.4, 150 mM NaCl, 2 mM $CaCl_2 \cdot 2H_2O$, 1 mM $MgCl_2 \cdot 6H_2O$, 1 mM $MnCl_2 \cdot 4H_2O$, 0.1 % (m/m) BSA) was added. The cells were incubated with ^{125}I-echistatin (120.000 – 140.000 cpm/well) and increasing concentrations of the RGD ligands (10-11 – 10^{-4} mol/L), both dissolved in binding buffer. The total incubation volume was adjusted to 500µL by addition of binding buffer. After the cells were incubated for 2 h

at r.t. the supernatant was removed and the cells were washed twice with cold PBS. The cells were lysed with 1 M sodium hydroxide solution and transferred to vials. Quantification of bound radioactivity was performed using a gamma counter. The experiments were performed in duplicate and repeated three times. The best-fit IC50 (inhibitory concentration of 50 %) values were calculated by fitting the data by nonlinear regression using GraphPad Prism (GraphPad Software, Inc.).

8.2.4 In vivo biodistribution study

To establish tumor growth, 1.5·107 M21 melanoma cells were injected subcutaneously into the shoulder of female CD1 nu/nu mice (Charles River, Sulzfeld, Germany).(*153*) At the time of the experiment (app. 6 weeks after cell inoculation), tumor masses ranged from 32-250 mg. For the biodistribution study, 740 kBq of [^{99m}Tc(L4)(CO)$_3$] in 100 µL of PBS were injected intravenously into the tail vein of the M21 tumor bearing nude mice (n=5). To demonstrate $\alpha_v\beta_3$ integrin specificity of tumor accumulation, mice (n=3) were co-injected with 590 µg Cilengitide per mouse (23.5 mg/kg body weight). At 60 min post injection (p.i.) mice were sacrificed, and the organs of interest were dissected, weighed and counted in a Gamma counter (Wallach, Turku). Data are given in percent of injected dose per gram tissue [%ID/g] and represent means ± standard deviation.

8.3 Synthesis and characterization of compounds in Chapter 3

Ethyl (hydroxyimino)cyanoacetate (3.1a) To a solution of $NaNO_2$ (7.5g, 0.1 mol) in water (40 ml) cooled in an ice bath was added ethyl cyanoacetate (10.2 g, 0.09 mol), followed by acetic acid (7.5 g, 0.12 mmol). The reaction mixture was stirred at 0 °C for two hours. The solution was filtered, and the yellow solid was treated with 12 % aq. HCl (22.5 ml). The resulting solution was extracted with diethyl ether, dried with anhydrous $CaCl_2$, and evaporated. The resulting white precipitate was recrystallized from water to yield (10 g, 78 %) of the product. ^{1}H NMR (200 MHz, D_2O): δ 4.32(q, 2H, *J* = 7.2 Hz), 1.25(t, 3H, *J* = 7.2 Hz).

Ethyl-2-amino-2-cyanoacetate (p-TsOH salt) (3.2a) To a solution of ethyl

(hydroxyimino)cyanoacetate (10 g, 70.4 mmol) in water (50 ml) and sat aq. $NaHCO_3$ (40 ml) was added $Na_2S_2O_4$ (15 g) and the resulting mixture was stirred at 35°C for 30 min. The mixture was extracted with CH_2Cl_2.The combined organic phase was then washed with brine and dried over $MgSO_4$, and the volatiles were removed under reduced pressure. The residue was dissolved in Et_2O and the solution treated with TsOH (9 g, 47.3 mmol) in EtOH. After addition of Et_2O and cooling, the precipitate was removed by filtration, washed with cold Et_2O, and dried under reduced pressure to provide (6.4 g, 30%) of compound **3.2** as a white solid. ^{1}H NMR (200 MHz, CD_3OD): δ 7.67-7.72(m, 2H), 7.20-7.25(m, 2H), 4.41(q, 2H, *J* = 7.2Hz), 2.36(s, 3H), 1.36(t, 3H, *J* = 7.2 Hz).

Ethyl 2-(tert-butoxycarbonylamino)-2-cyanoacetate (3.3a) To a solution of Ethyl-2-amino-2-cyanoacetate (p-TsOH salt) (4.80 g, 16 mmol) in toluene (17 ml) was added Boc_2O (6.11 g, 28 mmol) and DIPEA (2.07 g, 16 mmol).The reaction mixture was heated at 100 ºC in an oil bath for 5 h and was then cooled to room temperature, water(15 ml) was added and the mixture was extracted with EtOAc. The organic layer was separated, washed with aq.$NaHCO_3$, H_2O, and brine, dried ($MgSO_4$), and concentrated. Purification on silica gel eluting gradually with 20% EtOAc/hexanes, 50% EtOAc/hexanes provided compound **3.3** (3.1 g, 13.6 mmol, 85%) as a white solid. ^{1}H NMR (200 MHz, $CDCl_3$): δ 5.33(s, 1H), 5.27(s, 1H), 4.35(q, 2H, *J* = 7.2 Hz), 1.47(s, 9H), 1.34(t, 3H, *J* = 7.2Hz).

Compound **3.3** was synthesized according to the analogous procedure described for **3.3a**. Compound **3.4**, **3.5** were prepared according to the literature procedure.(*146, 147*)

Methanesulfonic acid 2-[2-(2-benzyloxy-ethoxy)-ethoxy]-ethylester (3.6) To a stirred solution of compound **3.5** (5 g, 0.02 mol) and methanesulfonylchloride (2.52, 0.022 mol) in dichloromethane (30 ml) cooled to 0 °C was slowly added TEA (2.22 g, 0.022 mol). The mixture was allowed to warm to room temperature, and stirring was continued for 2 h. The solution was diluted with 20ml dichloromethane and washed with water, brine, dried ($MgSO_4$), and concentrated to give a pale yellow oil (6.24 g, 98%). ^{1}H NMR (200 MHz, $CDCl_3$): 7.31-7.34(m, 5H), 4.53(s, 2H), 3.60-3.75(m, 12H), 3.00(s, 3H). ^{13}C NMR (50 MHz, $CDCl_3$): 138.17, 128.38, 127.75, 127.65, 73.20, 70.60, 70.54, 69.40, 68.98, 37.63.

1-((2-(2-(2-iodoethoxy)ethoxy)ethoxy)methyl)benzene (3.7) To a solution of **3.6** (8 g, 25.1 mmol) in 2-butanone (150 mL) was added sodium iodide (4.48 g, 29.9 mmol). The solution was refluxed for 6 h, concentrated, diluted with water, and extracted with EtOAc. The organic layer was separated, washed with 10% $Na_2S_2O_3$ and brine, dried, and evaporated. Silica gel chromatography, eluting with hexane-EtOAc (6:1), gave **3.7** (7.9 g, 90%) as a colourless oil. ^{1}H NMR (400 MHz, $CDCl_3$): δ 7.32-7.34(m, 5H), 4.55(s, 2H), 5.40(s, 1H), 3.75(t, 2H, *J* = 7.0 Hz), 3.62-3.68(m, 8H), 3.23(t, 2H, *J* = 6.8 Hz). ^{13}C NMR (100 MHz, $CDCl_3$): δ 138.31, 128.40, 127.75, 127.62, 73.27, 72.01, 70.77, 70.69, 70.28, 69.51, 3.12.

Methyl4-(2-(2-(benzyloxy)ethoxy)ethoxy)-2-(tert-butoxycarbonylamino)-2-cyano butanoate (3.8) Metallic sodium (0.23 g, 10 mmol) was dissolved in absolute methanol, and methyl 2-(tert-butoxycarbonylamino)-2-cyanoacetate (2.14g, 10 mmol) was added. After being stirred at 60°C for 30 min, all the methanol was removed under vacuum, the residue was dissolved in 30 ml DMSO, mesylate **3.6** (3.18 g, 10 mmol) was then added, the mixture was stirred at 70°C for 10 h. The DMSO was removed under high vacuum, the remaining material was taken into EtOAc and the solution washed with water, brine and dried over magnesium sulfate, and the volatiles were removed under reduced pressure. The resulting material was chromatographed on silica gel to afford 3.45 g (79%) of **3.8.** ^{1}H NMR (400 MHz, $CDCl_3$): δ 7.28-7.29(m, 5H), 6.63(s, 1H), 4.51(s, 2H), 3.57-3.77(m, 13H), 2.21-2.26(m, 2H), 1.40(s, 9H) ^{13}C NMR (100 MHz, $CDCl_3$) δ 167.08, 154.13, 138.17, 128.25, 128.23, 127.59, 127.49, 127.44, 116.86, 81.21, 73.09, 70.54, 70.45, 70.20, 69.43, 66.84, 58.84, 53.78, 35.78, 28.06, 27.91. HRMS (ESI): Calcd. for $[M + Na]^+$, 459.2102; Found, 459.2106.

Methyl4-(2-(2-(benzyloxy)ethoxy)ethoxy)-2-(tert-butoxycarbonylamino)-2-((tert-butoxycarbonylamino)methyl)butanoate (3.9) To a solution of **3.8** (1.75 g, 4 mmol) in dry MeOH (30 ml) cooled in an ice bath were added Boc_2O (1.74g, 8mmol)and $NiCl_2.6H_2O$ (0.096 g, 0.4 mmol). $NaBH_4$ (1.2 g, 32 mmol) was then added in small portions over 30 min. The solution was allowed to warm to room temperature, and stirring was continued for 3 h. The mixture was filtered through celite and the filtrate

evaporated to dryness *in vacuo*. The residue was taken up in EtOAc and washed with water, brine, dried ($MgSO_4$), and concentrated. Purification on a silica gel column with 33% EtOAc/hexane provided **3.9** (1.58 g, 73%)as a colorless oil. ^{1}H NMR (400 MHz, $CDCl_3$): δ 7.26-7.31(m, 5H), 6.00(s, 1H), 5.07(s, 1H), 4.54(s, 2H), 3.51-3.65(m, 15H), 2.24(s, 1H), 2.11(s, 1H), 1.40(s, 18H). ^{13}C NMR (100 MHz, $CDCl_3$): δ 173.21, 155.72, 154.61, 138.20, 128.32, 127.69, 127.56, 79.59, 79.27, 73.19, 70.58, 70.39, 70.29, 69.42, 66.83, 62.26, 52.47, 44.69, 32.62, 28.29. HRMS (ESI): Calcd. for $[M + Na]^+$, 563.2939; Found, 563.2936.

Methyl2-(tert-butoxycarbonylamino)-2-((tert-butoxycarbonyl)methylamino)-4-(2-(2-hydroxyethoxy)ethoxy)butanoate (3.10) To an anhydrous EtOH (50 ml) solution of **3.9** (2.5 g, 4.6 mmol)was added 10% palladium on carbon (150 mg), the resulting solution was constantly bubbled with hydrogen for 24 hours at room temperature. The catalyst was filtered off, and the solvent was removed under reduced pressure. The residue was purified by silica gel chromatography to yield **3.10** (1.87 g, 90%) as a colorless oil. ^{1}H NMR (400 MHz, $CDCl_3$): δ 6.00(s, 1H), 5.03(s, 1H), 3.51-3.68(m, 15H), 2.77(s, 1H), 2.23(s, 1H), 2.10(s, 1H), 1.38(s, 18H). ^{13}C NMR (100 MHz, $CDCl_3$): δ 173.38, 155.88, 154.58, 79.68, 79.38, 72.47, 70.21, 70.16, 66.73, 62.27, 61.69, 52.54, 44.58, 32.61, 28.28. HRMS (ESI): Calcd. for $[M + Na]^+$, 473.2470; Found, 473.2471.

Methyl4-(2-(2-bromoethoxy)ethoxy)-2-(tert-butoxycarbonylamino)-2-((tert-butoxycarbonylamino)methyl)butanoate (3.11) Compound **3.10** (1.5g, 3.3mmol) was dissolved in dry THF (10 ml), PPh_3 (0.95 g, 3.63 mmol) was added to the solution followed by CBr_4 (1.2 g, 3.63 mmol). The resulting mixture was stirred at RT for 3 h. The solvent was removed *in vacuo* and the residue was purified by silica gel chromatography with 4:1 hexane/ethyl acetate to give 1.05 g (62 %) of product as a colorless oil. ^{1}H NMR (400 MHz, $CDCl_3$): δ 5.96(s, 1H), 5.02(s, 1H), 3.41-3.77(m, 15H), 2.23(s, 1H), 2.10(s, 1H), 1.39(s, 18H) ^{13}C NMR (100 MHz, $CDCl_3$) δ 173.72, 156.40, 155.08, 1, 81.16, 79.83, 71.64, 70.78, 70.69, 67.42, 62.78, 53.00, 45.17, 33.17, 30.61, 28.80. HRMS (ESI): Calcd. for $[M + Na]^+$, 535.1626; Found, 535.1630.

Methyl4-(2-(2-(benzyloxy)ethoxy)ethoxy)-2-(2,2,2-trifluoroacetamido)-2-((2,2,2-trifluoroacetamido)methyl)butanoate (3.12) To a solution of compound **3.9** (810 mg, 1.5 mmol) in DCM (12 ml) was added dropwise TFA (4 mL). After stirring at room temperature for 3 h, the reaction mixture was concentrated *in vacuo* to give yellow oil that was used in the next step without further purification.

To a solution of the crude product in dichloromethane were added NEt_3 (0.8 mL) and trifluoroacetic anhydride (0.8 mL) at 0 °C. The reaction mixture was allowed to warm to room temperature and stirred for 40 min. The solvent was removed *in vacuo*, and the crude product was purified using flash column chromatography (silica gel, DCM/acetone, 60:1) to afford **3.12** as a colorless oil (510 mg, 0.96 mmol, 64%). ^{1}H NMR (400 MHz, $CDCl_3$): δ 8.63(br, 1H), 7.56(br, 1H), 7.33-7.25(m, 5H), 4.55(s, 2H), 3.61-3.98(m, 15H), 2.15-2.19(m, 2H). ^{13}C NMR (100 MHz, $CDCl_3$) δ 170.91, 157.62(q, 2×*C*OCF_3), 138.07, 128.39, 127.77, 127.70, 116.96(q, 2×CO*C*F_3), 73.27, 70.65, 70.58, 70.10, 69.35, 66.93, 63.01, 53.35, 42.98, 32.82. HRMS (ESI): Calcd. for $[M+Na]^+$, 555.1536; Found, 555.1537.

Methyl4-(2-(2-hydroxyethoxy)ethoxy)-2-(2,2,2-trifluoroacetamido)-2-((2,2,2-trifluoroacetamido)methyl)butanoate (3.13) To a solution of **3.12** (500 mg, 0.94 mmol) in ethanol (20 ml) was added 10% Pd/C (100 mg) and the suspension was stirred under hydrogen for 24 h. The suspension was then filtered and the filtrate was concentrated under reduced pressure to give **3.13** as a white solid (407 mg, 98 %). ^{1}H NMR (400 MHz, $CDCl_3$): δ 8.47(br, 1H), 7.68(br, 1H), 3.53-3.99(m, 15H), 2.21(s, 2H). ^{13}C NMR (100 MHz, $CDCl_3$) δ 170.73, 157.42(q, 2×*C*OCF_3), 116.82(q, 2×CO*C*F_3), 72.18, 70.45, 69.85, 66.64, 62.87, 61.46, 53.21, 42.82, 32.54. HRMS (ESI): Calcd. for $[M + H]^+$, 443.1248; Found, 443.1251.

4-(2-(2-(benzyloxy)ethoxy)ethoxy)-2-(tert-butoxycarbonylamino)-2-((tert-butoxycarbonylamino)methyl)butan-1-ol (3.14) To a solution of **3.9** (810 mg, 1.50 mmol) in THF (10.0 mL) was added lithium borohydride (66 mg, 3.03 mmol) at 0°C, The reaction mixture was stirred at room temperature for 20 h, and then treated with saturated aqueous ammonium chloride solution , followed by extraction with CH_2Cl_2, dried over $MgSO_4$ and filtrated. After evaporation of the solvent, the residue was

purified by chromatography on a silica gel column with AcOEt-*n*-hexane (1:2) to afford compound **3.14** (538 mg, 70% yield) as a colorless oil. ^{1}H NMR (400 MHz, $CDCl_3$): δ 7.31-7.32(m, 5H), 5.52(s, 1H), 5.44(s, 1H), 4.54(s, 2H), 3.25-3.64(m, 14H), 1.81-1.96(m, 2H), 1.40(s, 18H). ^{13}C NMR (100 MHz, $CDCl_3$): δ 157.18, 155.75, 138.17, 128.34, 128.31, 127.70, 127.60, 79.51, 79.33, 73.18, 70.61, 70.50, 70.33, 69.42, 66.94, 65.77, 58.96, 43.63, 32.07, 28.36. HRMS (ESI): Calcd. for $C_{26}H_{44}N_2NaO_8$ $[M+Na]^+$, 535.2990; Found, 535.2990.

1-((2-((3,4-bis(tert-butoxycarbonylamino)-3-((tert-butyldimethylsilyloxy)methyl) butoxy)ethoxy)ethoxy)methyl)benzene (3.15) A solution of alcohol **3.14** (800 mg, 1.56 mmol), TBSCl (423 mg, 2.80 mmol), and imidazole (234 mg, 3.43 mmol) in DMF (5 mL) was stirred at 50°C for 20 h. The mixture was then diluted with EtOAc washed with saturated aqueous ammonium chloride solution, water, brine, and dried over Mg_2SO_4. The solvent was evaporated under reduced pressure to afford the crude product which was purified by column chromatography using 15% EtOAc/nHexane (v/v) to afford **3.15** (743 mg, 1.18 mmol) in 76% yield as a colorless oil. ^{1}H NMR (400 MHz, $CDCl_3$): δ 7.29-7.31(m, 5H), 5.46(bs, 2H), 4.53(s, 2H), 3.37-3.80(m, 14H), 1.86-1.96(m, 2H), 1.40(s, 18H), 0.86(s, 9H), 0.03(s, 6H). ^{13}C NMR (100 MHz, $CDCl_3$): δ 157.18, 155.57, 138.77, 128.83, 128.20, 128.06, 79.91, 79.59, 73.73, 71.17, 71.02, 70.74, 69.97, 67.74, 66.37, 58.85, 45.95, 33.19, 28.90, 26.35, 18.62, -5.07.

General Procedure A: Removal of Benzyl protecting group: The benzyl protected alcohol was dissolved in absolute ethanol (40 mL) and 10% Pd/C (20% wt) was added. The mixture was subjected to hydrogenation for 24 h. The catalyst was removed by filtration on celite and the solvent evaporated to afford the alcohol in quantitative yield.

General Procedure B: Conversion of alcohol to azide: MsCl (1.1 equiv) was added to a solution of alcohol at room temperature. The solution was cooled to -78 °C with liquid nitrogen and Et_3N (1.1 equiv) was slowly added via a syringe. After being stirred for 3 h, the solution was diluted with 10ml CH_2Cl_2 and washed with water, brine, dried ($MgSO_4$). CH_2Cl_2 was evaporated completely (very important, to avoid the formation of explosive diazidomethane in the next step) and the residue was

dissolved in DMF. Sodium azide (1.5 equiv) was added to the solution, which was then heated to 70°C for 15 h. After being cooled to room temperature, water was added and the mixture was extracted with AcOEt. The combined organic layers were washed with water, dried over $MgSO_4$, filtered and evaporated. The crude product was purified by flash column chromatography.

General Procedure C: Conversion of azide to amine: To a solution of the azide in ethanol (15 ml) 10% Pd/C (10% wt) was added. The reaction mixture was cooled to 0°C and bubbled with hydrogen gas at pressure of 2 bar for 5 h. The catalyst was filtered off and the filtrate was concentrated under reduced pressure to yield a residue of the amine as colorless oil.

2-(2-(3,4-bis(tert-butoxycarbonylamino)-3-((tert-butyldimethylsilyloxy)methyl)butoxy)ethoxy)ethan-1-ol (3.16) Prepared according to General Procedure A. Starting with **3.15** (0.62 g, 1 mmol) the alcohol was obtained as a colorless oil (0.51 g, 96%). ^{1}H NMR (400 MHz, $CDCl_3$): δ 5.48-5.58(m, 2H), 3.87(d, 1H, *J* = 9.6Hz), 3.49-3.72(m, 13H), 1.88-2.03 (m, 2H), 1.41-1.43(m, 18H), 0.89(s, 9H), 0.05(s, 6H). ^{13}C NMR (100 MHz, $CDCl_3$): δ 156.56, 155.08, 79.02, 78.83, 72.62, 70.35, 67.18, 66.11, 61.73, 58.32, 45.54, 32.55, 28.39, 25.82, 18.11, -5.59. HRMS (ESI): Calcd. for $C_{25}H_{52}N_2NaO_8Si$ $[M + Na]^+$, 559.3385; Found, 559.3389.

1-(2-(3,4-bis(tert-butoxycarbonylamino)-3-((tert-butyldimethylsilyloxy)methyl)butoxy)ethoxy)azidoethane (3.17). Prepared according to General Procedure B. Starting with **3.16** (0.6 g, 1.12 mmol) the azide was obtained as a clear oil (0.5 g, 79%): ^{1}H NMR (400 MHz, $CDCl_3$): δ 5.41(bs, 2H), 3.80(d, 1H, *J* = 12Hz), 3.37-3.65(m, 13H), 1.91-2.01(m, 2H), 1.39-1.41(m, 18H), 0.87(s, 9H), 0.03(s, 6H). ^{13}C NMR (100 MHz, $CDCl_3$): δ 156.90, 155.30, 79.28, 79.10, 70.76, 70.45, 70.27, 67.53, 66.16, 58.50, 50.89, 45.70, 32.91, 28.62, 28.60, 26.05, 18.34, -5.36. HRMS (ESI): Calcd. for $C_{25}H_{51}N_5NaO_7Si$ $[M + Na]^+$, 584.3450; Found, 584.3453.

2-(2-(3,4-bis(tert-butoxycarbonylamino)-3-((tert-butyldimethylsilyloxy)methyl)butoxy)ethoxy)ethanamine (3.18) Prepared according to General Procedure C. Starting with azide **3. 17** the amine was obtained as a clear oil (0.38 g, 80%): ^{1}H NMR (400 MHz, $CDCl_3$): δ 5.44-5.48(m, 2H), 3.82(d, 1H, *J* = 12Hz), 3.37-3.59(m, 11H),

2.84(s, 2H), 1.81-1.91(m, 2H), 1.38-1.40(m, 18H), 0.86(s, 9H), 0.02(s, 6H). ^{13}C NMR (100 MHz, $CDCl_3$): δ 156.92, 155.27, 79.25, 79.02, 73.56, 70.40, 70.37, 67.43, 66.17, 58.52, 45.67, 41.96, 32.85, 28.59, 26.03, 18.31, -5.38. HRMS (ESI): Calcd. for $C_{25}H_{53}N_3NaO_7Si$ $[M + Na]^+$, 558.3545; Found, 558.3546.

Diethyl2-(2-(2-(2-(benzyloxy)ethoxy)ethoxy)ethyl)-2-(tert-butoxycarbonylamino) malonate (3.19) To a solution of diethyl 2-(*N*-(*tert*-butoxycarbonyl)amino)malonate (1.2 g, 4.27 mmol) in THF (30mL) was added NaH (60% in mineral oil, 170 mg , 4.25 mmol) and iodide **3.7** (1.0 g, 2.85mmol) at room temperature, The resulting solution was refluxed for 10 h. After evaporation of the solvent under reduced pressure, the crude product was purified by column chromatography over silica gel with n-hexane/EtOAc (v/v, 5/1) as the eluent to afford a colorless oil (1.3 g, 92%). ^{1}H NMR (400 MHz, $CDCl_3$): δ 7.33-7.34(m, 5H), 6.09(s, 1H), 4.55(s, 2H), 4.13-4.26(m, 4H), 3.48-3.64(m, 10H), 2.59(s, 2H), 1.42(s, 9H), 1.23(t, 6H, J = 7Hz). ^{13}C NMR (100 MHz, $CDCl_3$): δ 168.36, 154.10, 138.32, 128.38, 127.73, 127.60, 80.08, 73.25, 70.60, 70.49, 70.30, 69.50, 66.38, 64.61, 62.24, 32.92, 28.26, 13.95. MS-ESI: m/z 520.2(calcd. for $C_{25}H_{39}NNaO_9$: 520.25) [$(M + Na)^+$]. HRMS (ESI): Calcd. for $C_{25}H_{39}NNaO_9$ $[M + Na]^+$, 520.2517; Found, 520.2512.

2-amino-2-(2-(2-(2-(benzyloxy)ethoxy)ethoxy)ethyl)malonamide (3.23) To a solution of diester **3.19** (1.0 g, 2 mmol) in DCM (10 mL) was added trifluoroacetic acid (5 mL). The resulting mixture was stirred at room temperature for 3 h. After removal of volatile material, the residue was dissolved in MeOH (10 ml). 25% aq NH_3 (10 ml) was slowly added and the mixture was stirred at room temperature for 20 h. After this time, the solvent was evaporated to leave a white solid residue, which was dissolved in CH_2Cl_2 and washed with water. The organic phase was dried, filtered and concentrated and the residue was purified by column chromatography over silica gel with EtOAc as the eluent to afford the diamide **3.23** as a colorless oil(0.52 g, 76%).^{1}H NMR (400 MHz, $CDCl_3$): δ 7.83(bs, 2H), 7.26-7.34(m, 5H), 6.43(bs, 2H), 4.55(s, 2H), 3.53-3.65(m, 10H), 2.57(bs, 2H), 2.21(t, 2H, J=5.6Hz). ^{13}C NMR (100 MHz, $CDCl_3$): δ 175.53, 138.18, 128.37, 127.76, 127.62, 73.21, 70.53, 70.35, 70.29, 69.45, 68.01, 64.82, 32.45. MS-ESI: m/z 340.2 (calcd. for

$C_{16}H_{26}N_3O_5$:340.19)[(M + H)$^+$]. HRMS (ESI): Calcd. for $C_{16}H_{26}N_3O_5$ [M + H]$^+$, 340.1867; Found, 340.1866.

1-((2-((3,4-bis(tert-butoxycarbonylamino)-3-((tert-butoxycarbonylamino)methyl) butoxy)ethoxy)ethoxy)methyl)benzene (3.24) To a stirred solution of lithium aluminium hydride ($LiAlH_4$) (0.56 g, 14.76 mmol) in THF (33 ml) at 0 ^oC was added diamide **3.23** (1 g, 2.95 mmol) in THF (7 ml) via a syringe. The mixture was allowed to warm to room temperature and refluxed for 24 hours, after which time it was quenched with water (0.7 mL), 15% aqueous NaOH (0.7 ml), and water (1.8 mL) again. The resulting suspension was filtered through celite and evaporated to afford a colorless syrup that was used in the next step without purification. To a mixture of above residue and $NaHCO_3$ (0.76 g, 9.0 mmol) in H_2O (12 mL) was added Boc anhydride (1.97 g, 9.0 mmol) in dioxane (12 mL). The mixture was stirred for 24 h at room temperature. After this time, the solution was diluted with water and extracted with CH_2Cl_2. The organic phase was dried, filtered and concentrated to leave a crude product, which was purified by column chromatography using 25% EtOAc/hexanes as the eluent. Evaporation of the solvent afforded **3.24** as a colorless oil (0.9 g, 50%). ^{1}H NMR (400 MHz, $CDCl_3$): δ 7.27-7.28(m, 5H), 5.57-5.65(m, 3H), 4.50(s, 2H), 3.52-3.62(m, 10H), 3.31-3.32(m, 2H), 3.18-3.20(m, 2H), 1.90(t, 2H, *J* = 6 Hz), 1.34-1.38(m, 27H). ^{13}C NMR (100 MHz, $CDCl_3$): δ 157.64, 155.70, 138.73, 128.85, 128.20, 128.08, 79.87, 79.36, 73.72, 71.08, 70.95, 70.59, 69.97, 67.42, 59.63, 44.70, 33.20, 28.88, 28.86. HRMS (ESI): Calcd. for $C_{31}H_{53}N_3NaO_9$ [M + Na]$^+$, 634.3674; Found, 634.3670.

2-(2-(3,4-bis(tert-butoxycarbonylamino)-3-((tert-butoxycarbonylamino)methyl)b utoxy)ethoxy)ethan-1-ol (3.25) Compound **3.25** was prepared from **3.24** according to General Procedure A, quantitative yield, colorless oil. ^{1}H NMR (400 MHz, $CDCl_3$): δ 5.60-5.72(m, 3H), 3.52-3.67(m, 10H), 3.17-3.38(m, 4H), 1.90(s, 2H), 1.34-1.38(m, 27H). ^{13}C NMR (100 MHz, $CDCl_3$): δ 157.39, 155.42, 80.01, 79.76, 72.78, 70.52, 70.19, 67.14, 61.88, 59.37, 44.40, 32.91, 28.53, 28.50. HRMS (ESI): Calcd. for $C_{24}H_{47}N_3NaO_9$ [M + Na]$^+$, 544.3205; Found, 544.3205.

1-(2-(3,4-bis(tert-butoxycarbonylamino)-3-((tert-butoxycarbonylamino)methyl)b

utoxy)ethoxy)azidoethane (3.26) Compound **3.26** was prepared from **3.25** according General Procedure B**.** yield 84%; colorless oil; ^{1}H NMR (400 MHz, $CDCl_3$): δ 5.55-5.66(m, 3H), 3.53-3.64(m, 8H), 3.16-3.40(m, 6H), 1.92(s, 2H), 1.36-1.40(m, 27H). ^{13}C NMR (100 MHz, $CDCl_3$): δ 157.33, 155.37, 79.65, 79.10, 70.63, 70.20, 70.12, 67.16, 59.31, 50.79, 44.34, 32.90, 28.54, 28.52. HRMS (ESI): Calcd. for $C_{24}H_{46}N_6NaO_8$ $[M + Na]^+$, 569.3269; Found, 569.3267.

2-(2-(3,4-bis(tert-butoxycarbonylamino)-3-((tert-butoxycarbonylamino)methyl)butoxy)ethoxy)ethanamine (3.27) Compound **3.27** was prepared from **3.26** according to General Procedure C**.** yield 75%; colorless oil; ^{1}H NMR (400 MHz, $CDCl_3$): δ 5.71-5.76(m, 3H), 3.22-3.59(m, 12H), 2.96(s, 2H), 1.94(s, 2H), 1.36-1.40(m, 27H). ^{13}C NMR (100 MHz, $CDCl_3$): δ 157.53, 155.54, 79.75, 79.21, 70.52, 70.22, 67.25, 59.33, 44.40, 44.18, 32.91, 28.61, 28.59. HRMS (ESI): Calcd. for $C_{24}H_{49}N_4O_8$[M + H]$^+$, 521.3545; Found, 521.3546.

Diethyl2-(tert-butoxycarbonylamino)-2-(2-(2-(2-hydroxyethoxy)ethoxy)ethyl)malonate (3.20) Compound **3.20** was prepared from **3.19** according to General Procedure A, quantitative yield, colorless oil. ^{1}H NMR (400 MHz, $CDCl_3$): δ 6.02(s, 1H), 4.06-4.16(m, 4H), 3.61(t, 2H, *J* = 4.5Hz), 3.37-3.45(m, 8H), 2.47(s, 2H), 1.31(s, 9H), 1.15(t, 6H, *J* = 7Hz). ^{13}C NMR (100 MHz, $CDCl_3$): 168.40, 154.13, 80.15, 72.45, 70.24, 66.30, 64.59, 62.31, 61.73, 32.90, 28.24, 13.92. HRMS (ESI): Calcd. for $C_{18}H_{33}NNaO_9$: $[M + Na]^+$, 430.2048; Found, 430.2047.

diethyl2-(2-(2-(2-azidoethoxy)ethoxy)ethyl)-2-(tert-butoxycarbonylamino)malonate (3.21) Compound **3.21** was prepared from **3.20** according to General Procedure B**.** yield 77%; colorless oil; ^{1}H NMR (400 MHz, $CDCl_3$): δ 6.02(s, 1H), 4.10-4.22(m, 4H), 3.34-3.59(m, 10H), 2.53(s, 2H), 1.37(s, 9H), 1.19(t, 6H, *J* = 7Hz). ^{13}C NMR (100 MHz, $CDCl_3$): 168.47, 154.20, 80.25, 70.63, 70.35, 70.00, 66.59, 64.72, 62.36, 50.84, 33.00, 28.35, 14.05. MS-ESI: m/z 455.2 (calcd. for $C_{18}H_{32}N_4NaO_8$: 455.21) [$(M + Na)^+$]. HRMS (ESI): Calcd. for $C_{18}H_{32}N_4NaO_8$: $[M + Na]^+$, 455.2112; Found, 455.2110.

diethyl2-(2-(2-(2-aminoethoxy)ethoxy)ethyl)-2-(tert-butoxycarbonylamino)malonate (3.22) Compound **3.22** was prepared from **3.21** according to General Procedure C**.**

yield 75%; colorless oil; ^{1}H NMR (400 MHz, $CDCl_3$): δ 6.04(s, 1H), 4.10-4.20(m, 4H), 3.42-3.48(m, 8H), 2.83(s, 2H), 2.52(s, 2H), 2.18(s, 2H), 1.36(s, 9H), 1.19(t, 6H, *J* = 7Hz). ^{13}C NMR (100 MHz, $CDCl_3$): 168.48, 154.23, 80.25, 72.99, 70.33, 70.29, 66.48, 64.73, 62.39, 41.80, 33.02, 28.37, 14.06. MS-ESI: m/z 407.2(calcd. for $C_{18}H_{35}N_2O_8$:407.24) [$(M + H)^+$]. HRMS (ESI): Calcd. for $C_{18}H_{35}N_2O_8$: $[M + H]^+$, 407.2388; Found, 407.2391.

Ethyl4-(2-(2-(benzyloxy)ethoxy)ethoxy)-2-(tert-butoxycarbonylamino)-2-(hydroxymethyl)butanoate (3.28) To a solution of **3.19** (510 mg, 1.02 mmol) in THF (12 mL), a solution of LiOH monohydrate (64 mg, 1.52 mmol) in H_2O (6 mL) was added dropwise at 0 ˚C. The reaction mixture was warmed to room temperature and stirred for 24 h. the mixture was acidified and extracted with EtOAc. The organic layer was washed with water, dried ($MgSO_4$) and concentrated in *vacuo* to give the crude product which was directly used in the next step without purification.

N, N-Diisopropylethylamine (DIPEA) (210 ul, 1.20mmol) was added to a stirred suspension of above carboxylic acid (0.48 g, 1.02 mmol) and BOP (0.68 g, 1.53 mmol) in 6 ml of THF at room temperature, The resulting solution was stirred for 10 min, then $NaBH_4$ (57.9 mg, 1.53 mmol) was added. After stirring overnight, the solvent was evaporated and the residue was taken up in diethyl ether and washed with 5% HCl, saturated $NaHCO_3$ and brine, then dried ($MgSO_4$) and evaporated to give a colorless oil, which was chromatographed on silica gel (n-hexane : ethyl acetate = 2 : 1) to afford **12** as a colourless oil(0.25 g, 54%).^{1}H NMR (400 MHz, $CDCl_3$): δ 7.25-7.26(m, 5H), 5.93(s, 1H), 4.48(s, 2H), 4.15(q, 2H, *J* = 7Hz), 3.49-3.91(m, 12H), 2.09-2.18(m, 2H), 1.35(s, 9H), 1.18(t, 3H, *J* = 7Hz). ^{13}C NMR (400 MHz, $CDCl_3$): δ 173.20, 155.81, 138.73, 128.85, 128.21, 128.09, 80.26, 73.74, 71.15, 70.85, 70.80, 69.95, 67.52, 66.81, 63.89, 62.01, 33.07, 28.80, 14.60. HRMS (ESI): Calcd. for $C_{23}H_{37}NNaO_8$ $[M + Na]^+$, 478.2411; Found, 478.2413.

Ethyl4-(2-(2-(benzyloxy)ethoxy)ethoxy)-2-(tert-butoxycarbonylamino)-2-((tert-butyldimethylsilyloxy)methyl)butanoate (3.29) To a solution of **3.28** (0.46 g, 1.01 mmol) in DMF (6 mL) were added TBSCl (0.23 g, 1.5 mmol) and imidazole (0.10 g, 1.5 mmol), and the mixture was stirred for 20 h. After this time, the mixture was

diluted with water then extracted with ethyl acetate three times. The combined organic phase was dried, filtered and concentrated to leave a crude brown oil. This oil was purified by column chromatography using a 15% EtOAc/hexanes gradient as the eluent. Evaporation of the solvent afforded the O-protected compound **3.29** as a colorless oil (0.5 g, 87%) ^{1}H NMR (400 MHz, $CDCl_3$): δ 7.29-7.30(m, 5H), 5.72(s, 1H), 4.52(s, 2H), 4.08-4.18(m, 3H), 3.53-3.76(m, 11H), 2.30-2.33(m, 1H), 2.02-2.06(m, 1H), 1.39(s, 9H), 1.23(t, 3H, J=7Hz), 0.81(s, 9H), 0.03(s, 6H). ^{13}C NMR (400 MHz, $CDCl_3$): δ 172.91, 154.72, 138.80, 128.83, 128.20, 128.05, 79.44, 73.74, 71.12, 70.99, 70.75, 69.95, 67.22, 65.43, 63.91, 61.86, 31.64, 28.90, 26.20, 18.62, 14.61, -5.12. HRMS (ESI): Calcd. for $C_{29}H_{52}NO_8Si$ $[M + H]^+$, 570.3457; Found, 570.3459.

Ethyl2-(tert-butoxycarbonylamino)-2-((tert-butyldimethylsilyloxy)methyl)-4-(2-(2-hydroxyethoxy)ethoxy)butanoate (3.30) Prepared according to General Procedure A from **3.29**. The desired alcohol was obtained as a white solid(quantitative yield). ^{1}H NMR (400 MHz, $CDCl_3$): δ 5.71(s, 1H), 4.04-4.15(m, 3H), 3.63-3.70(m, 3H), 3.40-3.50(m, 8H), 2.62(s, 1H), 2.27-2.30(m, 1H), 1.98-2.04(m, 1H), 1.35(s, 9H), 1.19(t, 3H, *J* = 7Hz), 0.76(s, 9H), 0.07(s, 6H). ^{13}C NMR (400 MHz, $CDCl_3$): δ 173.04, 154.72, 79.52, 72.88, 70.78, 70.70, 67.13, 65.43, 63.91, 62.27, 61.97, 31.61, 28.89, 26.18, 18.61, 14.57, -5.15. HRMS (ESI): Calcd. for $C_{22}H_{45}NNaO_8Si$ $[M + Na]^+$, 502.2807; Found, 502.2812.

2-(2-(2-(3-(tert-butoxycarbonylamino)-3-((tert-butyldimethylsilyloxy)methyl)-4-ethoxy-4-oxobutoxy)ethoxy)ethoxy)acetic acid (3.31) To a stirred solution of alcohol **3.30** (0.63 g, 1.32 mmol) in dry THF (40 mL) was added sodium iodoacetate (0.35 g, 1.68 mmol) and NaH (67 mg, 1.68 mmol, 60% oil dispersion) at 0 °C. The reaction was allowed to warm to room temperature and stirred overnight. The mixure was diluted with water and acidified with 5% HCl. The aqueous phase was saturated with sodium chloride and extracted with EtOAc three times. The combined organic layers were dried over $MgSO_4$, filtered and concentrated. The residue was purified by flash chromatography over silica gel to yield carboxylic acid **3.31** (0.48 g, 67% yield) as a colourless oil. ^{1}H NMR (400 MHz, $CDCl_3$): δ 5.70(s, 1H), 4.10-4.16(m, 5H),

3.45-3.70(m, 11H), 2.30-2.33(m, 1H), 2.03-2.07(m, 1H), 1.39(s, 9H), 1.23(t, 3H, *J* = 6.8Hz), 0.80(s, 9H), 0.04(s, 6H). ^{13}C NMR (400 MHz, $CDCl_3$): δ 172.51, 154.27, 79.15, 71.35, 70.49, 70.13, 69.97, 68.92, 66.73, 64.96, 63.45, 61.49, 31.06, 28.41, 25.70, 18.13, 14.13, -5.56. MS-ESI: m/z 538.2 (calcd. for $C_{24}H_{48}NO_{10}Si$:538.30) [$(M + H)^+$].

8.4 Synthesis and characterization of compounds in Chapter 4

Compound **4.1**-**4.2**, **4.7**-**4.8** were prepared according to the literature method.(*105*)

(S)-benzyl 2-(benzyloxycarbonylamino)-6-(methylsulfonyloxy)hexanoate (**4.9**)**.** To a stirred solution of **4.8** (2g, 5.4 mmol) and H_3CSO_2Cl (0.466 mL, 6 mmol) in CH_2Cl_2 (10 mL) cooled to -78 °C, NEt_3 (0.797 mL, 6 mmol) was slowly added. The mixture was allowed to come to r.t., and stirring was continued for 3 h. The solution was diluted with 10 mL CH_2Cl_2, washed with H_2O, dried over $MgSO_4$, and evaporated. The crude product was purified by flash column chromatography (33% Et_2O in hexane) to give **7** as a pale yellow oil (2.3 g, 5.12 mmol, 95%). R_f =0.77 (SiO_2, TLC, Et_2O). ^{1}H NMR (400 MHz, $CDCl_3$): δ 7.26(s, 10H), 5.61(d, 1H, *J*=8Hz), 5.02-5.13(m, 4H), 4.34(d, 1H, *J* = 5.2Hz), 4.03(t, 2H, *J*= 6.2 Hz), 2.81(s, 3H), 1.32-1.78(m, 6H). ^{13}C NMR (100 MHz, $CDCl_3$): δ172.68, 156.58, 136.89, 135.91, 128.59-129.26, 70.12, 67.66, 67.44, 54.28, 37.66, 32.27, 29.02, 21.84. *Anal.* Calcd. for $C_{22}H_{27}NO_7S$: C, 58.78; H, 6.05; N, 3.12. Found: C, 58.39; H, 5.99; N, 3.04. MS-ESI: m/z 472.1(calcd. 472.15) [$(M + Na)^+$]

(S)-benzyl 2-(benzyloxycarbonylamino)-6-iodohexanoate (4.10) Sodium iodide (0.64 g, 4.26 mmol) was added to a solution of mesylate **4.9** (1.6 g, 3.6 mmol) in 2-butanone (30 ml) at room temperature. The reaction was stirred at 80°C for 3 h. After this time, the solvent was evaporated *in vacuo* to near dryness and the residue was partitioned between EtOAc and water. The organic extract was washed with 10% $Na_2S_2O_3$, dried over Na_2SO_4, and concentrated *in vacuo*. The crude product was purified by flash chromatography eluting with hexane/ethyl acetate (5:1) to give **4.10** as a colorless oil (1.44 g, 83%). ^{1}H NMR (400 MHz, $CDCl_3$): δ 7.30(s, 10H), 5.45(d, 1H, *J* = 8Hz), 5.15-5.20(m, 4H), 4.45-4.50(m, 1H), 3.13(t, 2H, *J* = 6.8Hz),

1.71-1.90(m, 4H), 1.38-1.48(m, 2H). ^{13}C NMR (100 MHz, $CDCl_3$): δ 172.15, 155.88, 136.26, 135.27, 128.70, 128.59, 128.44, 128.24, 128.14, 67.27, 67.06, 53.71, 32.76, 31.53, 26.03, 6.08. HRMS (ESI): Calcd. for $C_{21}H_{24}INNaO_4$ $[M + Na]^+$, 504.0642; Found, 504.0638.

(S)-tert-butyl 6-acetoxy-2-(benzyloxycarbonylamino)hexanoate (4.3) To a solution of **4.2** (3.5 g, 12.5 mmol) and sodium acetate (1.03 g , 12.5 mmol) in acetic acid (90 ml) was added sodium nitrite (2.8 g, 40.6 mmol) at room temperature. After stirring for 6 h at 40 °C, the reaction mixture was concentrated *in vacuo* and the pale yellow, oily residue was used in the next reaction without further purification.

To a solution of the carboxylic acid prepared above in *t*-BuOH (80 mL) was added 4-Dimethylaminopyridine (0.49 g, 4 mmol) and Boc_2O (4.36 g, 20 mmol). After stirring for 24 h, the reaction mixture was concentrated and the residue was purified via silica gel column chromatography eluting with 25% EtOAc/hexanes to give **4.3** (2.5 g, 53%) as a colorless oil. ^{1}H NMR (400 MHz, $CDCl_3$): δ 7.38-7.39(s, 5H), 5.35(d, 1H, *J* = 8Hz), 5.14(s, 2H), 4.26-4.30(m, 1H), 4.07(t, 2H, *J* = 6.5Hz), 2.06(s, 3H), 1.67-1.86(m, 4H), 1.36-1.49(m, 11H). ^{13}C NMR (100 MHz, $CDCl_3$): δ 171.10, 155.83, 136.36, 128.73, 128.52, 128.31, 128.16, 128.10, 82.12, 66.88, 64.09, 54.19, 32.54, 28.22, 27.99, 27.92, 21.57, 20.95. MS-ESI: m/z 402.2 (calcd. for $C_{20}H_{29}NNaO_6$:402.19) $[(M + Na)^+]$. HRMS (ESI): Calcd. for $C_{20}H_{29}NNaO_6$ $[M + Na]^+$, 402.1887; Found, 402.1890.

(S)-tert-butyl 2-(benzyloxycarbonylamino)-6-hydroxyhexanoate (4.4) To a stirred solution of **4.3** (1.3 g, 3.43 mmol) in methanol (15 mL) was added 1.4 M K_2CO_3 (1.25 g, 9 mmol) in H_2O. The resulting solution was stirred vigorously at rt for 12 h. Methanol was removed under vacuum, and the resulting aqueous solution was extracted with CH_2Cl_2. The organic layer was then dried over anhydrous magnesium sulfate and concentrated under vacuum to provide compound **4.4** as a yellow oil (1.04 g, 90%):. ^{1}H NMR (400 MHz, $CDCl_3$): δ 7.25-7.31(s, 5H), 5.48(d, 1H, *J* = 8Hz), 5.05(s, 2H), 4.18-4.23(m, 1H), 3.55(t, 2H, *J* = 6.2Hz), 2.26(s, 1H), 1.55-1.78(m, 4H). 1.36-1.41(m, 11H). ^{13}C NMR (100 MHz, $CDCl_3$): δ 171.8, 156.12, 136.46, 128.56, 128.18, 128.14, 82.08, 66.91, 62.29, 54.41, 32.63, 32.19, 28.05, 21.49. HRMS (ESI):

Calcd. for $C_{18}H_{27}NNaO_5$ $[M + Na]^+$, 360.1781; Found, 360.1777.

(S)-tert-butyl2-(benzyloxycarbonylamino)-6-(methylsulfonyloxy)hexanoate (4.5) Mesylate **4.5** was prepared from **4.4** according to the preparation of **4.9**: yield 95%. ^{1}H NMR (400 MHz, $CDCl_3$): δ 7.23-7.26(m, 5H), 5.26(d, 1H, *J* = 8Hz), 5.01(s, 1H), 4.09-4.18(m, 3H), 2.88(s, 3H), 1.59-1.75(m, 4H), 1.36-1.39(m, 11H). ^{13}C NMR (100 MHz, $CDCl_3$): δ 171.78, 156.37, 136.84, 129.03, 128.68, 128.60, 82.82, 69.97, 67.40, 54.54, 37.87, 32.78, 29.16, 28.48, 21.62. MS-ESI: m/z 438.3 (calcd. for $C_{19}H_{29}NNaO_7S$: 438.16) $[(M + Na)^+]$. HRMS (ESI): Calcd. for $C_{19}H_{29}NNaO_7S$ $[M + Na]^+$, 438.1557; Found, 438.1558.

(S)-tert-butyl 2-(benzyloxycarbonylamino)-6-iodohexanoate (4.6) Iodide **4.6** was prepared from **4.5** according to the preparation of **4.10**: yield 92%. ^{1}H NMR (400 MHz, $CDCl_3$): δ 7.25-7.29(m, 5H), 5.37(d, 1H, *J* = 8Hz), 5.04(s, 2H), 4.19-4.20(m, 1H), 3.07-3.10(m, 2H), 1.59-1.78(m, 4H), 1.40(s, 11H). ^{13}C NMR (100 MHz, $CDCl_3$): δ 171.87, 156.32, 136.91, 129.02, 128.63, 128.59, 82.69, 67.35, 54.59, 33.34, 32.22, 28.55, 26.38, 6.85. HRMS (ESI): Calcd. for $C_{18}H_{26}INNaO_4$ $[M + Na]^+$, 470.0799; Found, 470.0800.

(7S)-8-benzyl1-ethyl 2-(tert-butoxycarbonylamino)-7-(benzyloxycarbonylamino)-2-cyan ooctanedioate (4.16). Na (0.046 g, 2 mmol) was dissolved in abs. ethanol, and ethyl 2-(tert-butoxycarbonylamino)-2-cyanoacetate (0.46 g, 2 mmol) was added, the mixture was stirred at 60°C for 30 min. After cooling to r.t., ethanol was removed under vacuum, the residue dissolved in DMSO (5 mL), mesylate **4.9** (0.67 g, 1.5 mmol) was added and the resulting solution stirred at 70 °C for 10 h. DMSO was removed under high vacuum and the residue dissolved in EtOAc. The solution was washed with water, brine, dried over $MgSO_4$ and concentrated *in vacuo*. Purification on a silica gel column with EtOAc/hexane provided **4.16** (0.66 g, 76 %) as a colorless oil. R_f= 0.24 (SiO_2, TLC; hexane/EtOAc, 2/1). ^{1}H NMR (400 MHz, $CDCl_3$): δ 7.26(s, 10H), 5.41(d, 1H, *J* = 7.6Hz), 5.04-5.11(m, 4H), 4.33(s, 1H), 4.22(t, 2H, *J* = 7Hz), 1.58-1.96(m, 4H), 1.38(s, 9H), 1.18-1.31(m, 7H). ^{13}C NMR (100 MHz, $CDCl_3$) δ 172.00, 166.89, 155.85, 153.73, 136.09, 135.12, 128.03-128.59, 116.77, 81.60, 67.17, 66.97, 63.39, 57.88, 53.47, 36.23, 32.10, 28.03-28.15, 24.49, 23.31, 14.11. Anal. calcd. for $C_{31}H_{39}N_3O_8$: C, 64.01; H, 6.76; N, 7.22. Found: C, 63.92; H, 6.68; N, 7.18.

MS-ESI: m/z 582.4 (calcd. 582.27) [(M + H)$^+$]

(7S)-8-benzyl1-ethyl 2-(tert-butoxycarbonylamino)-7-(benzyloxycarbonylamino)-2-((tert-butoxycarbonylamino)methyl)octanedioate (4.17). Boc_2O (0.87 g, 4 mmol) was added to a solution of **4.16** (1.20 g, 2 mmol) in dry MeOH of 0° C followed by $NiCl_2 \cdot 6H_2O$(0.048 g, 0.2 mmol). $NaBH_4$ (0.606 g, 16 mmol) was then added in small portions over 30 min. The resulting mixture was allowed to warm to r.t. and left to stir for a further 2 h. The mixture was filtered through celite and the filtrate evaporated to dryness in vacuo. The residue was taken up in EtOAc, washed with water, brine, dried over $MgSO_4$ and concentrated. Flash chromatography on silica gel column eluting with EtOAc/hexane provided **4.17** (0.96 g, 70%) as a colorless oil. R_f = 0.4 (SiO_2, TLC; hexane/EtOAc, 2/1). ^{1}H NMR (500 MHz, $CDCl_3$): δ 7.24(s, 10H), 5.42(s, 1H), 5.35(d, 1H, J=7.5 Hz), 5.04-5.11(m, 4H), 4.82(s, 1H), 4.31(s, 1H), 4.11(d, 2H, J=6.5Hz), 3.60(m, 2H), 1.57-1.99(m, 4H), 1.41(s, 18H), 1.06-1.20(m, 7H). ^{13}C NMR (125 MHz, CDCl3) . δ 172.45, 172.16, 155.80, 155.60, 154.11, 136.17, 135.21, 127.99-128.52, 79.60, 79.32, 66.99, 66.84, 63.51, 61.84, 53.72, 44.47, 32.23, 28.15-28.21, 24.91, 23.07, 13.96. Anal. Calcd. for $C_{36}H_{51}N_3O_{10}$: C, 63.05; H, 7.50; N, 6.13. Found: C, 62.90; H, 7.23; N, 6.00. MS-ESI: m/z 708.5 (calcd. 708.35) [(M + Na)$^+$].

(2S)-2-amino-7-(tert-butoxycarbonylamino)-7-((tert-butoxycarbonylamino)methyl)-8-ethoxy-8-oxooctanoic acid (4.18). 30 mg of 10% Pd/C was added to an anhydrous EtOH (15 mL) solution of **4.17** (0.27 g, 0.4 mmol). H_2 was then bubbled through the solution for 2 days at r.t. The solution was filtered with celite to remove the catalyst and the solvent removed by rotary evaporation. The residue was purified by C18 RP chromatography (1:1 CH_3OH/H_2O) to give **4.18** (0.16 g, 88 %) as a white solid. ^{1}H NMR (400 MHz, $CDCl_3$): 7.94 (s, 1H), 5.73 (s, 1H), 5.15 (s, 1H), 4.12 (d, 1H, *J* = 6Hz), 3.57 (m, 3H), 1.41 (s, 18H), 1.18-1.82 (m, 11H). MS-ESI: m/z 484.4 (calcd. 484.27)[(M + Na)$^+$]. HRMS (ESI): Calcd. for [M + H]$^+$, 462.2815; Found, 462.2804.

(2S)-2-(((9H-fluoren-9-yl)methoxy)carbonylamino)-7-(tert-butoxycarbonylamino)-7-((tert-butoxycarbonylamino)methyl)-8-ethoxy-8-oxooctanoic acid (4.19). Compound **4.18** (0.6g, 1.3 mmol) was dissolved in dioxane (4 mL) and a 5% aqueous solution of Na_2CO_3 (8 mL). The reaction mixture was immersed in an ice bath and a

solution of FmocCl (0.336 g, 1.3 mmol) in dioxane (4 mL) was added. The solution was allowed to warm to r.t. and stirred for 3 h. The solvent was evaporated under high vacuum and the resulting material was purified on a silica gel column eluting with $CHCl_2$/MeOH. Compound **4.19** was received as a white solid (0.77 g, 87%). R_f =0.3 (SiO_2, TLC; CH_2Cl_2/MeOH, 30:1). ^{1}H NMR (400 MHz, $CDCl_3$): δ 7.26-7.77 (m, 8H), 5.53 (s, 1H), 4.89 (s, 1H), 4.19-4.50 (m, 5H), 3.68 (m, 2H), 1.41 (s, 18H), 1.25-2.10 (m, 11H). ^{13}C NMR (100 MHz, $CDCl_3$): δ 175.64, 172.61, 156.12, 155.88, 154.65, 143.92, 143.76, 141.30, 127.70, 127.08, 125.14, 119.96, 80.14, 79.94, 79.58, 67.07, 63.56, 62.02, 53.74, 47.16, 44.55, 32.08, 28.31, 25.01, 23.10, 14.09. MS-ESI: m/z 682.5 (calcd. 682.34)[(M - H)$^-$] HRMS (ESI): Calcd. for $[M + Na]^+$, 706.3315; Found, 706.3314.

(7S)-8-tert-butyl1-methyl7-(benzyloxycarbonylamino)-2-(tert-butoxycarbonylamino)-2-cyanooctanedioate (4.11) Methyl 2-(tert-butoxycarbonylamino)-2-cyanoacetate (0.23 g, 1.07 mmol) was added to a freshly prepared solution of NaOMe (59 mg, 1.09 mmol) in MeOH (5 mL) and stirred at 60°C for 30 min. After cooling to room temperature, methanol was removed under vacuum, the residue dissolved in DMSO (8 mL), mesylate **4.5** (0.4g, 0.96 mmol) was added and the resulting solution stirred at 70°C for 12 h. DMSO was removed under high vacuum and water was added, the mixture was extracted with EtOAc. The combined organic phases were washed with brine, dried overs $MgSO_4$ and filtered. The filtrate was concentrated *in vacuo* and the residue was purified by flash column chromatography (ethyl acetate/hexane = 1/2) to give **4.11** (0.36 g, 70%) as a colorless oil. ^{1}H NMR (500 MHz, $CDCl_3$): δ 7.22-7.27(m, 5H), 5.28-5.50(m, 2H), 5.00(s, 2H), 4.14(s, 1H), 3.77(t, 3H), 1.52-1.94(m, 4H), 1.25-1.39(m, 22H). ^{13}C NMR (125 MHz, $CDCl_3$): δ 171.92, 168.01, 156.52, 154.43, 136.86, 129.13, 128.80, 128.76, 128.72, 117.37, 83.12, 82.95, 67.57, 58.48, 54.36, 37.07, 33.12, 28.71, 28.58, 28.45, 25.14, 24.03. MS-ESI: m/z 556.6 (calcd. for $C_{27}H_{39}N_3NaO_8$:556.26) [(M + Na)$^+$]. HRMS (ESI): Calcd. for $C_{27}H_{39}N_3NaO_8$: $[M + Na]^+$, 556.2629; Found, 556.2631.

(7S)-8-tert-butyl1-methyl7-(benzyloxycarbonylamino)-2-(tert-butoxycarbonylamino)-2-((tert-butoxycarbonylamino)methyl)octanedioate (4.12) compound **4.12** was prepared according to the preparation of **4.17**: yield 72%, colorless oil. ^{1}H NMR

(400 MHz, $CDCl_3$): δ 7.22-7.28(m, 5H), 5.40(s, 1H), 5.21(s, 1H), 5.02(s, 2H), 4.79(s, 1H), 4.14(s, 1H), 3.58-3.69(m, 5H), 1.52-1.96(m, 4H), 1.34-1.37(m, 29H), 1.16-1.18(m, 2H). ^{13}C NMR (100 MHz, $CDCl_3$): δ 173.31, 171.69, 156.01, 155.91, 154.39, 136.55, 128.68, 128.30, 128.28, 82.21, 80.00, 67.03, 63.97, 54.39, 53.00, 44.85, 32.87, 28.17-28.49, 25.11, 25.08, 23.57. HRMS (ESI): Calcd. for $C_{32}H_{51}N_3NaO_{10}$: $[M + Na]^+$, 660.3467; Found, 660.3466.

(2S)-tert-butyl2-(benzyloxycarbonylamino)-7,8-bis(tert-butoxycarbonylamino)-7-(hydroxymethyl)octanoate (4.13) To a solution of **4.12** (180 mg, 0.28 mmol) in THF/H_2O (2:1, 10 mL) was added LiOH monohydrate (24 mg, 0.57 mmol) at 0 °C. The reaction mixture was warmed to rt and stirred for 48 h. The organic solvent was evaporated under reduced pressure. The remaining aqueous solution was carefully acidified with 1 N HCl and extracted with EtOAc three times. The combined organic phases were washed with water, dried over $MgSO_4$ and evaporated under reduced pressure to give a yellow oil that was used in the next step without further purification.

To a solution of the crude product in THF (4.0 ml) were added BOP (150 mg, 0.34 mmol) and DIPEA (59 μl, 0.34 mmol) at room temperature. The mixture was stirred for 10 min until it turned yellow, and cooled down to 0°C. Then $NaBH_4$ (15 mg, 0.4 mmol) was added portion wise. After stirring for 20 h, the reaction mixture was concentrated *in vacuo* and the residue was dissolved in diethyl ether. The resulting solution was washed with aqueous potassium bisulfate and brine, dried over $MgSO_4$ and concentrated. The residue was purified by column chromatography on silica gel to give **4.13** as a colorless oil (98 mg, 57%). ^1H NMR (400 MHz, $CDCl_3$): δ 7.30-7.33(m, 5H), 5.28(d, 1H), 5.07(s, 2H), 4.81(bs, 1H), 4.20(s, 1H), 3.23-3.44(m, 4H), 1.57-1.77(m, 4H), 1.39-1.42(m, 27H), 1.28-1.30(m, 4H). ^{13}C NMR (100 MHz, $CDCl_3$): δ 171.81, 156.10, 155.79, 136.55, 128.71, 128.34, 82.21, 80.38, 79.75, 67.09, 64.79, 59.61, 54.24, 43.88, 33.07, 32.32, 28.21-28.56, 25.58, 22.56. HRMS (ESI): Calcd. for $C_{31}H_{51}N_3NaO_9$: $[M + Na]^+$, 632.3518; Found, 632.3521.

(2S)-2-(benzyloxycarbonylamino)-7,8-bis(tert-butoxycarbonylamino)-7-(hydroxymethyl)octanoic acid(4.14) Compound **4.14** was prepared from **4.13** according to the

preparation of **4.22**. Yield: 79%. ^{1}H NMR (400 MHz, $CDCl_3$): δ 7.27(s, 5H), 5.26-5.62(m, 2H), 5.05(s, 2H), 4.25-4.28(m, 1H), 3.24-3.62(m, 4H), 1.60-1.80(m, 3H), 1.22-1.38(m, 23H). HRMS (ESI): Calcd. for $C_{27}H_{43}N_3NaO_9$ $[M + Na]^+$, 576.2892; Found, 576.2891.

(2S)-2-(((9H-fluoren-9-yl)methoxy)carbonylamino)-7,8-bis(tert-butoxycarbonylamino)-7-(hydroxymethyl)octanoic acid(4.15) Compound **4.15** was prepared from iodide **4.14** according to the preparation of **4.23**. Yield: 75%. ^{1}H NMR (400 MHz, $CDCl_3$): δ 7.29-7.79(m, 8H), 5.57(bs, 1H), 5.25-5.31(m, 1H), 5.05(bs, 1H), 4.41-4.44(m, 3H), 4.24(t, 1H. *J* = 6.8Hz), 3.32-3.50(m, 4H), 1.75-1.92(m, 3H), 1.30-1.45(m, 23H). MS-ESI: m/z 664.6 (calcd. 664.3) $[(M + Na)^+]$.

(S)-6-benzyl1,1-diethyl6-(benzyloxycarbonylamino)-1-(tert-butoxycarbonylamino)hexane-1,1,6-tricarboxylate (4.24) A solution of iodide **4.10** (0.5 g, 1.04 mmol) and diethyl 2-(*N*-(*tert*-butoxycarbonyl)amino)malonate (0.44 g, 1.6 mmol) was added to a flame-dried flask under nitrogen, then 38 mg of sodium hydride was added with vigorous stirring, and the mixture was stirred under reflux for 12 h. After cooling to room temperature, the solvent was removed and the residue was taken up in EtOAc. The solution was washed with brine, dried ($MgSO_4$), and concentrated. Flash chromatography on a silica gel column eluting with 25% EtOAc/hexanes provided **4.24** (0.59 g, 90%) as a colorless oil. ^{1}H NMR (400 MHz, $CDCl_3$): δ 7.31-7.32(m, 10H), 5.87(s, 1H), 5.23(d, 1H, *J* = 8Hz), 5.07-5.13(m, 4H), 4.13-4.36(m, 5H), 2.19(s, 2H), 1.61-1.77(m, 2H), 1.39(s, 9H), 1.18-1.22(m, 10H). ^{13}C NMR (100 MHz, $CDCl_3$): δ 172.43, 168.41, 156.01, 154.04, 136.41, 135.45, 128.29-128.83, 80.34, 67.34, 67.18, 66.55, 62.55, 62.54, 54.02, 32.73, 28.14, 25.08, 23.31, 14.18. HRMS (ESI): Calcd. for $C_{33}H_{44}N_2NaO_{10}$: $[M + Na]^+$, 651.2888; Found, 651.2890.

(S)-2-(((9H-fluoren-9-yl)methoxy)carbonylamino)-7-(tert-butoxycarbonylamino)-8-ethoxy-7-(ethoxycarbonyl)-8-oxooctanoic acid (4.25) To a solution of **4.24** (0.29 g, 0.46 mmol) in EtOH (12 mL) was added 10% Pd on carbon (60 mg). The mixture was stirred under H_2 (1 bar) for 20 h. The catalyst was filtered off, and the solvent was removed under reduced pressure. To the residue in acetone (15 ml) was added DIEA (87 µl, 0.5 mmol) followed by FmocOSu (0.17 g, 0.5 mmol), After the solution

was stirred overnight over night at room temperature, acetone was removed under reduced pressure and the residue was purified by silica gel chromatography to yield the title compound as a white solid (92% yield). ^{1}H NMR (400 MHz, $CDCl_3$): δ 7.30-7.79(m, 8H), 5.99(s, 1H), 5.42(s, 1H), 4.23-4.51(m, 8H), 2.28(s, 2H), 1.72-1.91(m, 2H), 1.46(s, 9H), 1.25-1.29(m, 10H). ^{13}C NMR (100 MHz, $CDCl_3$): δ 176.91, 168.25, 156.12, 154.03, 143.76, 141.31, 127.72, 127.10, 125.14, 119.96, 80.26, 67.06, 66.44, 62.43, 53.87, 47.18, 32.37, 32.15, 28.24, 24.98, 23.08, 14.00. HRMS (ESI): Calcd. for $C_{33}H_{42}N_2NaO_{10}$: $[M + Na]^+$, 649.2732; Found, 649.2733.

(S)-6-tert-butyl1,1-diethyl6-(benzyloxycarbonylamino)-1-(tert-butoxycarbonylamino)hexane-1,1,6-tricarboxylate (4.20) Compound **4.20** was prepared from iodide **4.6** according to the preparation of **4.24**. Yield: 95%. ^{1}H NMR (400 MHz, $CDCl_3$): δ 7.27-7.28(m, 5H), 5.84(s, 1H), 5.20(d, 1H, *J* = 8Hz), 5.02(s, 2H), 4.08-4.22(m, 5H), 2.18(s, 2H), 1.58-1.76(m, 2H), 1.35-1.37(m, 20H), 1.15-1.18(m, 8H). ^{13}C NMR (100 MHz, $CDCl_3$): δ 171.67, 168.40, 155.96, 153.99, 136.55, 128.66, 128.27, 128.23, 82.18, 80.29, 66.99, 66.56, 62.51, 62.49, 54.41, 32.90, 32.59, 28.38, 28.14, 25.00, 23.37, 14.15. HRMS (ESI): Calcd. for $C_{30}H_{46}N_2NaO_{10}$: $[M + Na]^+$, 617.3045; Found, 617.3039.

(7S)-8-tert-butyl1-ethyl7-(benzyloxycarbonylamino)-2-(tert-butoxycarbonylamino)-2-(hydroxymethyl)octanedioate (4.21) Compound **4.21** was prepared from **4.20** according to the preparation of **4.13**. Yield: 52%. ^{1}H NMR (400 MHz, $CDCl_3$): δ 7.28-7.29(m, 5H), 5.43(s, 1H), 5.22(s, 1H), 5.03(s, 2H), 4.15-4.21(m, 4H), 3.71(d, 1H, *J* = 12Hz), 1.58-1.97(m, 4H), 1.37-1.38(m, 20H), 1.20-1.24(m, 5H). ^{13}C NMR (100 MHz, $CDCl_3$): δ 173.13, 171.98, 156.32, 155.53, 136.85, 129.01, 128.64, 128.59, 82.58, 80.60, 67.37, 66.28, 65.58, 62.45, 54.69, 32.20, 32.56, 28.80, 28.49, 25.46, 23.72, 14.64. HRMS (ESI): Calcd. for $C_{28}H_{44}N_2NaO_9$ $[M + Na]^+$, 575.2939; Found, 575.2941.

(2S)-2-(benzyloxycarbonylamino)-7-(tert-butoxycarbonylamino)-8-ethoxy-7-(hydroxymethyl)-8-oxooctanoic acid (4.22) To the above alcohol **4.21** (160 mg, 0.29 mmol) in 2 mL of CH_2Cl_2 was added 1 mL of TFA and the mixture was stirred for 2.5 h at room temperature. Most of the volatile was removed by nitrogen flow. To a solution of the residue in dry acetonitrile was added $Me_4NOH \cdot 5H_2O$ (153 mg, 0.85

mmol) and 332 mg of Boc_2O (186 mg, 0.85 mmol). The resulting mixture was stirred for 20 h at room temperature, and concentrated under reduced pressure. The residue was diluted with water and extracted with diethyl ether, the aqueous phase was acidified with aqueous potassium bisulfate and extracted with ethyl acetate three times.The combined organic layers were washed with brine, dried ($MgSO_4$) and concentrated by rotary evaporation to provide 106 mg (yield 74%) of **4.22** as clear oil. ^{1}H NMR (400 MHz, $CDCl_3$): δ 7.31(s, 5H), 5.62-5.64(m, 1H), 5.07(s, 2H), 4.04-4.34(m, 4H), 3.76-3.78(m, 1H), 1.64-1.82(m, 4H), 1.40-1.41(m, 9H), 1.22-1.27(m, 7H). HRMS (ESI): Calcd. for $C_{24}H_{36}N_2NaO_9$ $[M + Na]^+$, 519.2313; Found, 519.2312.

(2S)-2-(((9H-fluoren-9-yl)methoxy)carbonylamino)-7-(tert-butoxycarbonylamino)-8-ethoxy-7-(hydroxymethyl)-8-oxooctanoic acid (4.23) To a solution of **4.22**(100 mg, 0.2 mmol) in ethanol (10 ml) was added 10% Pd/C (20 mg) and the solution was stirred under hydrogen for 20 h. The reaction mixture was then filtered and the filtrate was concentrated under reduced pressure. To a solution of the above residue and DIPEA (38 µl, 0.22 mmol) in dry acetone (6 mL) were added Fmoc-OSu (74 mg, 0.22 mmol) portionwise. After being stirred at room temperature overnight, the reaction mixture was concentrated and the residue was then purified by flash chromatography on silica gel (eluent: CH_2Cl_2/MeOH) to afford 91 mg of title compound **4.23** (yield 78%). ^{1}H NMR (500 MHz, $CDCl_3$): δ 7.22-7.73(m, 8H), 5.41-5.52(m, 2H), 4.04-4.37(m, 7H), 3.77-3.79(m, 1H), 1.69-2.14(m, 4H), 1.39-1.41(m, 9H), 1.22-1.26(m, 7H). HRMS (ESI): Calcd. for $C_{31}H_{40}N_2NaO_9$ $[M + Na]^+$, 607.2626; Found, 607.2632.

General procedure for synthesis of 4.29 to 4.31. The amine 3.18 or 3.22 or 3.27 was dissolved in THF and cooled to 0°C. This solution was treated with the Fmoc-Glu-OAll (1.1 eqiv), HOBt (1-hydroxybenzotriazole) (1.2 eqiv), EDC·HCl (1.2 eqiv), N-methylmorpholine (5 eqiv). The mixture was warmed to room temperature and stirring overnight. The solvent was removed *in vacuo*, and the residue was purified using flash column chromatography (silica gel, ethyl acetate/hexanes) to afford the desired compound as colorless oil.

(S)-diethyl2-(2-(2-(2-(4-(((9H-fluoren-9-yl)methoxy)carbonylamino)-5-(allyloxy)-

5-oxopentanamido)ethoxy)ethoxy)ethyl)-2-(tert-butoxycarbonylamino)malonate (4.29) (77% yield) ^{1}H NMR (400 MHz, $CDCl_3$): δ 7.28-7.78(m, 8H), 5.87-6.17(m, 3H), 5.24-5.37(m, 2H), 4.65(d, 2H, *J* = 5.4Hz), 4.16-4.44(m, 8H), 3.49-3.53(m, 10H), 2.62(s, 2H), 2.10-2.37(m, 4H), 1.44(s, 9H), 1.25(t, 6H, *J* = 7.2Hz). ^{13}C NMR (100 MHz, $CDCl_3$): δ 172.23, 171.77, 168.44, 156.28, 154.10, 144.01, 141.29, 131.61, 127.68, 127.08, 125.27, 119.94, 118.83, 80.26, 70.10, 70.00, 69.72, 67.10, 66.31, 65.98, 64.72, 62.35, 53.99, 47.17, 39.38, 32.79, 32.21, 28.23, 27.72, 13.92. MS-ESI: m/z 798.3 (calcd. for $C_{41}H_{56}N_3O_{13}$:798.38) [$(M + H)^+$]. HRMS (ESI): Calcd. for $C_{41}H_{55}N_3NaO_{13}$: $[M + Na]^+$, 820.3627; Found, 820.3626.

(2S)-allyl5-(2-(2-(3,4-bis(tert-butoxycarbonylamino)-3-((tert-butyldimethylsilyloxy)methyl)butoxy)ethoxy)ethylamino)-2-(((9H-fluoren-9-yl)methoxy)carbonylamino)-5-oxopentanoate (4.30) (83% yield) ^{1}H NMR (400 MHz, $CDCl_3$): δ 7.23-7.73(m, 8H), 5.19-5.89(m, 6H), 4.60(d, 2H, *J* = 5.6Hz), 4.20-4.39(m, 4H), 3.82(d, 1H, *J* = 8 Hz), 3.42-3.58(m, 12H)), 1.86-2.18(m, 6H), 1.37-1.39(m, 18H), 0.86(s, 9H), 0.04(s, 6H). ^{13}C NMR (100 MHz, $CDCl_3$): δ 171.97, 156.93, 156.48, 155.06, 144.22, 144.50, 131.79, 127.88, 127.29, 125.40, 120.14, 119.09, 79.46, 79.15, 70.44, 70.28, 70.11, 67.45, 67.31, 66.46, 66.22, 58.41, 54.11, 47.39, 45.82, 39.62, 32.76, 28.63, 26.04, 18.34, -5.36. HRMS (ESI): Calcd. for $C_{48}H_{74}N_4NaO_{12}Si$ $[M + Na]^+$, 949.4965; Found, 949.4966.

(S)-allyl5-(2-(2-(3,4-bis(tert-butoxycarbonylamino)-3-((tert-butoxycarbonylamino)methyl)butoxy)ethoxy)ethylamino)-2-(((9H-fluoren-9-yl)methoxy)carbonylamino)-5-oxopentanoate (4.31) (86% yield) ^{1}H NMR (400 MHz, $CDCl_3$): δ 7.30-7.66(m, 8H), 5.69-6.06(m, 4H), 5.26-5.38(m, 3H), 4.66(d, 2H, *J* = 5.6Hz), 4.26-4.45(m, 4H), 3.27-3.62(m, 14H)), 1.98-2.35(m, 6H), 1.43-1.46(m, 27H). ^{13}C NMR (100 MHz, $CDCl_3$): δ 171.80, 157.29, 156.30, 155.30, 143.98, 141.30, 131.56, 127.70, 127.08, 125.26, 119.95, 118.94, 79.69, 70.22, 69.94, 69.76, 67.12, 66.06, 59.20, 53.89, 47.17, 44.17, 39.41, 32.72, 32.36, 28.39. HRMS (ESI): Calcd. for $C_{47}H_{69}N_5NaO_{13}$: $[M + Na]^+$, 934.4784; Found, 934.4785.

General procedure for synthesis of 4.29a to 4.31a. To a solution of **4.29** or **4.30**, or **4.31** in THF, tetrakis(triphenylphosphane)palladium(0) (0.2 equiv) was added and

N-ethylaniline (10 equiv). After stirring for 30 min at room temperature, THF was removed *in vacuo* and the residue was purified by flash chromatography to afford 4.29a-4.31a as a white solid.

(S)-2-(((9H-fluoren-9-yl)methoxy)carbonylamino)-5-(2-(2-(3-(tert-butoxycarbonylamino)-4-ethoxy-3-(ethoxycarbonyl)-4-oxobutoxy)ethoxy)ethylamino)-5-oxopentanoic acid (4.29a) (quantitative yield). ^{1}H NMR (400 MHz, $CDCl_3$): δ 7.28-7.78(m, 8H), 6.01-6.17(m, 2H), 4.21-4.40(m, 8H), 3.49-3.51(m, 10H), 2.18-2.61(m, 6H), 1.44(s, 9H), 1.26(t, 6H, *J* = 7.2Hz). ^{13}C NMR (100 MHz, $CDCl_3$): δ 173.92, 168.51, 156.03, 154.17, 143.96, 141.28, 127.67, 127.09, 125.17, 119.93, 80.46, 70.07, 69.97, 69.35, 67.02, 66.21, 62.49, 53.61, 47.16, 39.61, 32.74, 32.23, 28.21, 13.90. HRMS (ESI): Calcd. for $C_{38}H_{51}N_3NaO_{13}$: $[M + Na]^+$, 780.3314; Found, 780.3319.

(2S)-5-(2-(2-(3,4-bis(tert-butoxycarbonylamino)-3-((tert-butyldimethylsilyloxy)methyl)butoxy)ethoxy)ethylamino)-2-(((9H-fluoren-9-yl)methoxy)carbonylamino)-5-oxopentanoic acid (4.30a) (quantitative yield) ^{1}H NMR (400 MHz, $CDCl_3$): δ 7.22-7.72(m, 8H), 5.41-5.98(m, 3H), 4.18-4.38(m, 5H), 3.85(d, 1H, *J* = 8 Hz), 3.32-3.51(m, 12H)), 1.85-2.13(m, 6H), 1.39-1.45(m, 18H), 0.85(s, 9H), 0.02(s, 6H). ^{13}C NMR (100 MHz, $CDCl_3$): δ 173.80, 171.37, 156.97, 156.14, 144.16, 144.50, 127.88, 127.29, 125.38, 120.14, 79.84, 70.2, 69.67, 67.24, 66.65, 58.69, 53.63, 47.38, 45.99, 39.79, 32.55, 28.64, 26.02, 18.31, -5.38. HRMS (ESI): Calcd. for $C_{45}H_{70}N_4NaO_{12}Si$: $[M + Na]^+$, 909.4651; Found, 909.4642.

(S)-5-(2-(2-(3,4-bis(tert-butoxycarbonylamino)-3-((tert-butoxycarbonylamino)methyl)butoxy)ethoxy)ethylamino)-2-(((9H-fluoren-9-yl)methoxy)carbonylamino)-5-oxopentanoic acid (4.31a) (quantitative yield) ^{1}H NMR (400 MHz, $CDCl_3$): δ 7.30-7.79(m, 8H), 5.74-6.09(m, 3H), 4.23-4.45(m, 4H), 3.27-3.58(m, 14H), 1.98-2.45(m, 6H), 1.44-1.46(m, 27H). ^{13}C NMR (100 MHz, $CDCl_3$): δ 174.20, 173.25, 157.43, 156.16, 143.93, 141.29, 131.56, 127.69, 127.10, 125.18, 119.94, 79.92, 79.31, 70.09, 69.87, 69.39, 67.08, 59.20, 53.43, 47.15, 44.26, 39.52, 32.62, 32.36, 28.39. MS-ESI: m/z 872.3 (calcd. for $C_{44}H_{66}N_5O_{13}$: 872.46) $[(M + H)^+]$. HRMS (ESI): Calcd. for $C_{44}H_{65}N_5NaO_{13}$: $[M + Na]^+$, 894.4471; Found, 894.4471.

(2R)-3-(4-(2-(2-(3,4-bis(tert-butoxycarbonylamino)-3-((tert-butyldimethylsilyloxy)methyl)butoxy)ethoxy)ethoxy)phenyl)-2-(((9H-fluoren-9-yl)methoxy)carbonylamino)propanoic acid(4.27a) To a solution of triphenylphosphine (0.29 g, 1.12 mmol), alcohol **3.16** (0.30 g, 0.56 mmol), and **4.26** (0.25 g, 0.56 mmol) in toluene(5 ml)was slowly added diethyl azodicarboxylate (DEAD, 40% in toluene, 0.44 ml ,1.12 mmol) with stirring at 0°C. The reaction mixture was stirred for 15 h and concentrated by rotary evaporator, the residue was purified by chromatography on silica gel (n-hexane/ethyl acetate 3:1) to give 4.27 as a colourless oil, which was used for the next step by dissolving it in THF (20 mL), N-methylaniline (0.73 mL, 6.7 mmol) and $Pd(PPh_3)_4$ (0.06 g, 0.05 mmol) were added to the solution. The mixture was stirred at room temperature for 30 min. The solvent was removed under reduced pressure and the oily residue was purified by column chromatography (eluent DCM/MeOH, 30:1 v/v) to afford **4.27a** (0.26 g, 50%) as a white solid . ^{1}H NMR (400 MHz, $CDCl_3$): δ 7.65-6.73 (m, 12H), 5.51(s, 1H), 5.40(s, 1H), 5.27(s, 1H), 4.54-3.98(m, 6H), 3.72-3.02(m, 12H), 1.82(s, 2H), 1.34(s, 18H), 0.8(s, 6H) . ^{13}C NMR (400 MHz, $CDCl_3$): δ 175.0, 158.50, 157.47, 156.33, 155.79, 144.47, 144.37, 141.90, 131.04, 128.68, 128.29, 127.66, 125.94, 125.67, 120.55, 115.42, 79.91, 79.57, 71.27, 70.81, 70.41, 68.09, 67.79, 67.66, 59.04, 58.84, 47.78, 46.14, 37.59, 33.33, 29.00, 26.44, 18.72, -5.01. MS-ESI: m/z 944.5 (calcd. for $C_{49}H_{71}N_3NaO_{12}Si$: 944.47) [$(M + Na)^+$]

8.5 Synthesis and characterization of compounds in Chapter 5

2,3,4,6-Tetra-*O*-acetyl-1-*O*-[2-(4-methoxy-4-oxo-3-(2,2,2-trifluoroacetamido)-3-((2,2,2-trifluoroacetamido)methyl)butoxy)ethoxy]-β-D-glucopyranose (5.1) β-Glucosepentaacetate (275 mg, 0.705 mmol) and alcohol **3.13** (240 mg, 0.543 mmol) were dissolved in anhydrous CH_2Cl_2 (2.5 mL), then $BF_3{\cdot}OEt_2$ (0.06 mL) was added slowly. The reaction mixture was stirred at room temperature for 24 h. and then poured into 5% aqueous $NaHCO_3$ (8 mL). The organic layer was separated, washed with water and brine, dried ($MgSO_4$) and concentrated. Purification on a silica gel column with DCM/Acetone(25:1) provided **5.1** (0.3 g, 72%) as a colorless oil. ^{1}H

NMR (500 MHz, $CDCl_3$): δ 8.57(s, 1H), 7.55(s, 1H), 5.19(t, 1H, J=9.5Hz), 5.06(t, 1H, *J* = 9.7Hz), 5.19(t, 1H, *J* = 9.0Hz), 4.56(d, 1H, *J* = 8Hz), 4.23(dd, 1H, *J* = 7.5Hz, *J* = 12Hz), 4.11-4.14(m, 2H), 3.58-4.01(m, 15H), 2.21(s, 1H), 1.99-2.07(m, 12H). ^{13}C NMR (125 MHz, $CDCl_3$) δ 170.73, 157.42(q, 2×*C*OCF_3), 116.82(q, 2×CO*C*F_3), 72.18, 70.45, 69.85, 66.64, 62.87, 61.46, 53.21, 42.82, 32.54. HRMS (ESI): Calcd. for $C_{28}H_{38}F_6N_2NaO_{16}$ $[M + Na]^+$, 795.2018; Found, 795.2018.

[Re(G1)(CO)$_3$] (5.2a) Lithium hydroxide monohydrate (42 mg, 1 mmol, 10.0 equiv.) and water (2.0 mL) were added sequentially to a solution of **5.1** (77 mg, 0.1 mmol) in THF (6 mL) at room temperature. The solution was stirred for 18 h. Amberlite IR-120 (H^+) resin was used to neutralize the above solution which was concentrated to afford viscous **G1** in quantitative yield. To a solution of above residue in water (5 mL) was added $[NEt_4]_2[Re(CO)_3Br_3]$ (76.8 mg, 0.1 mmol). The mixture was heated to 70˚C for 5 h. The solvent was then removed *in vacuo* and the residue was purified by silica gel chromatography (EtOAc/MeOH) to afford the product as a white solid (53.4 mg, 80%). ^1H NMR (500 MHz, D_2O): δ 4.53(d, 1H, *J* = 8Hz), 4.10-4.13(m, 1H), 3.96(dd, 1H, *J* = 2.5Hz, 12.5Hz), 3.87-3.90(m, 1H), 3.69-3.81(m, 9H), 3.32-3.55(m, 4H). 2.93-2.98(m, 1H), 2.76-2.82(m, 1H), 2.14-2.18(m, 1H), 2.00-2.04(m, 1H). HRMS (ESI): Calcd. for $C_{18}H_{29}N_2NaO_{13}Re$ $[M + Na]^+$, 691.1120; Found, 691.1117.

3,5,6-Tri-O-benzyl-1,2-O-isopropylidene-α-D-glucofuranose (5.3) A solution of 1,2-O-isopropylidene-a-D-glucofuranose (6 g), sodium hydride (8 g), and tetrabutylammonium iodide (catalytic amount) in dry N,N-dimethylformamide (70 mL) was cooled to 0 °C, and benzyl bromide (8 mL) was introduced dropwise. After 24 h, when TLC showed that the reaction was complete, the mixture was quenched with MeOH before filtered, filtrate evaporated, and the residue purified by column chromatography with 1:8 ethyl acetate-hexane as the eluent, giving a colorless syrup yield, 10.7g (80%). ^1H NMR (200 MHz, $CDCl_3$): δ 7.29-7.27(m, 15H), 5.91(d, 1H), 4.68(s, 2H), 4.60, 4.49(2d, 2H), 4.31(dd, 2H), 4.13(dd, 1H), 4.08(d, 1H), 4.04(m, 1H), 3.92(dd, 1H), 3.69(dd, 1H), 1.49(s, 3H), 1.32(s, 3H).

Methyl 3,5,6-tri-O-benzyl-α-D-glucofuranoside (5.4) A solution of the previous syrup (10 g) in methanol (150 mL) was boiled under reflux and stirred with Amberlite

IR-120 (H^+) ion-exchange resin (60 mL) for 5 days. TLC then showed that the starting material had disappeared completely. The suspension was filtered, the filtrate evaporated, the residue dissolved in 1: 1 hexane-ethyl acetate, and the mixture separated by column chromatography, with 1:3 ethyl acetate-hexane as the eluent, giving a colorless syrup yield, 4.2g (44%) ^{1}H NMR (400 MHz, $CDCl_3$): 7.30-7.38(m, 15H). 5.06(d, 1H, *J* = 4.4), 4.84(d, 1H, *J* = 11.5Hz), 4.72(d, 1H, *J* = 11.5Hz), 4.57-4.62(m, 4H), 4.36(dd, 1H, *J* = 4 Hz, 8Hz), 4.27-4.29(m, 1H), 4.07-4.10(m, 2H), 3.91(dd, 1H, *J* = 2Hz, 10.5Hz), 3.73(dd, 1H, *J* = 5.8Hz, 10.5Hz), 3.50(s, 3H).

Methyl3,5,6-tri-*O*-benzyl-2-O-[2-(3-(tert-butoxycarbonyl)-3-((tert-butoxycarbonyl)methyl)-4-methoxy-4-oxobutoxy)ethoxy]-α-D-glucofuranoside (5.5) To a solution of methyl 3,5,6-tri-O-benzyl-a-D-glucofuranoside(2) (410 mg, 0.88 mmol) in dry DMF (10 mL) in an ice bath was added sodium hydride (69 mg, 2.9 mmol)) under N_2. The reaction was stirred for half an hour and a solution of bromide **3.11** (1.2 g, 2.33 mmol) in DMF (1.2 mL) was added dropwise. The obtained suspension was stirred overnight with increasing temperature from 0°C to room temperature. The reaction was quenched with MeOH. The organic solvent was removed under vacuum, and the residue was extracted with EtOAc. The organic layer was dried with Na_2SO_4, then filtered, concentrated and the product isolated by column chromatography with a gradient of CH_2Cl_2/acetone (25:1) to yield (443 mg, 56%) of **5.5** as a colorless oil. ^{1}H NMR (400 MHz, $CDCl_3$) : δ 7.22-7.29(m, 15H), 5.95(s, 1H), 5.02(s, 1H), 4.93(d, J=4 Hz, 1H), 4.75(d, J=12 Hz, 1H), 4.62(d, J=12 Hz, 1H), 4.54-4.49(m, 4H), 4.29(t, J=8 Hz, 1H), 4.17(t, J=4 Hz, 1H), 3.99(t, J=8 Hz, 1H), 3.94(t, J=4 Hz, 1H), 3.84(d, J=4 Hz, 0.4H), 3.82(s, 0.6H), 3.70-3.47(m, 16H), 3.37(s, 3H), 2.22(s, 1H), 2.08(s, 1H), 1.40(s, 18H). ^{13}C NMR (100 MHz, $CDCl_3$): δ 173.40, 156.08, 154.77, 139.18, 138.86, 138.29, 128.47, 128.38, 127.77, 127.68, 127.57, 127.50, 101.70, 85.49, 82.00, 79.85, 79.53, 73.56, 72.75, 72.29, 71.60, 70.78, 70.62, 70.49, 70.40, 67.04, 62.50, 55.62, 52.72, 44.93, 32.84, 28.50. HRMS (ESI): Calcd. for $C_{48}H_{68}N_2NaO_{14}$ $[M + Na]^+$, 919.4563; Found, 919.4562.

Methyl3,5,6-tri-*O*-benzyl-2-O-[2-(4-methoxy-4-oxo-3-(2,2,2-trifluoroacetamido)-3-((2,2,2-trifluoroacetamido)methyl)butoxy)ethoxy]-α-D-glucofuranoside (5.6)

Trifluoroacetic acid (4.0 mL) was added dropwise to a solution of **5.5** (0.25 g, 0.28 mmol) in DCM (10 mL) under nitrogen. The resulting mixture was stirred at RT for 3h. The volatiles were removed under reduced pressure to give a crude oil which was used for the next step without further purification by dissolving it in DCM (15 mL) at 0°C, To the above solution was added triethylamine (0.2 mL) and trifluoroacetic anhydride (0.2 mL), The mixture was stirred at room temperature for 1 h. The solvent was removed under reduced pressure and the crude product was purified by flash chromatography (CH_2Cl_2/acetone 20:1) to afford the title compound **5.6** (180 mg, 73%). ^{1}H NMR (400 MHz, $CDCl_3$) : δ 8.63(bs, 1H), 7.58(bs, 1H), 7.30-7.22(m, 15H), 4.94(d, *J* = 3.76 Hz, 1H), 4.75(d, *J* = 11.67 Hz, 1H), 4.61(d, *J* = 12 Hz, 1H), 4.52(d, *J* = 12 Hz, 3H), 4.29(t, *J* = 6 Hz, 1H), 4.17(t, *J* = 6 Hz, 1H), 4.00-3.55(m, 20H), 3.37(s, 3H), 2.19-2.12(m, 2H). ^{13}C NMR (100 MHz, $CDCl_3$): δ 171.01, 157.74(q, 2×*C*OCF_3), 139.09, 138.80, 138.22, 127.35-128.49, 114.27(q, 2×CO*C*F_3), 101.65, 85.30, 81.93, 73.52, 72.69, 72.33, 72.31, 71.41, 70.84, 70.65, 70.30, 70.24, 67.08, 63.14, 55.59, 53.52, 43.20, 32.98. HRMS (ESI): Calcd. for $C_{42}H_{50}F_6N_2NaO_{12}$: $[M + Na]^+$, 911.3160; Found, 911.3160.

1,3,4,6-Tetra-*O*-acetyl-2-*O*-[2-(4-methoxy-4-oxo-3-(2,2,2-trifluoroacetamido)-3-((2,2,2-trifluoroacetamido)methyl)butoxy)ethoxy]-β-D-glucopyranose (5.7) 10% Pd/C (60 mg) was added to a solution of **5.6** (130 mg, 0.15 mmol) in MeOH (20 ml), and the reaction mixture was stirred overnight at room temperature under H_2 atmosphere. Then, the mixture was filtered through celite and solvent removal under reduced pressure gave 85 mg (94%) of **5** as a colorless oil that was used in the next step without further purification.

To a solution of above crude product (85 mg, 0.14 mmol) in acidic anhydride (1.9 mL) at 0˚C was added trimethylsilyl trifluoromethanesulphonate (25 µL). The reaction was allowed to stir for 1 h at 0˚C. After which it was poured into $NaHCO_3$-ice-water and extracted with DCM, The organic layer was dried with Na_2SO_4, then filtered and concentrated by rotary evaporation. The product was isolated by flash column chromatography using a gradient of $CHCl_2$/acetone to yield **5.7** (66 mg, 61%) as a colorless oil. ^{1}H NMR (400 MHz, $CDCl_3$) : δ 8.58(s, 1H), 7.56(s, 1H), 6.12(s, 1H),

5.29(m, 2H), 4.54-4.62(m, 2H), 4.10(dd, 1H, *J* = 12.4, 2.4Hz), 4.02(m, 1H), 3.91(m, 2H), 3.78(m, 6H), 3.60(m, 7H), 2.26(m, 2H), 2.00-2.16(m, 12H). HRMS (ESI): Calcd. for $C_{28}H_{38}F_6N_2NaO_{16}$:$[M + Na]^+$, 795.2018; Found, 795.2017.

[Re(G2)(CO)$_3$] (5.8a) Lithium hydroxide monohydrate (21 mg, 0.5 mmol) and water (1.0 mL) were added sequentially to a solution of **5.7** (39 mg, 0.05 mmol) dissolved in THF (3.0 mL) at room temperature. After stirring the mixture for 20 h, The solution was treated with Amberlite IR-120 (H^+) resin and stirred for 2 h. The solution was then filtered and evaporated to afford **G2** as an oil, which was dissolved in water. $[NEt_4]_2[ReBr_3(CO)_3]$ (38 mg, 0.05 mmol) was added and the mixture was heated to 70˚C for 5 h. The solvent was then removed *in vacuo* and the residue was purified by silica gel chromatography to afford the product as a hydroscopic solid (29 mg, 87%). ^{1}H NMR (500 MHz, D_2O): δ 5.27(d, 0.4H, *J* = 3.5Hz), 4.64(d, 0.6H, *J* = 8Hz), 4.39(m, 1H), 3.61-3.99(m, 13H), 3.30-3.42(m, 2H). 2.84-2.88(m, 1H), 2.70-2.73(m, 1H), 2.07-2.10(m, 1H), 1.93-1.96(m, 1H). *Anal*. Calcd. for $C_{18}H_{31}N_2O_{14}Re$: C, 31.53; H, 4.56; N, 4.09. Found: C, 31.39; H, 4.48; N, 3.91. MS-ESI: m/z 691.1 (calcd. for $C_{18}H_{29}N_2NaO_{13}Re$ 691.11) $[(M + Na)^+]$

1,2:5,6-di-O-isopropylidene-α-D-glucofuranoside (5.9) To a slurry of D-glucose (1.8 g, 10 mmol) in dry acetone (35 mL) was added H_2SO_4-silica (200 mg). The mixture was refluxed for 3 h. Then it was filtered through a pad of Celite and the solvent was removed *in vacuo* and the crude product was purified by silica gel comlum to give the target compound **5.9** as a white solid(1.7 g, 65%). ^{1}H NMR (400 MHz, $CDCl_3$) : δ 5.97(d, 1H, *J* = 3.6Hz), 4.56(d, 1H, *J* = 3.6Hz), 4.35-4.40(m, 2H), 4.20(dd, 1H, *J* = 6.2Hz, 8.6Hz), 4.11(dd, 1H, *J* = 2.8Hz, 7.6 Hz), 4.00(dd, 1H, *J* = 5.4Hz, *J* = 8.6Hz), 1.35-1.53(m, 12H). MS-ESI: m/z 283.1 (calcd. for $C_{12}H_{20}NaO_6$ 283.12) $[(M + Na)^+]$.

3-O-([2-(3-(tert-butoxycarbonyl)-3-((tert-butoxycarbonyl)methyl)-4-methoxy-4-oxobutoxy)ethoxy])-1,2:5,6-di-O-isopropylidene-α-D-glucofuranoside (5.10) To a solution of 0.030 g (0.12 mmol)) of **5.9** in 3 mL of DMF was added 10 mg of NaH (0.42 mmol). After stirring this mixture at room temperature for 30 min, a solution of bromide **3.11**(0.15 g, 0.29 mmol) in 0.5 ml DMF was added. The obtained suspension

was stirred overnight with slowly increasing temperature from 0 °C to room temperature. The solvent was removed *in vacuo* and the residue was purified by column chromatography (over SiO_2 eluting with 2:1 Hexane/EtOAc) gave **5.10** as a clear oil (70%). ^{1}H NMR (400 MHz, $CDCl_3$): δ 5.95(s, 1H), 5.82(d, 1H, *J* = 3.6Hz), 5.02(s, 1H), 4.53(d, 1H, *J* = 3.6Hz), 4.25-4.28(m, 1H), 4.04-4.09(m, 2H), 3.93-3.96(m, 1H), 3.88(d, 1H, *J* = 2.8Hz), 3.44-3.75(m, 15H), 2.23-2.26(m, 1H), 2.05-2.09(m, 1H), 1.27-1.45(m, 30H). ^{13}C NMR (100 MHz, $CDCl_3$): δ 173.23, 155.90, 154.61, 111.72, 108.89, 105.24, 82.71, 81.12, 79.69, 79.38, 72.54, 70.47, 70.33, 70.04, 69.92, 67.20, 62.29, 52.51, 44.71, 32.59, 28.32, 26.80, 26.25, 25.44. HRMS (ESI): Calcd. for $C_{32}H_{56}N_2NaO_{14}$: $[M + Na]^+$, 715.3624; Found, 715.3627.

[Re(G3)(CO)$_3$] (5.11a) Compound **5.10** (21mg, 0.03mmol) was added to a trifluoroacetic acid/water (1:1) mixture and the solution was stirred at room temperature for 3 h. Concentration of the solution give a yellow oily residue that was dissolved in THF:H_2O (1:1), Lithium hydroxide monohydrate (4 mg, 0.09 mmol) was added and the solution was stirred for 5 h. Amberlite IR-120 (H^+) resin was used to neutralize the above solution which was concentrated to afford a syrup **G3** in quantitative yield. To a solution of above syrup in water (2 mL) was added $[NEt_4]_2[Re(CO)_3Br_3]$ (23 mg, 0.03 mmol). The resulting solution was heated to 70˚C for 4 h. The solvent was then removed *in vacuo* and the residue was purified by silica gel chromatography to afford the product **5.11a** as a hydroscopic solid (15 mg, 75%). ^{1}H NMR (400 MHz, D_2O): δ 5.17(d, 0.5H, *J* = 3Hz)), 4.60(d, 0.5H, *J* = 8Hz), 4.38-4.41(m, 1H), 3.95-3.97(m, 2H), 3.47-3.86(m, 13H), 2.87-2.90(m, 1H), 2.70-2.73(m, 1H), 2.07-2.09(m, 1H), 1.94-1.97(m, 1H). HRMS (ESI): Calcd. for $C_{18}H_{29}N_2NaO_{13}Re$ $[M + Na]^+$, 691.1120; Found, 691.1126.

Benzyl 2,3,4,6-tetra-O-benzyl-β-D-glucopyranoside (5.12) To a solution of powdered KOH (3.5 g, 63.5 mmol) in 4 mL of Me_2SO cooled in an ice bath was added D-Glucose (1.0 g, 5.6 mmol). BnBr (4.8 mL, 40.3 mmol) was immediately added dropwise over a period of 30 min. The reaction was allowed to come slowly to room temperature. After stirring for 24 h, the reaction was diluted with 60 mL of cold water and then extracted with methyl *tert*-butyl ether, the combined organics were

washed with water, brine, dried ($MgSO_4$) and concentrated. The residue was purified by silica gel chromatography (EtOAc/hexane 1:10) to afford the product (2.12 g, 60%) as a white solid. ^{1}H NMR (300 MHz, $CDCl_3$): δ 7.37-7.15(m, 25H), 5.02-4.52(m, 11H), 3.77-3.63(m, 6H).

Benzyl 6-O-acetyl-2,3,4-tri-O-benzyl-β-D-glucopyranoside (5.13) To a solution of **5.12** (2.5 g, 4 mmol) in 15 ml Ac_2O/HOAc (5:1) was added a solution of freshly fused $ZnCl_2$ (2.7 g, 20 mmol) in 15 ml Ac_2O/HOAc (5:1), the mixture was stirred at room temperature for 90 min, and then water was added, the mixture was extracted with dichloromethane three times, and the combined organic phase was washed with saturated sodium carbonate, water, brine, dried over Na_2SO_4, and concentrated to give a syrup. Purification by chromatography gave 13 (1.20 g, 52%) as a white solid. ^{1}H NMR (400 MHz, $CDCl_3$): δ 7.21-7.32(m, 20H), 4.89-4.94(m, 3H), 4.46-4.84(m, 6H), 4.35(d, *J* = 11.6 Hz, 1H), 4.22(dd, *J* = 12.0 Hz, 4.8 Hz, 1H), 3.61-3.65(m, 1H), 3.45-3.50(m, 3H), 2.02(s, 3H). MS-ESI: m/z 605.3(calcd. for $C_{36}H_{38}NaO_7$ 605.25) $[(M + Na)^+]$.

Benzyl 2,3,4-tri-O-benzyl-β-D-glucopyranoside (5.14) A suspension of **5.13**(1.19g, 2mmol) in 15 mL of 0.025 M NaOMe in MeOH was stirred for 10 h. The reaction mixture was evaporated to dryness. The residue was dissolved in methyl tert-butyl ether and washed with water and brine, dried (Na_2SO_4), and concentrated. Purification by chromatography give 14 (0.96g, 89%) as a white solid. ^{1}H NMR (400 MHz, $CDCl_3$): δ 7.30-7.33(m, 20H), 4.66-5.00(m, 8H), 4.62(d, 1H, 8Hz), 3.89-3.92(m, 1H), 3.68-3.73(m, 2H), 3.60(t, 1H, *J* = 9 Hz), 3.52(dd, 1H, *J* = 8Hz, 9Hz), 3.39-3.41(m, 1H). MS-ESI: m/z 563.3 (calcd. for $C_{34}H_{36}NaO_6$ 563.24) $[(M + Na)^+]$

Benzyl2,3,4,-tri-O-benzyl-6-O-([2-(3-(tert-butoxycarbonyl)-3-((tert-butoxycarbonyl)methyl)-4-methoxy-4-oxobutoxy)ethoxy])-β-D-glucopyranoside (5.15) To a stirred solution of **5.14** (520 mg, 0.96 mmol) in DMF(10 ml) at 0 °C was added sodium hydride (80 mg, 3.33 mmol). The mixture was stirred at room temperature for 30 min, and then a solution of bromide **3.11**(1.55 g, 3.02 mmol) in DMF (1.5 mL) was added dropwise. The obtained suspension was stirred overnight with increasing temperature from 0 °C to room temperature. The excess of sodium hydride was then destroyed by addition of methanol (1.0 ml). The volatiles were removed under

reduced pressure, and the residue was taken up into EtOAc and washed with brine, dried ($MgSO_4$), and concentrated. Purification by chromatography gave **5.15** as a colourless oil(485mg, 52%). ^{1}H NMR (400 MHz, $CDCl_3$) : δ 7.21-7.28(m, 20H), 5.94(s, 1H), 5.00(s, 1H), 4.60-4.89(m, 8H), 4.46(d, 1H, *J* = 8Hz), 3.41-3.67(m, 21H), 2.05-2.19(m, 2H), 1.38(s, 18H). ^{13}C NMR (100 MHz, $CDCl_3$): δ 173.39, 156.05, 154.76, 137.61-138.77, 127.74-128.57, 102.75, 84.85, 82.25, 80.08, 79.82, 79.49, 75.10, 71.28, 70.72, 70.56, 70.32, 66.25, 62.44, 52.67, 44.87, 32.81, 28.54.

[Re(G4)(CO)$_3$] (5.16a) Trifluoroacetic acid (1.5 mL) was added dropwise to a solution of **5.15** (80 mg, 0.082 mmol) in DCM (4 mL) under nitrogen. The resulting mixture was stirred at RT for 5 h. The volatiles were removed under reduced pressure to give a crude oil which was dissolved in MeOH (15 ml). To the above solution was added 10% Pd/C (100 mg). The reaction mixture was stirred for 24 h at room temperature under H_2 atmosphere. The suspension was then filtered over a Celite pad and concentrated to dryness to afford a colorless oil which was dissolved in THF:H_2O (1:1), LiOH was added and the solution was stirred overnight. The solution was neutralized with Amberlite IR-120 (H^+) resin. After removing the resin by filtration, the solution was concentrated to afford a syrup **G4** (20.0 mg, 0.05 mmol) which was dissolved in water (3mL), $[NEt_4]_2[ReBr_3(CO)_3]$ (38.4 mg, 0.05 mmol) was added and the solution was heated to 70˚C for 5 h. The solvent was then removed *in vacuo* and the residue purified by silica gel chromatography to afford the product as a white solid(27.7 mg, 83%). ^{1}H NMR (400 MHz, D_2O): δ 4.58(d, 1H, J=8Hz), 4.38-4.40(m, 1H), 3.90-3.92(m, 1H), 3.80(dd, 1H, *J* = 2.0 Hz, 11.3Hz), 3.61-3.72(m, 13H). 2.85-2.89(m, 1H), 2.70-2.74(m, 1H), 2.06-2.10(m, 1H), 1.94-1.98(m, 1H). *Anal*. Calcd. for $C_{18}H_{31}N_2O_{14}Re$: C, 31.53; H, 4.56; N, 4.09. Found: C, 31.80; H, 4.46; N, 3.99. MS-ESI: m/z 669.1(calcd. for $C_{18}H_{30}N_2O_{13}Re$ 669.13) $[(M + H)^+]$

8.6 Synthesis and characterization of compounds in Chapter 6

BBN analogues synthesis

Peptides were prepared either on an automated peptide synthesizer or by manual

synthesis using Fmoc chemistry. The BBN analogs prepared and characterized were: NH_2-Lys(Dap)-Gln-Trp-Ala-Val-Gly-His-Leu-Met-$CONH_2$ (N-terminal, **L1**), NH_2-Gln-Trp-Ala-Val-Lys(Dap)-Gly-His-Leu-Met-$CONH_2$ (integrated, **L2**), and NH_2-Gln-Trp-Ala-Val-Gly-His-Leu-Met-Lys(Dap)-$CONH_2$ (C-terminal, **L3**). Peptide synthesis used traditional Fmoc chemistry with HBTU or HATU activation of the carboxylate groups on the reactant for coupling with the N-terminal amino group on the growing peptide anchored via the C-terminus to the resin. Rink Amide MBHA resin and Fmoc-protected amino acids with appropriate side-chain protection were used for the synthesis. A fourfold excess of Fmoc amino acid and two equivalent of SAAC 40 were employed for each coupling. The final products were cleaved from the resin by a standard procedure using a cocktail containing thioanisol, water, phenol, and trifluoroacetic acid in a ratio of 5:5:5:85 and precipitated into methyl-*t*-butyl ether. Crude peptides were purified by preparative HPLC monitored at 278 nm (gradient from 0 to 100% solvent B over the course of 60 min). ESI-MS was used to determine the molecular constitution of the conjugates. ESI-MS for **L1**, **L2**, **L3**: m/z: 1183.7 [$(M + H)^+$].

Cyclic RGD peptide (L4) synthesis

The peptide was synthesized by solid-phase peptide synthesis (SPPS) on 2-chlorotrityl chloride resin using Fmoc-strategy. L-glycine was loaded on the 2-chlorotrityl chloride resin as a first amino acid. 2-chlorotrityl chloride resin (1g, loading: 1.56mmol/g) was placed in a sintered glass funnel and the resin was washed and swelled twice with dry DMC. Then a solution of Fmoc-Gly-OH (208mg, 0.7mmol) and DIEA (0.44ml, 2.8mmol) in dry DCM (10ml) was added immediately to the resin. The flask was sealed and the reaction mixture was agitated for 1 hour at room temperature. After the coupling reaction, the unreacted sites on the resin was capped by washing with a mixture of DCM/MeOH/DIEA (17:2:1) (3×) fellowed by washing with dry DCM (3×), dry DMF (2×), dry DCM (2×). Then the resin was dried in vacuum. To determine the amino acid loading 1-2 mg of resin were placed in a cuvette and 20%(vv) piperidine/DMF was added in order to deprotect Fmoc. The OD_{290} was measured against a blank (20% piperidine/DMF). The amino acid loading

was then calculated according to the following equation: Fmoc-loading = (OD_{290}(sample)-OD_{290}(blank))/(1.75×mg(resin)). The amount of resin needed for the peptide synthesis was calculated.

Subsequently, Fmoc-Arg(Pbf)-OH, SAAC, Fmoc-D-Tyr(tBu)-OH, and Fmoc-Asp(OtBu) were coupled with HBTU (4 equiv), HOBt (4 equiv) and DIEA(10 equiv) in DMF. Cleavage of protected linear peptide from the resin was performed without affecting the side chain protecting groups by using a mild 0.8% TFA/CH_2Cl_2 (1:1:8) mixture. Head-to-tail cyclization was carried out in DMF with HBTU (4 equiv), HOBt (4 equiv) and DIEA (10 equiv). The side chain protecting groups were removed by treatment with trifluoroacetic acid/water/triisopropylsilane (TIS)) (95:2.5:2.5) at room temperature for 1.5 h. The reaction mixture was concentrated and precipitated with ice-cold ether and purified by preparative HPLC monitored at 226nm(Method for L4, L7, L9, L6: Gradient E; L5, L8: Gradient F) ESI-MS for L4 m/z: 707.3 $[(M + H)^+]$, 354.1 $[(M + 2H)^{2+}]$; L5: m/z: 909.2 $[(M + H)^+]$, 455.2 $[(M + 2H)^{2+}]$; L6: m/z: 823.3 $[(M + H)^+]$, 412.3 $[(M + 2H)^{2+}]$; L7: m/z: 824.2 $[(M + H)^+]$, 412.7 $[(M + 2H)^{2+}]$; L8: m/z: 778.2 $[(M + H)^+]$, 389.7 $[(M + 2H)^{2+}]$; L9: m/z: 795.4 $[(M + H)^+]$, 398.3 $[(M + 2H)^{2+}]$.

Synthesis of Re-peptide conjugates. An excess of $(NEt_4)_2[ReBr_3(CO)_3]$ was added to 6 mg of an aqueous solution of **L1-L9** respectively. The solution was heated at 70°C for 6-20h (longer times do not reduce the yields) with stirring. Microwave was used to speed up the reactions. Quality control of the reaction mixture was done by RP-HPLC. The desired product was purified by HPLC, lyophilized and characterized by ESI-MS. ESI-MS for 6.1a, 6.2a, 6.3a: m/z: 1425.6 $[(M + H)^+]$, 713.3 $[(M + 2H)^{2+}]$; 6.7a: m/z: 1121.2 $[M^-]$; 6.8a: m/z: 1093.5 $[M^+]$; 6.9a: m/z: 990.2 $[M^-]$; 6.10a: m/z: 1094.5 $[(M + H)^+]$.

$[^{99m}Tc(OH_2)_3(CO)_3]^+$ Labeling. The precursor $[^{99m}Tc(OH_2)_3(CO)_3]^+$ was prepared using an IsoLink® Kit with 1.0–2.5 GBq of $Na^{99m}TcO_4$ in 1-2 ml saline.(*154*) After neutralization to pH = 7 with HCl, quantitative labeling was achieved by mixing an aliquot of the $[^{99m}Tc(OH_2)_3(CO)_3]^+$ precursor with a 0.1 mM stock solution of **L1-L9** at 90°C for 30 min. Quality control (radiochemical yield and purity determination) of

the product was determined by RP-HPLC. The identity was assessed by comparing HPLC retention times with the corresponding rhenium compounds (coinjection).

HPLC and MS analysis of peptide conjugates

The HPLC-MS (UV) trace of **L1**(Nucleodur C18 Column, Gradient A)

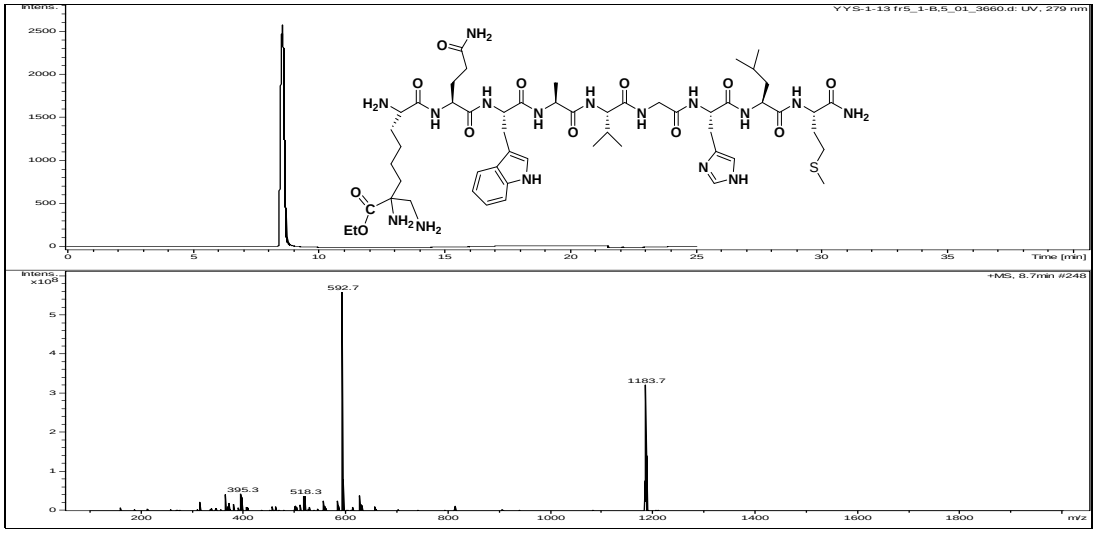

The HPLC-MS (UV) trace of compound **6.1a**(Nucleodur C18 Column, Gradient A)

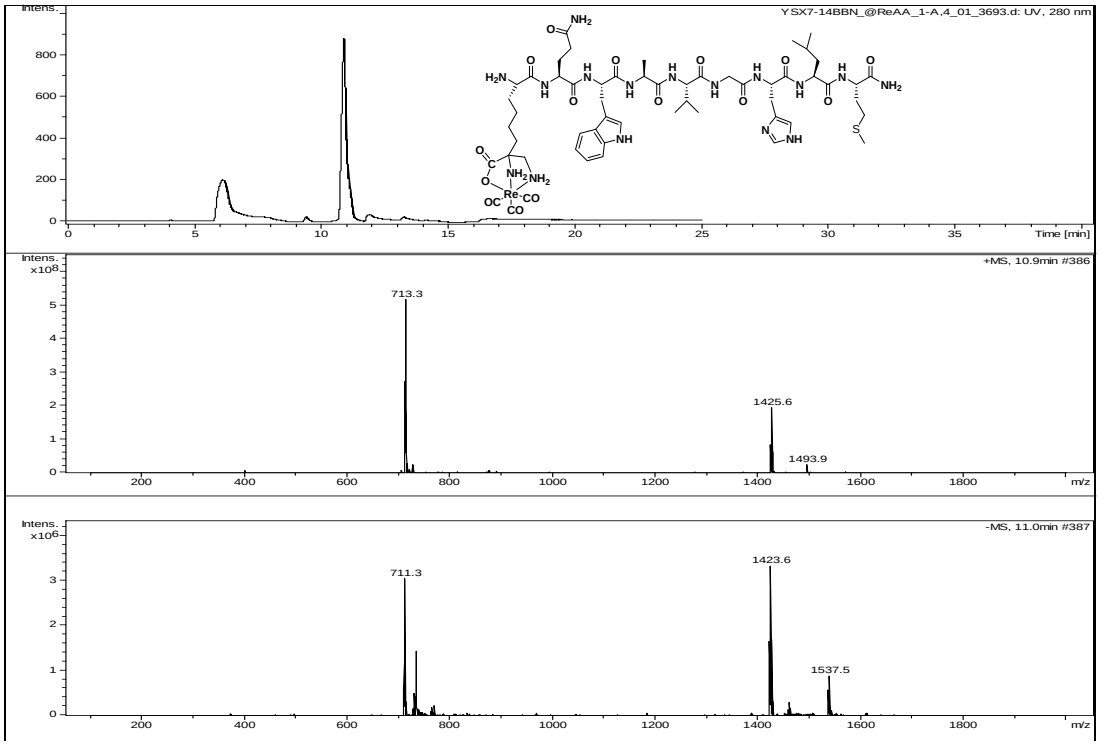

The HPLC-MS (UV) trace of **L2 (**Nucleosil C18 Column, Gradient A)

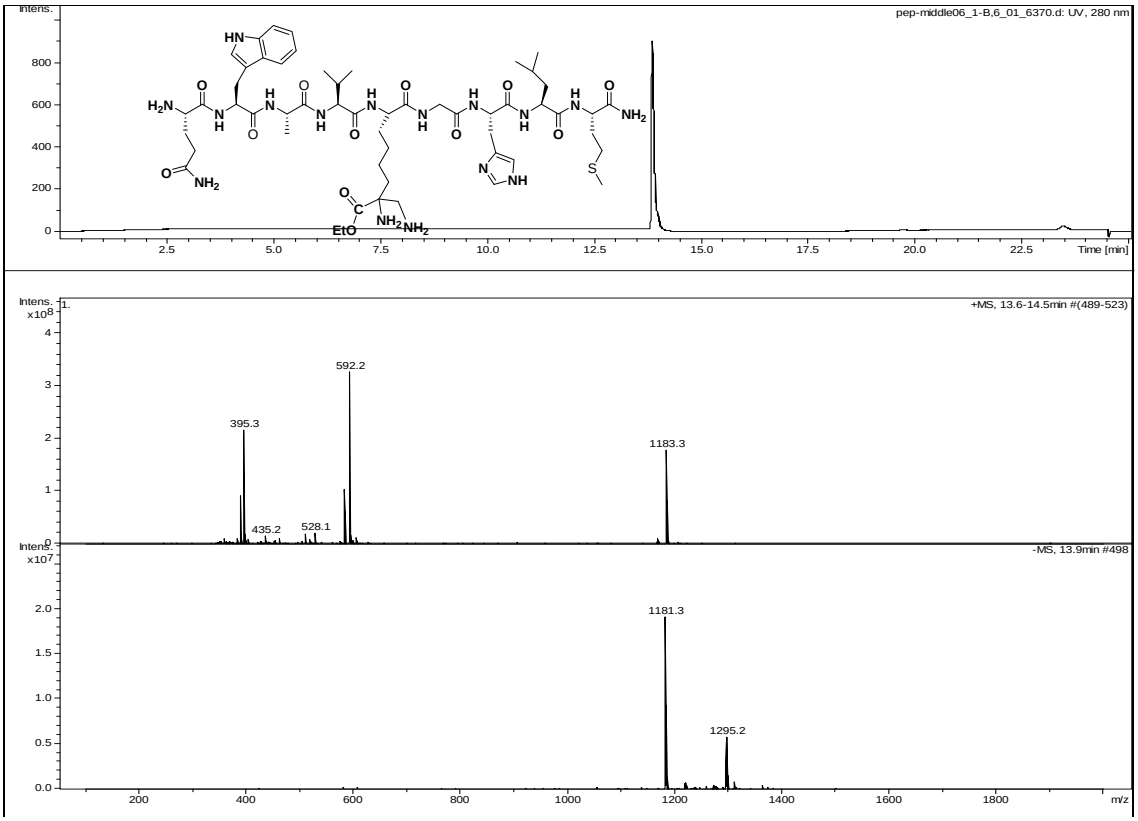

The HPLC traces of compound **6.2a, 6.2b** (Gradient C)

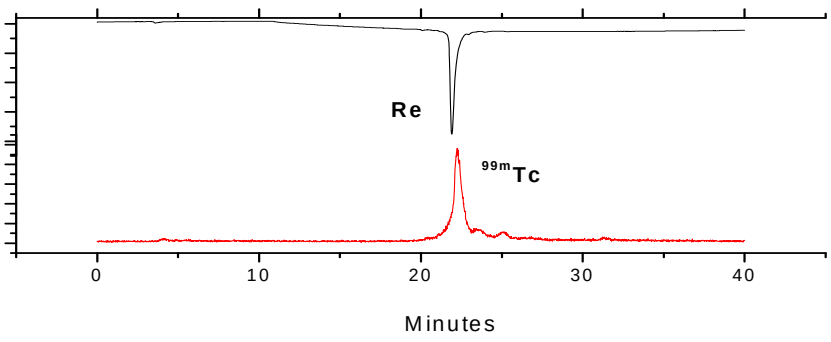

Mass Spectrum of compound **6.2a**

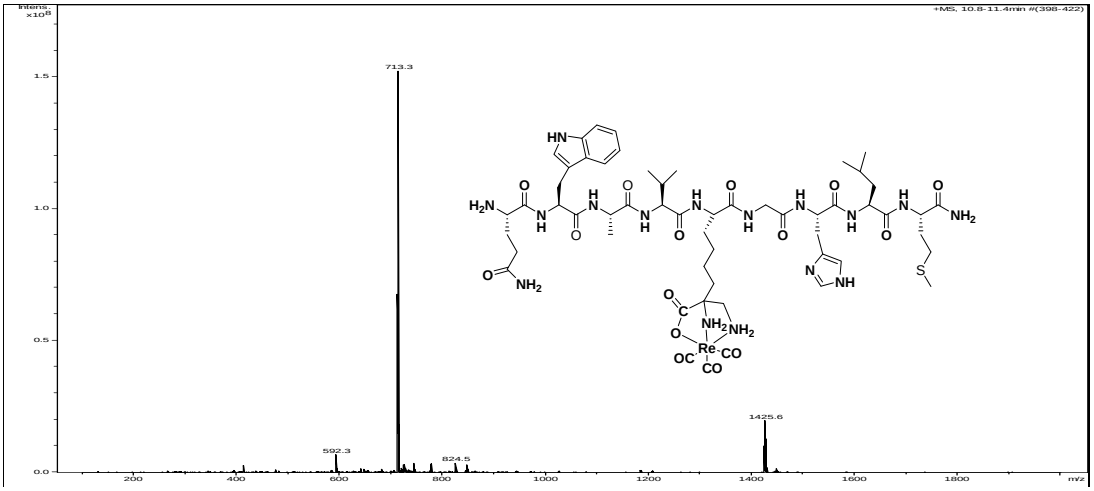

The HPLC-MS (UV) trace of **L3 (**Nucleosil C18 Column, Gradient A)

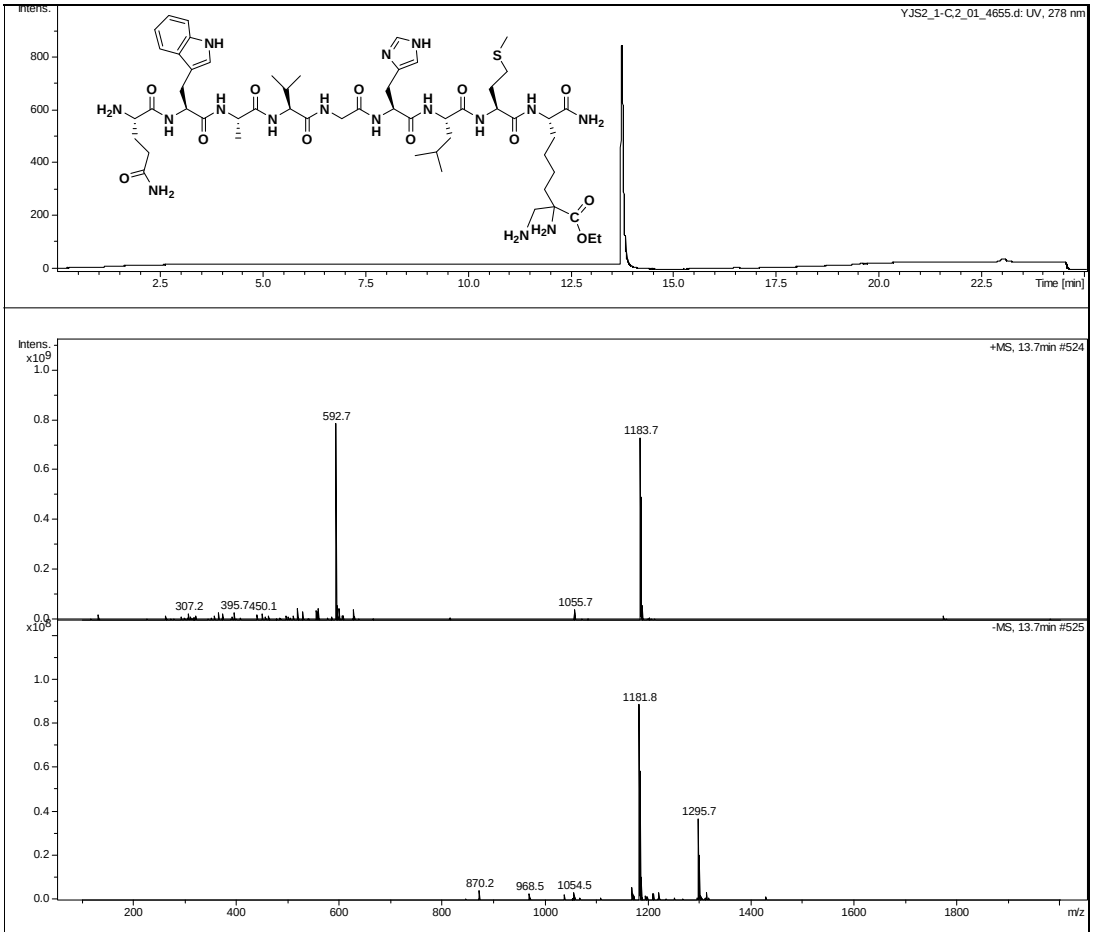

The HPLC traces of compound **6.3a, 6.3b** (Gradient B)

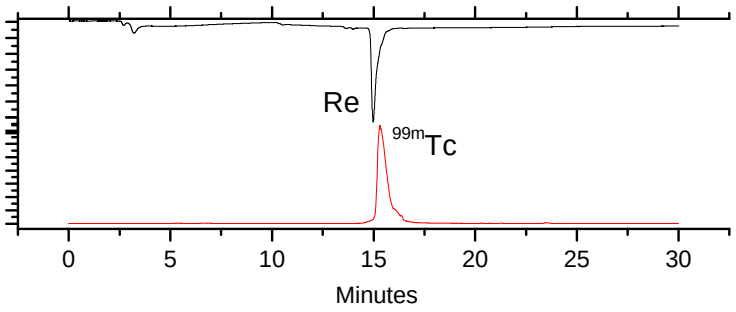

Mass Spectrum of compound **6.3a**

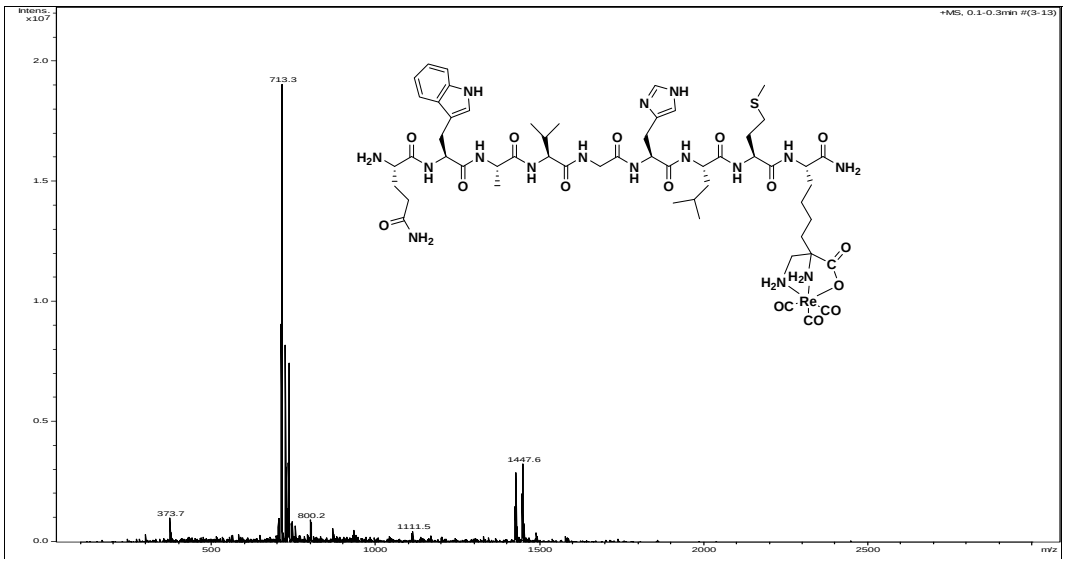

The HPLC trace of compound **L4**(Gradient D)

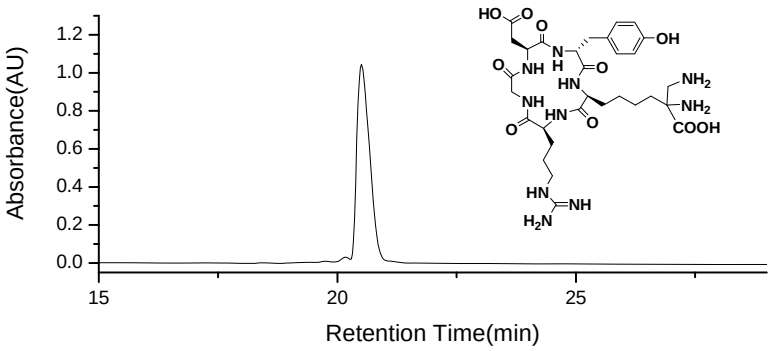

Mass Spectrum of compound **L4, 6.6a**

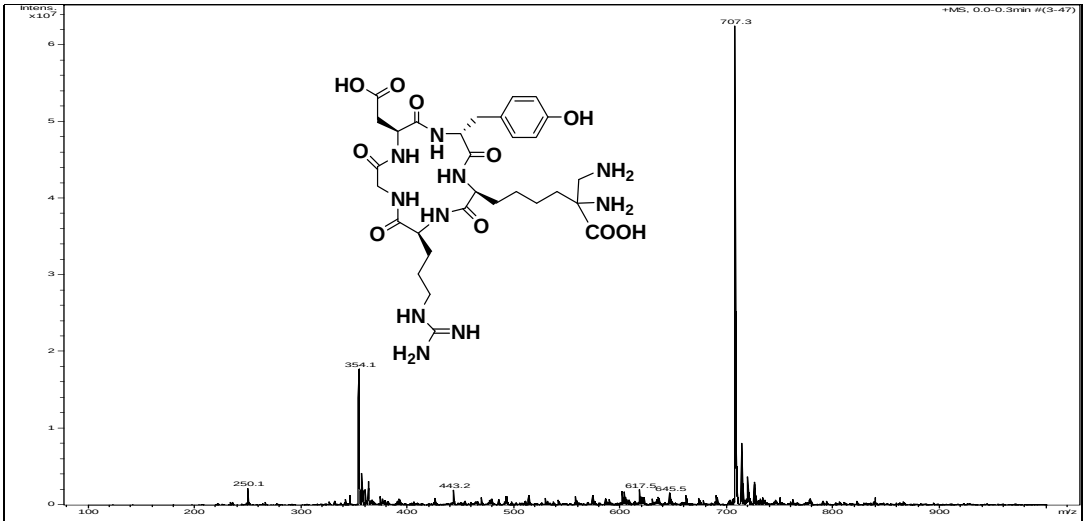

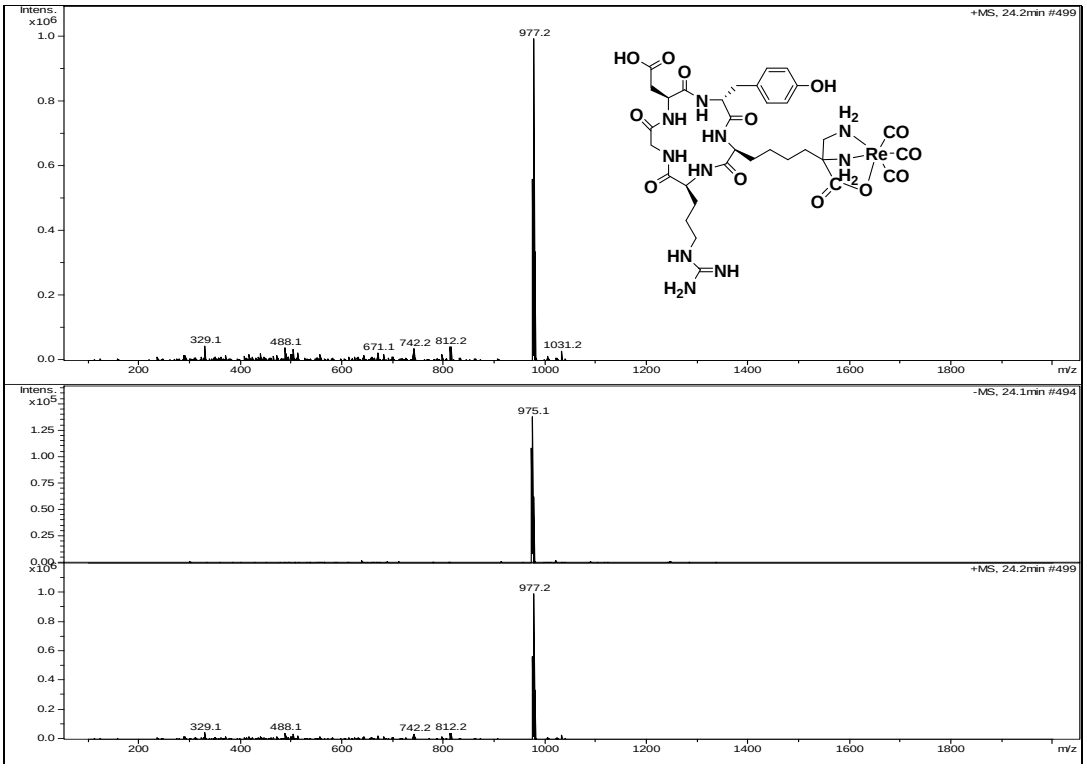

9 Reference

(1) Edwards, C. L. (1979) Tumor-Localizing Radionuclides in Retrospect and Prospect. *Semin. Nucl. Med. 9*, 186-189.

(2) Seidlin, S. M., Marinelli, L. D., and Oshry, E. (1946) Radioactive Iodine Therapy - Effect on Functioning Metastases of Adenocarcinoma of the Thyroid. *JAMA-J. Am. Med. Assoc. 132*, 838-847.

(3) Terpogossian, M. M., Phelps, M. E., Hoffman, E. J., and Mullani, N. A. (1975) Positron-Emission Transaxial Tomograph for Nuclear Imaging (Pett). *Radiology 114*, 89-98.

(4) Everett, D. B., Fleming, J. S., Todd, R. W., and Nightingale, J. M. (1977) Gamma-Radiation Imaging-System Based on Compton-Effect. *Proc. Inst. Electr. Eng-London. 124*, 995-1000.

(5) Patz, E. F., Lowe, V. J., Hoffman, J. M., Paine, S. S., Burrowes, P., Coleman, R. E., and Goodman, P. C. (1993) Focal Pulmonary Abnormalities - Evaluation with F-18 Fluorodeoxyglucose Pet Scanning. *Radiology 188*, 487-490.

(6) Messa, C., Perani, D., Lucignani, G., Zenorini, A., Zito, F., Rizzo, G., Grassi, F., Del Sole, A., Franceschi, M., Gilardi, M. C., and Fazio, F. (1994) High-Resolution Technetium-99m-Hmpao Spect in Patients with Probable Alzheimers-Disease - Comparison with Fluorine-18-Fdg Pet. *J. Nucl. Med. 35*, 210-216.

(7) Sharir, T., Ben-Haim, S., Merzon, K., Prochorov, V., Dickman, D., Ben-Haim, S., and Berman, D. S. (2008) High-Speed Myocardial Perfusion Imaging Initial Clinical Comparison With Conventional Dual Detector Anger Camera Imaging. *JACC-Cardiovasc. Imag. 1*, 156-163.

(8) Murphy, P. H. (1987) Acceptance Testing and Quality-Control of Gamma-Cameras, Including Spect. *J. Nucl. Med. 28*, 1221-1227.

(9) Audi, G., Bersillon, O., Blachot, J., and Wapstra, A. H. (1997) The NUBASE evaluation of nuclear and decay properties. *Nucl. Phys. A. 624*, 1-124.

(10) Eary, J. F., and Brenner, W. (2007) *Nuclear Medicine Therapy*, Informa Healthcare USA, Inc., New York.

(11) Vanarthos, W. J., Ganz, W. I., Vanarthos, J. C., Serafini, A. N., and Tehranzadeh, J. (1992) Diagnostic Uses of Nuclear-Medicine in Aids. *Radiographics 12*, 731-749.

(12) Steenvoorde, P., Pauwels, E. K. J., Harding, L. K., Bourguignon, M., Mariere, B., and Broerse, J. J. (1998) Diagnostic nuclear medicine and risk for the fetus. *Eur. J. Nucl. Med. 25*, 193-199.

(13) Santana-Boado, C., Candell-Riera, J., Castell-Conesa, J., Aguade-Bruix, S., Garcia-Burillo, A., Canela, T., Gonzalez, J. M., Cortadellas, J., Ortega, D., and Soler-Soler, J. (1998) Diagnostic accuracy of technetium-99m-MIBI myocardial SPECT in women and men. *J. Nucl. Med. 39*, 751-755.

(14) Kim, H. J., Boyd, J., Dunphy, F., and Lowe, V. (1998) F-18 FDG PET scan after radiotherapy for early-stage larynx cancer. *Clin. Nucl. Med. 23*, 750-752.

(15) Cheng, K. C., Yeung, H. W., Macapinlac, H. A., and Larson, S. M. (2000) Fluorine-18 fluorodeoxyglucose (18F-FDG) positron emission tomographic imaging in assessing recurrence of head and neck tumors. *Radiology 217*, 497-497.

(16) Dockx, Y., Huizing, M. T., Van den Wyngaert, T., Altintas, S., Huyghe, I., Geboers, I., Vervliet, J., Molderez, C., van Goethem, M., van Marck, V., Sonnemans, H., and Tjalma, W. (2012)

18F-fluorodeoxyglucose (FDG) positron emission tomography (PET) as early imaging biomarker of axillary sentinel lymph node (SLN) status in locally advanced node-positive breast cancer (NPBC) patients (pts) receiving neoadjuvant chemotherapy (NACT). *J. Clin. Oncol. 30*.

(17) Saisho, S., Yasuda, K., Maeda, A., Yukawa, T., Okita, R., Hirami, Y., Shimizu, K., and Nakata, M. (2013) Role of 2-[18F]fluoro-2-deoxyglucose positron emission tomography in preoperative management of solid-type small-sized lung cancer. *Ann. Nucl. Med. 27*, 515-522.

(18) Blake, P., Johnson, B., and VanMeter, J. W. (2003) Positron emission tomography (PET) and single photon emission computed tomography (SPECT): Clinical applications. *J. Neuro-Ophthal. 23*, 34-41.

(19) Richards, P., and Obrien, M. J. (1969) Rapid Determination of 99mo in Separated 99mtc. *J. Nucl. Med. 10*, 517-&.

(20) Jurisson, S., Berning, D., Jia, W., and Ma, D. S. (1993) Coordination-Compounds in Nuclear-Medicine. *Chem. Rev. 93*, 1137-1156.

(21) Hilton, T. C., Thompson, R. C., Williams, H. J., Saylors, R., Fulmer, H., and Stowers, S. A. (1994) Tc-99m Sestamibi Myocardial Perfusion Imaging in the Emergency Room Evaluation of Chest Pain. *J. Am. Chem. Soc. 23*, 1016-1022.

(22) Bisi, G., Sciagra, R., Santoro, G. M., Rossi, V., and Fazzini, P. F. (1995) Technetium-99m-Sestamibi Imaging with Nitrate Infusion to Detect Viable Hibernating Myocardium and Predict Postrevascularization Recovery. *J. Nucl. Med. 36*, 1994-2000.

(23) Ciavolella, M., Greco, C., Tavolaro, R., Tanzilli, G., Scopinaro, F., and Campa, P. P. (1998) Acute oral trimetazidine administration increases resting technetium 99m sestamibi uptake in hibernating myocardium. *J. Nucl. Cardiol. 5*, 128-133.

(24) Yap, C., Vranjesevic, D., Cameron, R., and Czernin, J. (2003) F18-fluoro-thymidine: A new molecular probe for PET imaging of cancer. *Ann. Surg. Oncol. 10*, S38-S38.

(25) Lim, K., Price, R. R., and Baldwin, R. M. (2007) Automated synthesis of [C11]DTBZ for PET molecular imaging study. *Abstr. Pap. Am. Chem. Soc 234*.

(26) Macfarlane, D. J., Shulkin, B. L., Murphy, K., and Wolf, G. T. (1995) Fdg Pet Imaging of Paragangliomas of the Neck - Comparison with Mibg Spet. *Eur. J. Nucl. Med. 22*, 1347-1350.

(27) Sabri, O., Schneider, R., and Buell, U. (1997) Comparison of PET, SPET, neuropsychological and morphological findings in vascular dementia. *Eur. J. Nucl. Med. 24*, 348-349.

(28) Schwarzbach, M., Willeke, F., DimitrakopoulouStrauss, A., Mechtersheimer, G., Lehnert, T., Strauss, L. G., and Herfarth, C. (1997) Positron emission tomography (PET) and single photon emission tomography (SPET): Biological characterization of soft-tissue sarcoma. Preliminary results. *Eur. J. Cancer. 33*, 489-489.

(29) Schwochau, K. (1994) Technetium Radiopharmaceuticals - Fundamentals, Synthesis, Structure, and Development. *Angew. Chem. Int. Ed. 33*, 2258-2267.

(30) Mastrostamatis, S. G., Papadopoulos, M. S., Pirmettis, I. C., Paschali, E., Varvarigou, A. D., Stassinopoulou, C. I., Raptopoulou, C. P., Terzis, A., and Chiotellis, E. (1994) Tridentate Ligands Containing the Sns Donor Atom Set as a Novel Backbone for the Development of Technetium Brain-Imaging Agents. *J. Med. Chem. 37*, 3212-3218.

(31) Tsiapa, I., Loudos, G., Varvarigou, A., Fragogeorgi, E., Psimadas, D., Tsotakos, T., Xanthopoulos, S., Mihailidis, D., Bouziotis, P., Nikiforidis, G. C., and Kagadis, G. C. (2013) Biological evaluation of an ornithine-modified Tc-99m-labeled RGD peptide as an

angiogenesis imaging agent. *Nucl. Med. Biol. 40*, 262-272.

(32) Alberto, R., Schibli, R., Egli, A., Schubiger, A. P., Abram, U., and Kaden, T. A. (1998) A novel organometallic aqua complex of technetium for the labeling of biomolecules: Synthesis of [Tc-99m(OH2)(3)(CO)(3)](+) from [(TcO4)-Tc-99m](-) in aqueous solution and its reaction with a bifunctional ligand. *J. Am. Chem. Soc. 120*, 7987-7988.

(33) Alberto, R. (2003) [Tc(CO)(3)](+) chemistry: a promising new concept for SPET? *Eur. J. Nucl. Med. Mol. Imag. 30*, 1299-1302.

(34) Alberto, R., Ortner, K., Wheatley, N., Schibli, R., and Schubiger, A. P. (2001) Synthesis and properties of boranocarbonate: A convenient in situ CO source for the aqueous preparation of [(TC)-T-99m(OH2)(3)(CO)(3)](+). *J. Am. Chem. Soc. 123*, 3135-3136.

(35) Alberto, R. (2005) New organometallic technetium complexes for radiopharmaceutical imaging. *Contrast Agents III: Radiopharmaceuticals - from Diagnostics to Therapeutics 252*, 1-44.

(36) Hagenbach, A., Athenstadt, S., Daroczi, H. E., Abram, U., and Alberto, R. (2004) Rhenium(I) and technetium(I) tricarbonyl complexes with phosphoraneimines. *Z. Anorg. Allg. Chem. 630*, 2709-2716.

(37) Bernard, J., Ortner, K., Spingler, B., Pietzsch, H. J., and Alberto, R. (2003) Aqueous synthesis of derivatized cyclopentadienyl complexes of technetium and rhenium directed toward radiopharmaceutical application. *Inorg. Chem. 42*, 1014-1022.

(38) van Staveren, D. R., Waibel, R., Mundwiler, S., Schubiger, P. A., and Alberto, R. (2004) Conjugates of vitamin B12 with N-epsilon-functionalized histidine for labeling with [Tc-99m(OH2)(3)(CO)(3)](+): synthesis and biodistribution studies in tumor bearing mice. *J. Organomet. Chem. 689*, 4803-4810.

(39) Zobi, F., Spingler, B., Fox, T., and Alberto, R. (2003) Toward novel DNA binding metal complexes: Structure and basic kinetic data of [M(9MeG)(2)(CH3OH)(CO)(3)](+) (M=Tc-99, Re). *Inorg. Chem. 42*, 2818-2820.

(40) Alberto, R., Pak, J. K., van Staveren, D., Mundwiler, S., and Benny, P. (2004) Mono-, bi-, or tridentate ligands? The labeling of peptides with Tc-99m-carbonyls. *Biopolymers 76*, 324-333.

(41) Benny, P., Pak, J. K., Spingler, B., Kurz, P., and Alberto, R. (2004) Synthesis of novel amino acid derivatized ligands for complexation of fac-M(Co)(3+), M=Tc-99m, Re. *Abstr. Pap. Am. Chem. Soc 228*, U6-U6.

(42) Haefliger, P., Agorastos, N., Renard, A., Giambonini-Brugnoli, G., Marty, C., and Alberto, R. (2005) Cell uptake and radiotoxicity studies of an nuclear localization signal peptide-intercalator conjugate labeled with [Tc-99m(CO)(3)](+). *Bioconjugate Chem. 16*, 582-587.

(43) Hafliger, P., Agorastos, N., Spingler, B., Georgiev, O., Viola, G., and Alberto, R. (2005) Induction of DNA-double-strand breaks by Auger electrons from Tc-99m complexes with DNA-binding ligands. *Chembiochem 6*, 414-421.

(44) Mundwiler, S., Waibel, R., Spingler, B., Kunze, S., and Alberto, R. (2005) Picolylamine-methylphosphonic acid esters as tridentate ligands for the labeling of alcohols with the fac-[M(CO)(3)](+)core (M=Tc-99m, Re): synthesis and biodistribution of model compounds and of a Tc-99m-labeled cobinamide. *Nucl. Med. Biol. 32*, 473-484.

(45) van Staveren, D. R., Benny, P. D., Waibel, R., Kurz, P., Pak, J. K., and Alberto, R. (2005) S-functionalized cysteine: Powerful ligands for the labelling of bioactive molecules with

triaquatricarbonyltechnetium-99m(1+) ([Tc-99m(OH2)(3)(CO)(3)](+)). *Helv. Chim. Acta. 88*, 447-460.

(46) van Staveren, D. R., Mundwiler, S., Hoffmanns, U., Pak, J. K., Spingler, B., Metzler-Nolte, N., and Alberto, R. (2004) Conjugation of a novel histidine derivative to biomolecules and labelling with [Tc-99m(OH2)(3)(CO)(3)](+). *Org. Biomol. Chem. 2*, 2593-2603.

(47) Egli, A., Alberto, R., Tannahill, L., Schibli, R., Abram, U., Schaffland, A., Waibel, R., Tourwe, D., Jeannin, L., Iterbeke, K., and Schubiger, P. A. (1999) Organometallic Tc-99m-aquaion labels peptide to an unprecedented high specific activity. *J. Nucl. Med. 40*, 1913-1917.

(48) Fonti, R., Salvatore, B., Quarantelli, M., Sirignano, C., Cammarano, F., Segreto, S., Petruzziello, F., Catalano, L., Rotoli, B., Del Vecchio, S., Pace, L., and Salvatore, M. (2006) 18F-FDG-PET/CT, 99mTc-MIBI and MRI in the evaluation of patients with multiple myeloma. *Eur. J. Nucl. Med. Mol. Imag. 33*, S188-S188.

(49) Uematsu, T., Yuen, S., Yukisawa, S., Aramaki, T., Morimoto, N., Endo, M., Furukawa, H., Uchida, Y., and Watanabe, J. (2005) Comparison of FDG PET and SPECT for detection of bone metastases in breast cancer. *Am. J. Roentgenol. 184*, 1266-1273.

(50) Liu, Y., Oliveira, B. L., Correia, J. D. G., Santos, I. C., Santos, I., Spingler, B., and Alberto, R. (2010) Syntheses of bifunctional 2,3-diamino propionic acid-based chelators as small and strong tripod ligands for the labelling of biomolecules with Tc-99m. *Org. Biomol. Chem. 8*, 2829-2839.

(51) Liu, Y., Pak, J. K., Schmutz, P., Bauwens, M., Mertens, J., Knight, H., and Alberto, R. (2006) Amino acids labeled with [Tc-99m(CO)(3)](+) and recognized by the L-type amino acid transporter LAT1. *J. Am. Chem. Soc. 128*, 15996-15997.

(52) Oliveira, B. L., Liu, Y., Correia, J. D. G., Santos, I., Gano, L., Spingler, B., and Alberto, R. (2010) 2,3-Diamino propionic acid based chelators for labeling biomolecules with Tc-99m(I). *Nucl. Med. Biol. 37*, 704-704.

(53) Pak, J. K., Benny, P., Spingler, B., Ortner, K., and Alberto, R. (2003) N-epsilon functionalization of metal and organic protected L-histidine for a highly efficient, direct labeling of biomolecules with [Tc(OH2)(3)(CO)(3)](+). *Chem. Eur. J. 9*, 2053-2061.

(54) Ernst, B., and Magnani, J. L. (2009) From carbohydrate leads to glycomimetic drugs. *Nat. Rev. Drug Discov. 8*, 661-677.

(55) Tiwari, V. K., Mishra, R. C., Sharma, A., and Tripathi, R. P. (2012) Carbohydrate based Potential Chemotherapeutic Agents: Recent Developments and their Scope in Future Drug Discovery. *Mini-Rev. Med. Chem. 12*, 1497-1519.

(56) Pauwels, E. K. J., Sturm, E. J. C., Bombardieri, E., Cleton, F. J., and Stokkel, M. P. M. (2000) Positron-emission tomography with [F-18]fluorodeoxyglucose Part I. Biochemical uptake mechanism and its implication for clinical studies. *J. Cancer Res. Clin. Oncol. 126*, 549-559.

(57) Berger, L., Slein, M. W., Colowick, S. P., and Cori, C. F. (1946) Isolation of Hexokinase from Bakers Yeast. *J. Gen. Physiol. 29*, 379-391.

(58) Bustamante, E., Morris, H. P., and Pedersen, P. L. (1981) Energy-Metabolism of Tumor-Cells - Requirement for a Form of Hexokinase with a Propensity for Mitochondrial Binding. *J. Biol. Chem. 256*, 8699-8704.

(59) Geschwind, J. F. H., Ko, Y. H., Torbenson, M. S., Magee, C., and Pedersen, P. L. (2002) Novel therapy for liver cancer: Direct intraarterial injection of a potent inhibitor of ATP production. *Cancer Res. 62*, 3909-3913.

(60) Bertoni, J. M., and Weintraub, S. T. (1984) Competitive-Inhibition of Human-Brain Hexokinase by Metrizamide and Related-Compounds. *J. Neurochem. 42*, 513-518.

(61) Medina, R. A., and Owen, G. I. (2002) Glucose transporters: expression, regulation and cancer. *Biol. Res. 35*, 9-26.

(62) Carvalho, K. C., Cunha, I. W., Rocha, R. M., Ayala, F. R., Cajaiba, M. M., Begnami, M. D., Vilela, R. S., Paiva, G. R., Andrade, R. G., and Soares, F. A. (2011) GLUT1 expression in malignant tumors and its use as an immunodiagnostic marker. *Clinics 66*, 965-972.

(63) Olson, A. L., and Pessin, J. E. (1996) Structure, function, and regulation of the mammalian facilitative glucose transporter gene family. *Annu. Rev. Nutr. 16*, 235-256.

(64) Manolescu, A. R., Witkowska, K., Kinnaird, A., Cessford, T., and Cheeseman, C. (2007) Facilitated hexose transporters: New perspectives on form and function. *Physiology 22*, 234-240.

(65) Zhang, M., Zhang, Z. H., Blessington, D., Li, H., Busch, T. M., Madrak, V., Miles, J., Chance, B., Glickson, J. D., and Zheng, G. (2003) Pyropheophorbide 2-deoxyglucosamide: A new photosensitizer targeting glucose transporters. *Bioconjugate Chem. 14*, 709-714.

(66) Speizer, L., Haugland, R., and Kutchai, H. (1985) Asymmetric Transport of a Fluorescent Glucose Analog by Human-Erythrocytes. *Biochim. Biophys. Acta. 815*, 75-84.

(67) Yoshioka, K., Saito, M., Oh, K. B., Nemoto, Y., Matsuoka, H., Natsume, M., and Abe, H. (1996) Intracellular fate of 2-NBDG, a fluorescent probe for glucose uptake activity, in Escherichia coli cells. *Biosci. Biotechnol. Biochem. 60*, 1899-1901.

(68) Achilefu, S. (2010) Introduction to Concepts and Strategies for Molecular Imaging. *Chem. Rev. 110*, 2575-2578.

(69) Okarvi, S. M. (2004) Peptide-based Radiopharmaceuticals: Future Tools for Diagnostic Imaging of Cancers and other Diseases (vol 24, pg 357, 2004). *Med. Res. Rev. 24*, 685-686.

(70) Virgolini, I., Traub, T., Novotny, C., Leimer, M., Fuger, B., Li, S. R., Patri, P., Pangerl, T., Angelberger, P., Raderer, M., Andreae, F., Kurtaran, A., and Dudczak, R. (2001) New Trends in Peptide Receptor Radioligands. *Q. J. Nucl. Med. 45*, 153-159.

(71) Bolzati, C., Refosco, F., Marchiani, A., and Ruzza, P. (2010) (99m)Tc-Radiolabelled Peptides for Tumour Imaging: Present and Future. *Curr. Med. Chem. 17*, 2656-2683.

(72) Herschman, H. R. (2003) Molecular imaging: Looking at problems, seeing solutions. *Science 302*, 605-608.

(73) Yang, D. J., Kim, E. E., and Inoue, T. (2006) Targeted Molecular Imaging in Oncology. *Ann. Nucl. Med. 20*, 1-11.

(74) Weissleder, R. (2006) Molecular imaging in cancer. *Science 312*, 1168-1171.

(75) Banerjee, S. R., Maresca, K. P., Francesconi, L., Valliant, J., Babich, J. W., and Zubieta, J. (2005) New Directions in the Coordination Chemistry of Tc-99m: a Reflection on Technetium Core Structures and a Strategy for New Chelate Design. *Nucl. Med. Biol. 32*, 1-20.

(76) Maresca, K. P., Hillier, S. M., Femia, F. J., Zimmerman, C. N., Levadala, M. K., Banerjee, S. R., Hicks, J., Sundararajan, C., Valliant, J., Zubieta, J., Eckelman, W. C., Joyal, J. L., and Babich, J. W. (2009) Comprehensive Radiolabeling, Stability, and Tissue Distribution Studies of Technetium-99m Single Amino Acid Chelates (SAAC). *Bioconjugate Chem. 20*, 1625-1633.

(77) Lane, S. R., Bhadrasetty Veerendra, Tammy L. Rold, Gary L. Sieckman, Timothy J. Hoffman, Silvia S. Jurisson, Charles J. Smith. (2008) 99mTc(CO)3-DTMA bombesin conjugates having

high affinity for the GRP receptor. *Nucl. Med. Biol.*, 263–272.

(78) Bolzati, C., Carta, D., Salvarese, N., and Refosco, F. (2012) Chelating Systems for Tc-99m/Re-188 in the Development of Radiolabeled Peptide Pharmaceuticals. *Anti-Cancer Agents Med. Chem. 12*, 428-461.

(79) Chakraborty, S., and Liu, S. (2010) Tc-99m and In-111-Labeling of Small Biomolecules: Bifunctional Chelators and Related Coordination Chemistry. *Curr. Top. Med. Chem. 10*, 1113-1134.

(80) Guzman, F., Barberis, S., and Illanes, A. (2007) Peptide synthesis: chemical or enzymatic. *Electron. J. Biotechnol. 10*, 279-314.

(81) Merrifield, R. B. (1963) Solid Phase Peptide Synthesis .1. Synthesis of a Tetrapeptide. *J. Am. Chem. Soc. 85*, 2149-&.

(82) Fields, G. B., and Noble, R. L. (1990) Solid-Phase Peptide-Synthesis Utilizing 9-Fluorenylmethoxycarbonyl Amino-Acids. *Int. J. Pept. Protein Res. 35*, 161-214.

(83) Mcdonald, T. J., Jornvall, H., Nilsson, G., Vagne, M., Ghatei, M., Bloom, S. R., and Mutt, V. (1979) Characterization of a Gastrin Releasing Peptide from Porcine Non-Antral Gastric Tissue. *Biochem. Biophys. Res. Commun. 90*, 227-233.

(84) Smith, C. J., Volkert, W. A., and Hoffman, T. J. (2005) Radiolabeled peptide conjugates for targeting of the bombesin receptor superfamily subtypes. *Nucl. Med. Biol. 32*, 733-740.

(85) Okarvi, S. M. (2004) Peptide-based radiopharmaceuticals: Future tools for diagnostic imaging of cancers and other diseases. *Med. Res. Rev. 24*, 357-397.

(86) Karra, S. R., Schibli, R., Gali, H., Katti, K. V., Hoffman, T. J., Higginbotham, C., Sieckman, G. L., and Volkert, W. A. (1999) Tc-99m-labeling and in vivo studies of a bombesin analogue with a novel water-soluble dithiadiphosphine-based bifunctional chelating agent. *Bioconjugate Chem. 10*, 254-260.

(87) Van de Wiele, C., Dumont, F., Vanden Broecke, R., Oosterlinck, W., Cocquyt, V., Serreyn, R., Peers, S., Thornback, J., Slegers, G., and Dierckx, R. A. (2000) Technetium-99m RP527, a GRP analogue for visualisation of GRP receptor-expressing malignancies: a feasibility study. *Eur. J. Nucl. Med. 27*, 1694-1699.

(88) Van de Wiele, C. V., Dumont, F., Dierckx, R. A., Peers, S. H., Thornback, J. R., Slegers, G., and Thierens, H. (2001) Biodistribution and dosimetry of Tc-99m-RP527, a gastrin-releasing peptide (GRP) agonist for the visualization of GRP receptor-expressing malignancies. *J. Nucl. Med. 42*, 1722-1727.

(89) Nock, B., Nikolopoulou, A., Chiotellis, E., Loudos, G., Maintas, D., Reubi, J. C., and Maina, T. (2003) [Tc-99m]Demobesin 1, a novel potent bombesin analogue for GRP receptor-targeted tumour imaging. *Eur. J. Nucl. Med. Mol. Imag. 30*, 247-258.

(90) Weide, T., Modlinger, A., and Kessler, H. (2007) Spatial screening for the identification of the bioactive conformation of integrin Ligands. *Bioactive Conformation I 272*, 1-50.

(91) Hynes, R. O. (2002) Integrins: Bidirectional, allosteric signaling machines. *Cell 110*, 673-687.

(92) Muto, P., Lastoria, S., Varrella, P., Vergara, E., Salvatore, M., Morgano, G., Listerjames, J., Bernardy, J. D., Dean, R. T., Wencker, D., and Borer, J. S. (1995) Detecting Deep Venous Thrombosis with Tc-99m-Labeled Synthetic Peptide P280. *J. Nucl. Med. 36*, 1384-1391.

(93) Zhou, Y., Chakraborty, S., and Liu, S. (2011) Radiolabeled Cyclic RGD Peptides as Radiotracers for Imaging Tumors and Thrombosis by SPECT. *Theranostics 1*, 58-82.

(94) Decristoforo, C., Faintuch-Linkowski, B., Rey, A., von Guggenberg, E., Rupprich, M.,

Hernandez-Gonzales, I., Rodrigo, T., and Haubner, R. (2006) [99mTc]HYNIC-RGD for imaging integrin alpha(v)beta(3) expression. *Nucl. Med. Biol. 33*, 945-952.

(95) Alves, S., Correia, J. D. G., Gano, L., Rold, T. L., Prasanphanich, A., Haubner, R., Rupprich, M., Alberto, R., Decristoforo, C., Santos, I., and Smith, C. J. (2007) In vitro and in vivo evaluation of a novel Tc-99m(CO)(3)-pyrazolyl conjugate of cyclo-(Arg-Gly-Asp-D-Tyr-Lys). *Bioconjugate Chem 18*, 530-537.

(96) Arhjoul, L., and Bentourkia, M. (2007) Assessment of glucose metabolism from the projections using the wavelet technique in small animal pet imaging. *Comput. Med. Imaging Graph. 31*, 157-165.

(97) Converse, A. K., Moirano, J. M., Larson, J. A., Kronenfeld, K. V., Oakes, T. R., Holden, J. E., Moore, C. F., and Schneider, M. L. (2009) PET imaging of cerebral glucose metabolism during executive function in normal rhesus. *J. Cereb. Blood Flow Metab. 29*, S591-S592.

(98) Faria, D. D., Copray, J. C. V. M., Sijbesma, J. W. A., Dierckx, R. A. J. O., and de Vries, E. F. J. (2013) PET imaging of neuroinflammation, glucose metabolism and demyelination in the lysolecithin rat model for multiple sclerosis. *J. Label. Compd. Radiopharm. 56*, S480-S480.

(99) Furst, A., Mormino, E., Lal, R., Rabinovici, G., Patel, P., Madison, C., Baker, S., Miller, B., and Jagust, W. (2008) The impact of amyloid burden on glucose metabolism in Alzheimer's disease: Evidence from [11C]PIB and [18F]FDG PET imaging for a differential effect along the anterior-posterior axis. *Neurology 70*, A449-A449.

(100) Mirrione, M. M., Schiffer, W. K., Siddiq, M., Dewey, S. L., and Tsirka, S. E. (2006) PET imaging of glucose metabolism in a mouse model of temporal lobe epilepsy. *Synapse 59*, 119-121.

(101) Suzuki, N., Suzuki, T., Ota, Y., Nakano, T., Kurihara, M., Okuda, H., Yamori, T., Tsumoto, H., Nakagawa, H., and Miyata, N. (2009) Design, Synthesis, and Biological Activity of Boronic Acid-Based Histone Deacetylase Inhibitors. *J. Med. Chem. 52*, 2909-2922.

(102) Zaugg, H. E., Dunnigan, D. A., Sommers, A. H., Michaels, R. J., Swett, L. R., Wang, T. S., and Denet, R. W. (1961) Specific Solvent Effects in Alkylation of Enolate Anions .3. Preparative Alkylations in Dimethylformamide. *J. Org. Chem. 26*, 644-&.

(103) Lange, M., Pettersen, A. L., and Undheim, K. (1998) Synthesis of secondary amines by reductive dimerization of azides. *Tetrahedron 54*, 5745-5752.

(104) McGeary, R. P. (1998) Facile and chemoselective reduction of carboxylic acids to alcohols using BOP reagent and sodium borohydride. *Tetrahedron Lett. 39*, 3319-3322.

(105) Baldwin, J. E., Killin, S. J., Adlington, R. M., and Spiegel, U. (1988) Synthesis of N-Benzyloxycarbonyl-L-Alpha-Aminoadipic Acid, Alpha-Benzyl Ester. *Tetrahedron 44*, 2633-2636.

(106) Bence, A. K., and Crooks, P. A. (2002) Synthesis of L-indospicine. *Synth. Commun. 32*, 2075-2082.

(107) Wu, Y. Q., Limburg, D. C., Wilkinson, D. E., Vaal, M. J., and Hamilton, G. S. (2000) A mild deprotection procedure for tert-butyl esters and tert-butyl ethers using ZnBr2 in methylene chloride. *Tetrahedron Lett. 41*, 2847-2849.

(108) Marcantoni, E., Massaccesi, M., Torregiani, E., Bartoli, G., Bosco, M., and Sambri, L. (2001) Selective deprotection of N-Boc-protected tert-butyl ester amino acids by the CeCl3 center dot 7H(2)O-NaI system in acetonitrile. *J. Org. Chem. 66*, 4430-4432.

(109) Cativiela, C., Lopez, P., and Lasa, M. (2004) Synthesis and preparative resolution of the

trans-cyclohexane analogues of phenylalanine. *Eur. J. Org. Chem.*, 3898-3908.

(110) Khalil, E. M., Subasinghe, N. L., and Johnson, R. L. (1996) An efficient and high yield method for the N-tert-butoxycarbonyl protection of sterically hindered amino acids. *Tetrahedron Lett. 37*, 3441-3444.

(111) Hsieh, Y. S. Y., Taleski, D., Wilkinson, B. L., Wijeyewickrema, L. C., Adams, T. E., Pike, R. N., and Payne, R. J. (2012) Effect of O-glycosylation and tyrosine sulfation of leech-derived peptides on binding and inhibitory activity against thrombin. *Chem. Commun. 48*, 1547-1549.

(112) Humphries, P. S., T Do, Q. Q., and Wilhite, D. M. (2006) ADDP and PS-PPh3: an efficient Mitsunobu protocol for the preparation of pyridine ether PPAR agonists. *Beilstein J. Org. Chem. 2*.

(113) Seebach, D., Dubost, E., Mathad, R. I., Jaun, B., Limbach, M., Loweneck, M., Flogel, O., Gardiner, J., Capone, S., Beck, A. K., Widmer, H., Langenegger, D., Monna, D., and Hoyer, D. (2008) New open-chain and cyclic tetrapeptides, consisting of alpha-, beta(2)-, and beta(3)-amino-acid residues, as somatostatin mimics - A survey. *Helv. Chim. Acta. 91*, 1736-1786.

(114) Smits, E., Engberts, J. B. F. N., Kellogg, R. M., and vanDoren, H. A. (1996) Reliable method for the synthesis of aryl beta-D-glucopyranosides, using boron trifluoride-diethyl ether as catalyst. *J. Chem. Soc., Perkin Trans. 1.*, 2873-2877.

(115) Kim, I. B., Erdogan, B., Wilson, J. N., and Bunz, U. H. F. (2004) Sugar-poly(para-phenylene ethynylene) conjugates as sensory materials: Efficient quenching by Hg2+ and Pb2+ ions. *Chem. Eur. J. 10*, 6247-6254.

(116) Tsai, C. S., Yu, T. B., and Chen, C. T. (2005) Gold nanoparticle-based competitive colorimetric assay for detection of protein-protein interactions. *Chem. Commun.*, 4273-4275.

(117) Pozsgay, V., Dubois, E. P., and Pannell, L. (1997) Synthesis of kojidextrins and their protein conjugates. Incidence of steric mismatch in oligosaccharide synthesis. *J. Org. Chem. 62*, 2832-2846.

(118) Dumas, C., Schibli, R., and Schubiger, P. A. (2003) Versatile routes to C-2- and C-6-functionalized glucose derivatives of iminodiacetic acid. *J. Org. Chem. 68*, 512-518.

(119) Lee, D. S., and Perlin, A. S. (1984) Acid-Catalyzed Conversion of 2-O-(2-Hydroxypropyl)-D-Glucose Derivatives into 1,2-O-(1-Methyl-1,2-Ethanediyl)-D-Glucose Acetals - Studies Related to O-(2-Hydroxy-Propyl)Cellulose. *Carbohydr. Res. 125*, 265-282.

(120) Angibeaud, P., and Utille, J. P. (1990) Stereoselective Reaction of Methyl Alpha-D-Glycopyranoside and Beta-D-Glycopyranoside with Acetic-Anhydride in the Presence of Trimethylsilyl Trifluoromethanesulfonate. *J. Chem. Soc., Perkin Trans. 1.*, 1490-1492.

(121) Lu, W., Navidpour, L., and Taylor, S. D. (2005) An expedient synthesis of benzyl 2,3,4-tri-O-benzyl-beta-D glucopyranoside and benzyl 2,3,4-tri-O-benzyl-beta-D-mannopyranoside. *Carbohydr. Res. 340*, 1213-1217.

(122) Azema, L., Claustre, S., Alric, I., Blonski, C., Willson, M., Perie, J., Baltz, T., Tetaud, E., Bringaud, F., Cottem, D., Opperdoes, F. R., and Barrett, M. P. (2004) Interaction of substituted hexose analogues with the Trypanosoma brucei hexose transporter. *Biochem. Pharmacol. 67*, 459-467.

(123) Willson, M., and Perie, J. (1999) Inhibition of yeast hexokinase: a kinetic and phosphorus

nuclear magnetic resonance study. *Spectroc. Acta Pt. A-Molec. Biomolec. Spectr. 55*, 911-917.

(124) Ogawa, Z., Kanashima, M., and Nishioka, H. (2001) Improvement of the quantitative method for glucose determination using hexokinase and glucose 6-phosphate dehydrogenase. *Clin. Chem. Lab. Med. 39*, 396-400.

(125) Schibli, R., Dumas, C., Petrig, J., Spadola, L., Scapozza, L., Garcia-Garayoa, E., and Schubiger, P. A. (2005) Synthesis and in vitro characterization of organometallic rhenium and technetium glucose complexes against glut 1 and hexokinase. *Bioconjugate Chem. 16*, 105-112.

(126) Ferreira, C. L., Marques, F. L. N., Okamoto, M. R. Y., Otake, A. H., Sugai, Y., Mikata, Y., Storr, T., Bowen, M., Yano, S., Adam, M. J., Chammas, R., and Orvig, C. (2010) Cationic technetium and rhenium complexes with pendant carbohydrates. *Appl. Radiat. Isot. 68*, 1087-1093.

(127) Dirscherl, G., Knape, R., Hanson, P., and Konig, B. (2007) Solid-phase synthesis of metal-complex containing peptides. *Tetrahedron 63*, 4918-4928.

(128) Huang, H., and Rabenstein, D. L. (1999) A cleavage cocktail for methionine-containing peptides. *J. Pept. Res. 53*, 548-553.

(129) Chen, X. Y., Park, R., Shahinian, A. H., Bading, J. R., and Conti, P. S. (2004) Pharmacokinetics and tumor retention of I-125-labeled RGD peptide are improved by PEGylation. *Nucl. Med. Biol. 31*, 11-19.

(130) Kaiser, E., Colescot.Rl, Bossinge.Cd, and Cook, P. I. (1970) Color Test for Detection of Free Terminal Amino Groups in Solid-Phase Synthesis of Peptides. *Anal. Biochem. 34*, 595-&.

(131) Schottelius, M., Laufer, B., Kessler, H., and Wester, H. J. (2009) Ligands for Mapping alpha(v)beta(3)-Integrin Expression in Vivo. *Accounts Chem. Res. 42*, 969-980.

(132) Schottelius, M., and Wester, H. J. (2009) Molecular imaging targeting peptide receptors. *Methods 48*, 161-177.

(133) Kerr, J. S., Slee, A. M., and Mousa, S. A. (2000) Small molecule alpha(v) integrin antagonists: novel anticancer agents. *Expert Opin. Inv. Drug 9*, 1271-1279.

(134) Decristoforo, C., Santos, I., Pietzsch, H. J., Kuenstler, J. U., Duatti, A., Smith, C. J., Rey, A., Alberto, R., Von Guggenberg, E., and Haubner, R. (2007) Comparison of in vitro and in vivo properties of [Tc-99m]cRGD peptides labeled using different novel Tc-cores. *Q. J. Nucl. Med. Mol. Im. 51*, 33-41.

(135) Haubner, R., Wester, H. J., Weber, W. A., Mang, C., Ziegler, S. I., Goodman, S. L., Senekowitsch-Schmidtke, R., Kessler, H., and Schwaiger, M. (2001) Noninvasive imaging of alpha(v)beta(3) integrin expression using F-18-labeled RGD-containing glycopeptide and positron emission tomography. *Cancer Res. 61*, 1781-1785.

(136) Kraft, S., Diefenbach, B., Mehta, R., Jonczyk, A., Luckenbach, G. A., and Goodman, S. L. (1999) Definition of an unexpected ligand recognition motif for alpha nu beta 6 integrin. *J. Biol. Chem. 274*, 1979-1985.

(137) Knappe, T. A., Manzenrieder, F., Mas-Moruno, C., Linne, U., Sasse, F., Kessler, H., Xie, X. L., and Marahiel, M. A. (2011) Introducing Lasso Peptides as Molecular Scaffolds for Drug Design: Engineering of an Integrin Antagonist. *Angew. Chem. Int. Edit. 50*, 8714-8717.

(138) Goodman, S. L., Holzemann, G., Sulyok, G. A. G., and Kessler, H. (2002) Nanomolar small molecule inhibitors for alpha v beta 6, alpha v beta 5, and alpha v beta 3 integrins. *J. Med. Chem. 45*, 1045-1051.

(139) Dechantsreiter, M. A., Planker, E., Matha, B., Lohof, E., Holzemann, G., Jonczyk, A., Goodman, S. L., and Kessler, H. (1999) N-methylated cyclic RGD peptides as highly active and selective alpha(v)beta(3) integrin antagonists. *J. Med. Chem. 42*, 3033-3040.

(140) Mas-Moruno, C., Rechenmacher, F., and Kessler, H. (2010) Cilengitide: The First Anti-Angiogenic Small Molecule Drug Candidate. Design, Synthesis and Clinical Evaluation. *Anti-Cancer Agent Med. 10*, 753-768.

(141) Pohle K, Notni J, Bussemer J, Kessler H, Schwaiger M, and AJ, B. (2012) 68Ga-NODAGA-RGD is a suitable substitute for 18F-Galacto-RGD and can be produced with high specific activity in a cGMP/GRP compliant automated process. *Nucl. Med. Biol. in press*.

(142) Wester, H. J., Schottelius, M., and Schwaiger, M. (2001) Tc-99m (CO)(3)-labeled Carbohydrated SSTR-ligands: Synthesis, Internalization Kinetics and Biodistribution on a Rat Pancreatic Tumor Model. *J. Nucl. Med. 42*, 115p-115p.

(143) Yu, G., Wang, S. Z., Wang, K., Hu, Y. F., and Hu, H. W. (2004) A novel approach to 1,2-dihydro-2-oxo-3-pyridinecarboxylic ester via aromatization induced by deamidation. *Synthesis*, 1021-1028.

(144) Heitsch, H., Wagner, A., YadavBhatnagar, N., and GriffoulMarteau, C. (1996) Synthesis of the imidazole-derived AT(1)-selective ANG II receptor antagonist HR 720 utilizing reductive amination as key step. *Synthesis*, 1325-+.

(145) Poulsen, T. B., Dickmeiss, G., Overgaard, J., and Jorgensen, K. A. (2008) Organocatalytic asymmetric synthesis of versatile gamma-lactams. *Angew. Chem. Int. Ed. 47*, 4687-4690.

(146) Langlois, M., Quintard, D., and Abalain, C. (1994) Synthesis of Symmetrical Pseudopeptides as Potential Inhibitors of the Human Immunodeficiency Virus-1 Protease. *Eur. J. Med. Chem. 29*, 639-647.

(147) Bonnet, N., O'Hagan, D., and Hahner, G. (2007) Ionic strength mediated hydrophobic force switching of CF3-terminated ethylene glycol self-assembled monolayers (SAMs) on gold. *Chem. Commun.*, 5066-5068.

(148) Peng, Y. G., Pang, H. W., and Ye, T. (2004) Stereocontrolled synthesis of onchidins. *Org. Lett. 6*, 3781-3784.

(149) Rajput, V. K., and Mukhopadhyay, B. (2006) Sulfuric acid immobilized on silica: an efficient reusable catalyst for the synthesis of O-isopropylidene sugar derivatives. *Tetrahedron Lett. 47*, 5939-5941.

(150) Marugan, J. J., Manthey, C., Anaclerio, B., Lafrance, L., Lu, T. B., Markotan, T., Leonard, K. A., Crysler, C., Eisennagel, S., Dasgupta, M., and Tomczuk, B. (2005) Design, synthesis, and biological evaluation of novel potent and selective alpha(v)beta(3)/alpha(v)beta(5) integrin dual inhibitors with improved bioavailability. Selection of the molecular core. *J. Med. Chem. 48*, 926-934.

(151) Stragies, R., Osterkamp, F., Zischinsky, G., Vossmeyer, D., Kalkhof, H., Reimer, U., and Zahn, G. (2007) Design and synthesis of a new class of selective integrin alpha 5 beta 1 antagonists. *J. Med. Chem. 50*, 3786-3794.

(152) Hartman, G. D., Egbertson, M. S., Halczenko, W., Laswell, W. L., Duggan, M. E., Smith, R. L., Naylor, A. M., Manno, P. D., Lynch, R. J., Zhang, G. X., Chang, C. T. C., and Gould, R. J. (1992) Nonpeptide Fibrinogen Receptor Antagonists .1. Discovery and Design of Exosite Inhibitors. *J. Med. Chemistry 35*, 4640-4642.

(153) Haubner, R., Bruchertseifer, F., Bock, M., Kessler, H., Schwaiger, M., and Wester, H. (2004) Synthesis and biological evaluation of a Tc-99m-labelled cyclic RGD pepticle for imaging the alpha v beta 3 expression. *Nuklearmedizin 43*, 26-32.

(154) Alberto, R., Ortner, K., Wheatley, N., Schibli, R., and Schubiger, A. P. (2001) Synthesis and Properties of Boranocarbonate: A Convenient in Situ CO Source for the Aqueous Preparation of [99mTc(OH2)3(CO)3]+. *J. Am. Chem. Soc. 123*, 3135-3136.

Curriculum Vitae

PERSONAL INFOS

Surname: SHEN
First name: Yunjun
Date of birth: 16th September, 1981
Nationality: China

EDUCATIONAL BACKGROUND

09.2009-present Ph. D. in Inorganic Chemistry, Anorganisch-chemisches Institut, Universität Zürich, Zurich, Switzerland
Supervisor: Prof. Dr. Roger Alberto

09.2008-08.2009 Ph. D Candidate of Chemical Engineering. South China University of Technology, Guangzhou, China

09.2005-07.2008 M.S. in Applied Chemistry. Wuhan Institute of Technology, Wuhan, China
Master thesis: Synthesis, Characterization and Biolgical Activities of Superoxide Dismutase and peroxidase Model Complexes
Supervisor: Prof. Dr. Qingxiang Li

09.2001-07.2005 B.S. in chemical Technology, Wuhan Institute of Technology, Wuhan, China

09.1998-07.2001 No.4 High school of Suizhou, Suizhou, China

SCHOLARSHIPS & HONORS

2013 Grant from European corporation in science and technology
2009 CSC scholarship for PhD study
2002-2004 School scholarships in wuhan institute of technology

ACADEMIC PUBLICATIONS

[1]. Yunjun Shen, Raposinho, P., Alberto, R*. Synthesis of Carbohydrate conjugates for potential use in ^{99m}Tc molecular imaging. *Journal of biological inorganic chemistry*. To be submitted.

[2]. Yunjun Shen, Raposinho, P., Alberto, R*. Radiolabeled $_{\alpha v\beta 3}$ Integrin Binding Peptides for Tumor Targeting. In preparation.

[3]. Yunjun Shen, Alberto, R*. Design and Synthesis of functionalised chelating agents for

conjugation to RGD peptide. In preparation.

[4]. Yunjun Shen, Alberto, R* (2013) Orthogonally Protected Artificial Amino Acid as Tripod Ligand for Automated Peptide Synthesis and Labeling with $[^{99m}Tc(OH_2)_3(CO)_3]^+$. *Bioconjugate. Chem. 24*, 26.

[5]. Li, Q. X*., Yunjun Shen, and Meng, X. G. (2008) Synthesis and crystal structures of 1-(benzimidazol-2-ylmethyl)-1,4,7-triazacyclononane and its copper complex $[Cu(_{C14H21N5})Br_{]2}.[CuB_{r4}]$. *Acta. Chim. Sinica*. 66, 266**.**

[6]. Li, Q. X*., Yunjun Shen, Du, Y., and Wang, Z. H. (2006) 1,4- bis (1H–benzimi d a z o l-2-ylmethyl)1,4,7-triazacyclononane 4.5-hydrate. *Acta. Crystallogr. E.* 62, O1682

[7]. Li, Q. X*, Yunjun Shen, J., Liu, C. L., and Yu, G. P. (2006) Propane-1,3-diyl bis-(p-toluenesulfonate). Acta. Crystallogr. E. 62, O2464

[8]. Li, Q. X*., He, B. Z., Yunjun Shen, and Xiao, H. Y. (2007) [(4RS,7SR)-1-(1H-B-enzimidazol-2-ylmethyl-kappaN-3)-1,4,7-triazacyclononane-kappaN-3] bromido-copper(II) bromide. *Acta. Crystallogr. E.* 63, M1482-M1483

[9]. Li, Q. X*., Li, Q. A., Yunjun Shen, Meng, X. G., Luan, F. P., and Xiang, A. H. (2010) Synthesis and Crystal Structure of a Copper(II)-Sodium(I) Coordination Polymer. *J. Chem. Crystallogr.* 40, 1155.